PREFACE

We are pleased to offer our readers the scientific Activity Report of the Frank Laboratory of Neutron Physics for 2014. Its first part presents a brief review of the experimental and theoretical results achieved in the main research areas – condensed matter physics, neutron nuclear physics, applied research and in the development and creation of elements of neutron spectrometers for condensed matter investigations. The second part includes the reports on the operation of the modernized IBR-2 pulsed reactor, the development of the IREN neutron source and investigations carried out at the EG-5 accelerator. A list of publications in 2014, the information about seminars and conferences organized in FLNP and statistical data on the FLNP personnel structure are presented as well.

In 2014 the main achievements of the Laboratory were:

- successful fulfillment of the user program at the IBR-2 spectrometers;
- construction of a full-scale stand of a pelletized cryogenic moderator for the central IBR-2 reactor beamlines and the successful conduct of experiments to study the possibilities of feeding moderating material.

In 2014 the IBR-2 reactor operated for physical experiments for 2492 hours, the IREN facility – for 1358 hours and EG-5 – for 665 hours.

FLNP has cooperation agreements in the field of neutron investigations with almost 200 scientific institutes and universities from 42 countries from all over the world. A significant contribution to this cooperation is made by the JINR Member States.

The FLNP personnel include more than 450 employees. Among them are 79 Ph.D. and 17 D.Sci. researchers. 64 scientists and specialists are from the JINR Member States (besides the Russian Federation) with more than two thirds of them being under 35 years of age.

The organization of annual conferences and schools covering all FLNP research fields helps to recruit young specialists — one of the top priority tasks of the FLNP Directorate.

We can state with assurance that the Laboratory continues to develop successfully and dynamically, carrying out investigations for the benefit of the JINR Member States.

V.N. Shvetsov

Director

Members of the Directorate of the Frank Laboratory of Neutron Physics:

SHVETSOV
Valeryi
Nikolaevich
Director
since 2013

Deputy Directors for Science

CULICOV
Otilia
Ana
since 2013

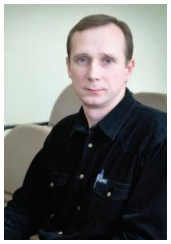

LYCHAGIN
Egor
Valerievich
since 2013

KUCERKA
Norbert
since 2014

KOZENKOV
Sergey
Vyacheslavovich
Deputy Director
for General Issues
since 1989

VINOGRADOV
Alexander
Vital'evich
Chief Engineer
since 2007

CHUDOBA
Dorota
Marta
Scientific secretary
since 2013

1. SCIENTIFIC RESEARCH

CONDENSED MATTER PHYSICS

The main objectives of research in the framework of the theme involved the application of neutron scattering techniques and complementary methods to investigate the structure, dynamics and microscopic properties of nanosystems and novel materials, which are of great importance for the development of nanotechnologies in the fields of electronics, pharmacology, medicine, chemistry, modern condensed matter physics and interdisciplinary sciences.

The greater part of experimental research was carried out on spectrometers of the modernized IBR-2 reactor in accordance with the Topical Plan for JINR Research and International Cooperation and FLNP User Program. A number of scientific experiments were performed in neutron and synchrotron centers in Russia and abroad under the existing cooperation agreements and accepted beam time application proposals. Also, the activities on the modernization of the available spectrometers and the development of new instruments were carried out in accordance with the development program plan for the IBR-2 spectrometers. Most attention was given to the realization of the top-priority projects (construction of a new DN-6 diffractometer for studying microsamples and a multipurpose GRAINS reflectometer).

Within the framework of investigations under the theme the employees of the FLNP Department of Neutron Investigations of Condensed Matter (NICM) maintained broad cooperation with many scientific organizations in Russia and abroad. The cooperation, as a rule, was documented by joint protocols or agreements. In Russia, especially active collaboration was with the thematically-close organizations, such as RRC KI, PNPI, SSC RF IPPE, MSU, IMP UB RAS, IC RAS, INR RAS and others.

A list of the main scientific topics studied by the employees of the NICM Department includes:

- Investigation of structure and properties of novel crystal materials and nanosystems by neutron diffraction;
- Investigation of magnetic colloidal systems in bulk and at interfaces;
- Investigation of structure of carbon nanomaterials;
- Magnetism of layer nanostructures;
- Investigation of nano-scale structure and functional characteristics of biological, colloidal and polymeric nanodispersed materials;
- Investigation of nanostructure and properties of lipid membranes and lipid complexes;
- Investigation of atomic dynamics of nanosystems and materials by neutron inelastic scattering;
- Investigation of texture and properties of minerals and rocks;
- Analysis of internal stresses in bulky materials and factory-made goods.

I. Scientific results

Structure investigations of novel oxide, intermetallic and nanostructured materials

The structural, magnetic, and vibrational properties of $PbFe_{0.5}Nb_{0.5}O_3$ relaxor multiferroic were studied by means of x-ray, neutron diffraction, and Raman spectroscopy at pressures up to 30 GPa in a temperature range from 10 to 300 K [1] (**Fig. 1**). With increasing pressure in a given compound two successive structural phase transitions from the initial R3m rhombohedral polar phase to Cm and Pm monoclinic polar phases were observed at P = 5.5 and 8.5 GPa, respectively. The G-type antiferromagnetic order remains stable in the pressure range under study and the Néel temperature increases with a pressure coefficient $(1/T_N)dT_N/dP$ = 0.012 GPa^{-1}. The existence of high-pressure polar phases in combination with the magnetic order characterized by an increase in T_N in $PbFe_{0.5}Nb_{0.5}O_3$ implies the stability of the magnetoelectric effect and is a unique phenomenon, which

is in drastic contrast with a general tendency towards a suppression of polar phases and/or magnetoelectric coupling in the majority of conventional oxide multiferroics under pressure.

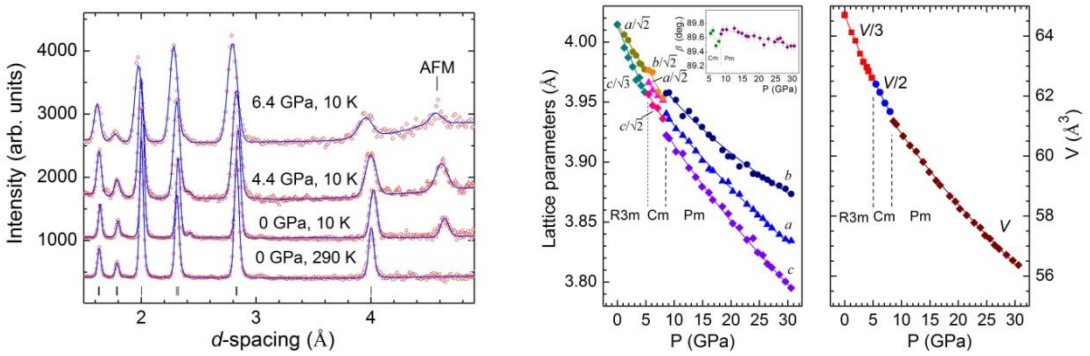

Fig. 1. Neutron diffraction patterns of $PbFe_{0.5}Nb_{0.5}O_3$ (DN-12 diffractometer, IBR-2) measured under high pressures of up to 6.4 GPa and at temperatures of 10 and 290 K (left). The most intense magnetic peak is marked as AFM. The pressure dependencies of lattice parameters and unit cell volume of different phases of $PbFe_{0.5}Nb_{0.5}O_3$ obtained in X-ray diffraction experiments in a wide pressure range of up to 30 GPa (right).

The atomic and magnetic structures of intermetallic cobalt compounds RCo_2 were studied using neutron diffraction in the range of high pressures of 0-4 GPa and temperatures of 10-300 K [2, 3]. For many years these compounds have been considered as model systems demonstrating a phenomenon of itinerant electron metamagnetism (IEM). This phenomenon involves the appearance of transition metal sublattice magnetization as a response to the action of the magnetic field of the rare-earth metal sublattice in intermetallic compounds. In the course of the experiments it was found that the concept of IEM is valid for compounds with sufficiently high magnetic ordering temperatures T_C ~ 150-200 K (R = Tb, Ho), but it cannot describe the magnetic properties of compounds with low values of T_C ~ 30-40 K. Using $ErCo_2$ as an example, the inconsistent behavior of Er and Co sublattice magnetizations and the suppression of Co sublattice magnetism were demonstrated at stable magnetic properties of the Er sublattice under pressure (**Fig. 2**). The obtained results in combination with the theoretical calculations call for further refinement of the IEM concept taking into account the peculiarities of the electronic structure of RCo_2 compounds.

The structural features of promising high-voltage cathode materials based on $LiNi_{0.5}Mn_{1.5}O_4$ - $LiNi_{0.5-x}Mn_{1.5-y}M_{x+y}O_4$ (M = Co, Cr, Ti, Al, Mg; x + y = 0.05), synthesized in the Institute of Chemistry and Mechanochemistry, Siberian Branch of the Russian Academy of Sciences (Novosibirsk) were investigated in order to improve the electrochemical properties of these materials. The unsubstituted $LiNi_{0.5}Mn_{1.5}O_4$ has a high electrochemical potential (4.7 V) corresponding to a flat plateau in the charge-discharge curve at a mean capacity of 120 mAh/g, which significantly increases specific stored energy of the battery as compared to other materials ($LiCoO_2$ ~ 3.8 V, $LiFePO_4$ ~ 3.2 V at the same capacity). Depending on the method of synthesis, $LiNi_{0.5}Mn_{1.5}O_4$ can have either a primitive cubic structure, symmetry $P4_332$, with an ordered arrangement of cations (temperature of synthesis does not exceed 700°C) or face-centered cubic structure, symmetry Fd-3m, with a disordered arrangement of cations (temperatures of synthesis are above 800°C). Because of structural transformations during the cycling the compound $LiNi_{0.5}Mn_{1.5}O_4$ with the space group $P4_332$ shows worse electrochemical behavior as compared to $LiNi_{0.5}Mn_{1.5}O_4$ with the structure Fd-3m.

1. SCIENTIFIC RESEARCH

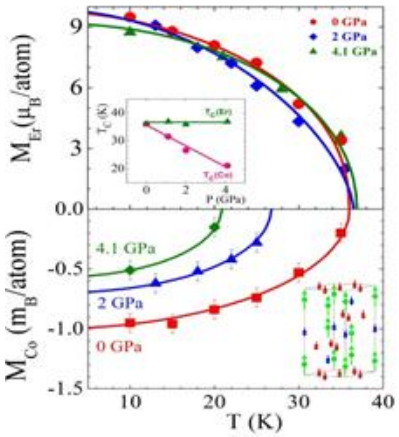

Fig. 2. Temperature dependences of Er and Co sublattice magnetizations in $ErCo_2$ at different pressures, illustrating their independent behavior which is beyond the IEM concept. The insets show the pressure dependences of the Curie temperatures of Er and Co sublattices and the character of the magnetic ordering in these compounds.

The samples under study were synthesized at T < 800°C by means of a small substitution of transition metals for Ni and Mn cations, as well as by using the mechanoactivation procedure for the reactant mixture in a planetary mill. As a result of the treatment of the neutron diffraction spectra using the Rietveld method it was found that all the samples have a two-phase structure. The main phase is the Fd-3m phase, and the extra phase $P4_332$ comprises from 1 to 20% depending on the added metal and the temperature of synthesis. It was observed that the ions of the added metal preferably occupy positions of Ni, which in turn causes the formation of the impurity phase NiO in small amounts (1-2%). The average size of the blocks was 70-80 nm for the samples synthesized at 700°C, and 100-150 nm for the samples synthesized at 800°C. Large microstrains were found mostly, as expected, in the samples with the lower temperature of synthesis.

Investigations of magnetic fluids and nanoparticles

The study of the influence of magnetic nanoparticle loading on the structure of the protein shell in magnetoferritin (synthetic biological complex of apoferritin with different content of magnetic material in the protein cavity) was continued for a wide range of loading factor LF (the number of iron atoms per complex) of the magnetic material [4, 5]. The increase in the magnetic loading up to LF = 910 leads to the loss of solution stability and partial sedimentation. At the same time the small-angle neutron scattering (SANS) from the supernatant solution has a form typical for pure appoferritin (**Fig. 3a**). The results of the experiments on contrast variation (**Fig. 3b**) showed a shift in the effective match point of the complex with increasing LF and growth of the residual scattering in it, which is associated with an increase in the structural polydispersity of the system. As a result, there is a considerably greater (in comparison with the expected value) volume fraction of the magnetic material in the complex, which increases with the loading factor growth, thus pointing to a partial destruction of the apoferritin shell. The work has been done in collaboration with the Institute of Experimental Physics, Slovak Academy of Sciences (Kosice, Slovakia) and the Faculty of Physics of the Taras Shevchenko National University of Kiev (Kiev, Ukraine).

As a part of a comprehensive study of the nanoparticle impact on biological macromolecules in solutions, the data of small-angle scattering of synchrotron radiation (SAXS) for mixtures of fibrillar amyloid protein aggregates of lysozyme (egg white) with magnetoferritin were analyzed. It was revealed from SAXS experiments (**Fig. 4**) and fluorescence analysis that the addition of magnetoferritin to amyloid solutions of lysozyme reduces the amyloid aggregation of proteins [6].

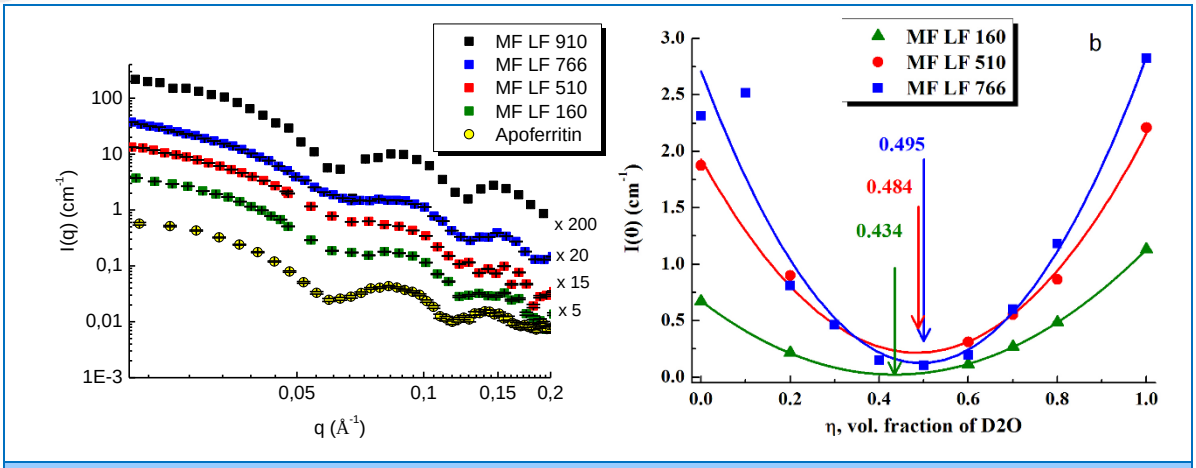

Fig. 3. SANS data for solutions of apoferritin and magnetoferritin with varying load (a). Results of experiments on contrast variation for magnetoferritin with different loading factor (b).

The pair distance distribution functions (**Fig. 4**) obtained using SAXS data strongly suggest the reduction in the size of amyloid aggregates in the mixture with the magnetoferritin complex. The effect was found to be more pronounced for larger loads of the magnetic material. The work has been done in collaboration with the Institute of Experimental Physics, Slovak Academy of Sciences (Kosice, Slovakia), Helmholtz Research Centre Geesthacht (Geesthacht, Germany) and the Faculty of Physics of the Taras Shevchenko National University of Kiev (Kiev, Ukraine).

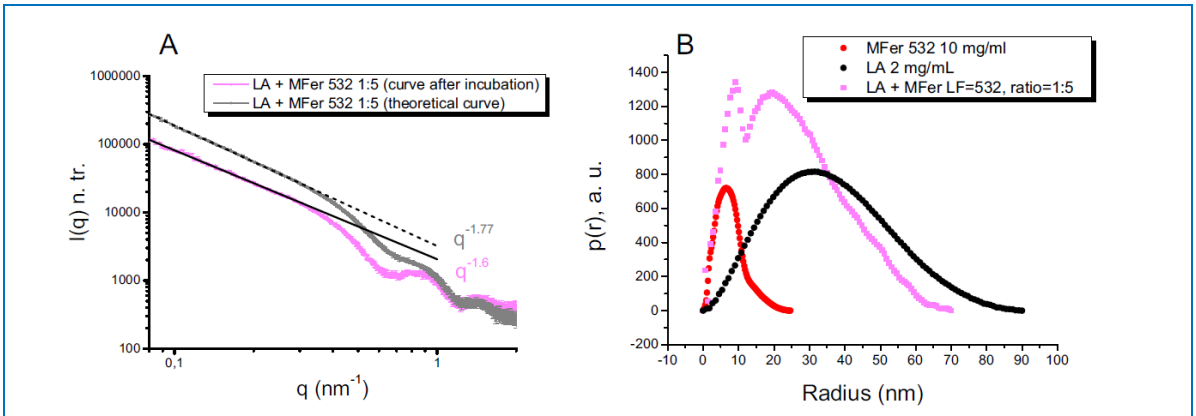

Fig. 4. (A) The experimental scattering curve for a mixture of lysozyme amyloids and magnetoferritin with LF = 532 is compared with the theoretical curve based on the scattering from unmixed solutions. (B) The corresponding pair distance distribution function for the mixture is compared with the similar functions for neat solutions of amyloids and magnetoferritin.

A detailed study of aqueous micellar solutions of sodium oleate and its mixtures with polyethylene glycol PEG (PEG) was carried out within the investigations of the structural reorganization effects previously detected in aqueous magnetic fluids stabilized by sodium oleate on addition of the polymer as a biocompatibiity enhancement component. The SANS data revealed changes in the structure and interactions between the micelles of sodium oleate. The neat aqueous solutions of sodium oleate showed a typical behavior for the solutions of charged micelles characterized by the transition from spherical to cylindrical micelles at 2% surfactant content in the system. The structural parameters of micelles and micellar interaction in solutions of sodium oleate with and without PEG in the system were obtained. The addition of a small (about 2%) amount of

1. SCIENTIFIC RESEARCH

PEG resulted in a decrease in the micelle aggregation number and changes in the degree of aggregation with growing surfactant concentration in the solution. At a high (10%) content of PEG some kind of screening of the intermicellar interaction in the system was observed, presumably due to the effective micelle surface coating by the polymer [7]. The work has been performed in collaboration with Helmholtz Research Centre Geesthacht (Geesthacht, Germany), Institute of Experimental Physics, Slovak Academy of Sciences (Kosice, Slovakia) and the Faculty of Physics of the Taras Shevchenko National University of Kiev (Kiev, Ukraine).

Investigations of carbon nanomaterials

In the framework of research for developing synthesis of biologically active fullerene derivatives, integrated studies (atomic force microscopy, small-angle neutron scattering and infrared spectroscopy) were carried out on aqueous colloidal C60 solutions produced by different methods. It was shown that along with C60 monomers (size of about 0.7 nm) spherical aggregates in a broad size range of 2-50 nm were present in the solutions. The size characteristics (radius of gyration and maximum size) of the aggregates in bulk solutions of three- and six-month age were derived from the SANS data analysis (**Fig. 5**) and were in good agreement with the AFM data obtained for the dried samples. To identify possible additional bonds in the aqueous fullerene solutions, experiments on infrared spectroscopy were performed. The spectra revealed additional peaks that correspond to O-H, C-OH and C-O bonds. This fact indicates that a hydroxyl shell exists on the surface of the fullerene clusters providing for the solution stabilization [8]. The work has been done in collaboration with the Taras Shevchenko National University of Kiev (Kiev, Ukraine).

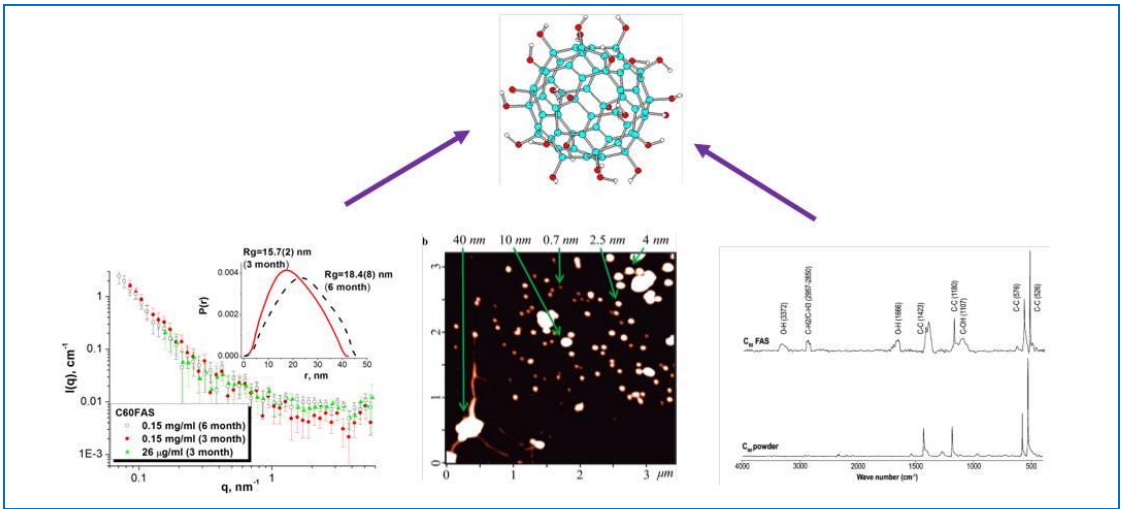

Fig. 5. The proposed model for stabilization of fullerene molecules in water according to the results of the experiments (SANS, AFM and infrared microscopy).

A general theory of small-angle scattering from spherical nanoparticles with a diffuse surface was developed and tested in practice [9] within the framework of structural studies of nanodiamonds. The approximation of low diffusivity and a large width of the diffusive layer, which are observed in SANS experiments on detonation nanodiamonds, was considered. The expressions for the parameters of the particle size distribution function in the lognormal approximation were derived. The dependences of the scattering invariants as a function of the solvent scattering length density in the contrast variation experiments on liquid dispersions of such particles were studied. The theoretical results were used in the analysis of the SANS data on cluster solutions of detonation nanodiamonds in water and dimethylsulfoxide from different manufacturers. Full agreement with the predicted behavior of the scattering invariants with the contrast changes was obtained. The presence of a

transitional diamond-graphite region in detonation nanodiamonds in the form of a specific power-law dependence for the average radial density was confirmed. The work has been performed in collaboration with the Ioffe Physical-Technical Institute (St. Petersburg, Russia), Helmholtz Research Centre Geesthacht (Geesthacht, Germany), Nanocarbon Research Institute (Nagano, Japan) and Faculty of Physics of Taras Shevchenko National University of Kiev (Kiev, Ukraine).

The modeling of the kinetics of cluster formation and growth in C60 fullerene solutions was continued. In the extrapolation of numerical solutions of the kinetic equations over time, first estimates of the time evolution of the cluster size distribution function *f*(*R*, *t*) were obtained for a polar saturated solution of C60 (time interval of seven days). Using these data the SANS curves for the solution after various time intervals were calculated. It was shown that according to the model calculations the maximum SANS intensity is observed for the interval ranging from several hours to one day after the solution preparation (**Fig. 6**). The accuracy of the estimates and possibilities of making more accurate calculations for concrete systems are under discussion. The prospects of these studies are linked to the use of new equations including the population balance equation (PBE) method. For the application of this approach, the solution of the model problems was extended to longer periods of the evolution time of the system by using the dynamic grid sampling. In addition to the cases of pure decay and pure particle aggregation we considered a model that takes into account both processes; as the initial interaction "cores" the mathematically simple cores (constant, summation and others) were used.

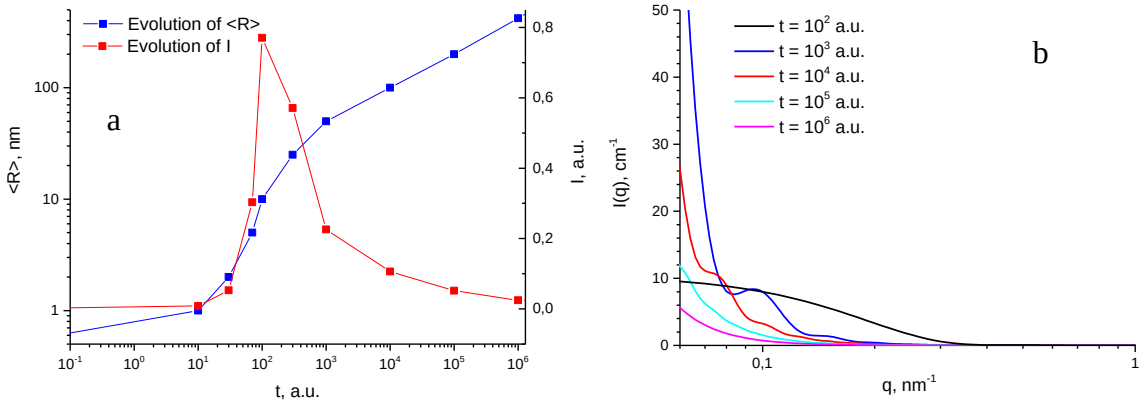

Fig. 6. (a) Model evolution of the average cluster size and average SANS intensity for a polar fullerene solution. (b) Examples of calculated SANS spectra from the cluster size distribution function for the time intervals ranging from several hours to one day after solution preparation.

Investigations of layered nanostructures

On the REMUR reflectometer the nonreciprocal transmission of neutrons through a noncoplanar magnetic system (NCMS) was investigated [10]. The new generation of spintronics elements is based on complex noncoplanar magnetic systems (NCMS), in which the spatial dependence of three orthogonal components of the magnetic field induction takes place. Neutrons, like electrons, have spin s = 1/2, therefore the investigation of neutron transmission processes is of importance for the identification of common features inherent in both kinds of particles. The approximation of the electron-type behavior by neutrons is justified in ferromagnets, where the exchange field is large and the Lorentz force can be neglected. A noncoplanar magnetic system, in accordance with the solution of the Schrödinger equation, is characterized by the properties, which are not inherent in a coplanar magnetic system (CMS), namely, the dependence of the transmission

1. SCIENTIFIC RESEARCH

of unpolarized neutrons (or electrons) on the direction of their propagation. To verify this result, a NCMS was created in which the interface between regions with different directions of magnetization does not exceed 10 nm, providing a non-adiabatic regime for the neutron spin transmission through them. NCMS consisted of two magnetic mirrors with magnetization vectors orthogonal to each other and lying in the mirror planes. It was placed in a magnetic field perpendicular to the mirrors. **Figure 7** shows two schemes of experiments to study the behavior of neutrons transmitted through CMS and NCMS. In the first scheme (**Fig. 7**, at the top), the neutron beam was directed in such a way that the sequences "first mirror–magnetic field–second mirror" and "second mirror–magnetic field–first mirror" were realized.

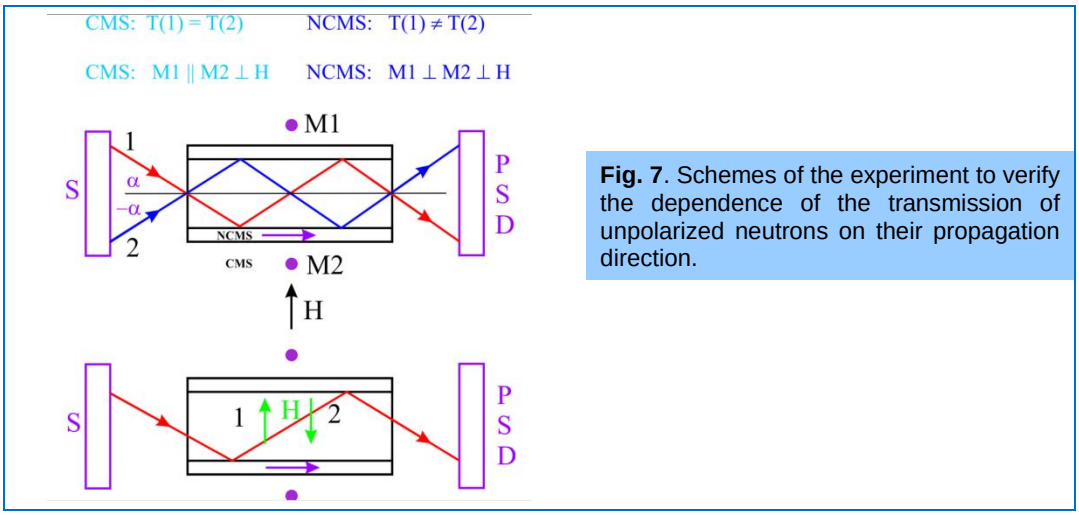

Fig. 7. Schemes of the experiment to verify the dependence of the transmission of unpolarized neutrons on their propagation direction.

Figure 8 shows the neutron intensities for CMS and NCMS, respectively. In the case of NCMS an antiphase behavior of the transmission curves was observed. The second scheme in **Fig. 7** (at the bottom) illustrates the second variant of verification, when the direction of the magnetic field is reversed. In accordance with this scheme **Figure 8** shows the dependences of transmission of unpolarized neutrons for CMS and NCMS, respectively.

Thus, it was shown that the transmission in NCMS depends on the neutron propagation direction, which in its turn is a consequence of non-commutativity of the spin algebra for S = ½.

The film coatings based on titanium nitride were studied by neutron and X-ray reflectometry in order to determine the structural parameters (thickness of layers, roughness of the layer interfaces and the scattering length density of individual layers). The monolayer (TiN) and multilayer (TiN/WN) coatings reduce the wear of cutting and shaping tools, increase the surface hardness and reduce the coefficient of friction. The studies were carried out on the neutron reflectometer REFLEX at the IBR-2 reactor and the Bruker X-ray reflectometer at Saint-Petersburg State University. On the basis of the obtained reflection coefficients from the 32-nm-thick film of titanium nitride deposited on a silicon substrate (TiN(32nm)/Si) by magnetron sputtering, the scattering length density (SLD) profiles (DRP) in the direction of the normal to the interface were determined (**Fig. 9**).

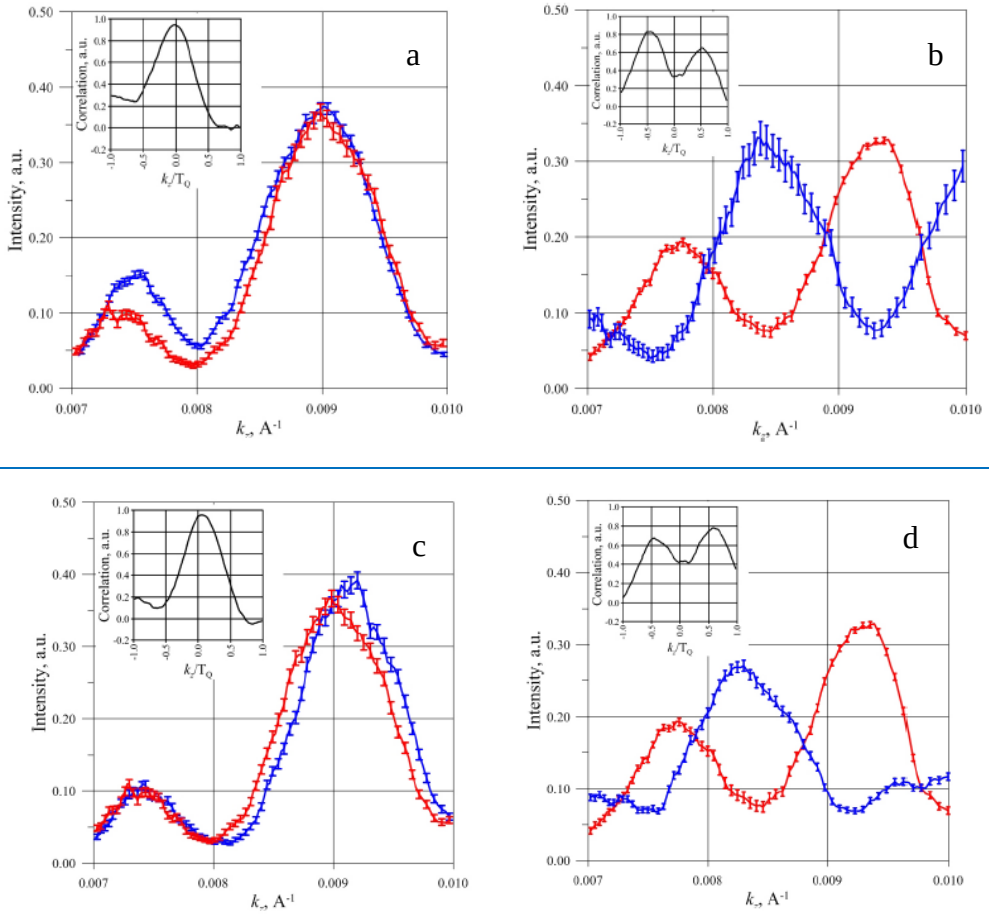

Fig. 8. The transmission for unpolarized neutrons obtained using the first experimental scheme for CMS (a) and NCMS (b). The transmission of unpolarized neutrons obtained by using the second experimental scheme for CMS (c) and NCMS (d).

1. SCIENTIFIC RESEARCH

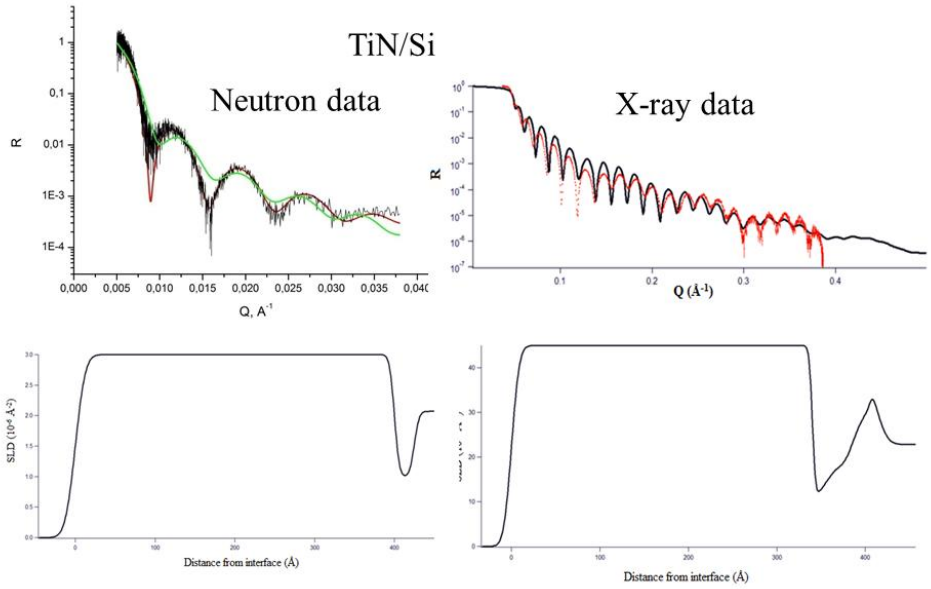

Fig. 9. Neutron (left) and X-ray (right) reflection coefficients from a 36-nm-thick titanium nitride film. The determined scattering length density profiles in both cases (below) show the presence of a transitional layer between the film and the substrate with a relatively low SLD-value. This is indicative of poor adhesion of the film to the substrate surface.

Investigations of biological nanosystems, lipid membranes and complexes

The self-organization and structural parameters of pH-sensitive micelles of surfactants – amine oxides synthesized in the Comenius University (Bratislava, Slovakia) – were studied by small-angle neutron scattering at the Yellow Submarine (Budapest, Hungary) and YuMO instruments. Earlier it has been shown that pH variation provides wide possibilities of controlling properties of specific surfactant molecules – amine oxides. According to the SANS data, at pH < 3 and pH > 8 charged micelles can be observed in solutions, but according to the literature, amine oxides can possess a charge only in acidic media. To obtain more detailed information about the charge, additional studies involving the analysis of ζ-potential in the solutions.

The effect of sucrose on the structure of the lipid bilayer of unilamellar vesicles was studied by small-angle neutron synchrotron radiation scattering [11]. It has been found that when the concentration of sucrose exceeds 40% there is a significant decrease in the thickness of the lipid bilayer.

The model lipid membranes of the lipid matrix of the stratum corneum of the skin were investigated by neutron and X-ray diffraction. The main result obtained is that the superstrong membrane interaction retains after complete membrane hydration.

Polymeric materials

Synthesis and investigation of the structure and physical properties of magnetic elastomers are one of the intensively developing fields of technologies aimed at creating novel "smart" nanomaterials with molecular anisotropy and ferromagnetic nanoparticles. The magnetic elastomers synthesized in the West University of Timisoara, Romania, were investigated by small-angle neutron scattering in the transverse (Pi) and longitudinal (Bi) magnetic fields. Measurements were made on the initial elastomer P1(B1) without ferromagnetic inclusions (matrix) and elastomers P12-P32, P13-

P33, P14-P34 and B2-B4 with ferroparticles of different concentrations polymerized in the absence and presence of an external magnetic field of varying magnitude.

According to the results of neutron studies the initial polymer matrix is anisotropic itself (polymeric clusters of the developed branched chains are more extended in the direction transverse to the film plane). The magnetic field applied in the same transverse direction results in the attraction and convergence of ferroparticles along the field lines. Thus, the polymer is squeezed out of the gaps between the particles, and the polymer cluster anisotropy changes (cluster size increases in the film plane and decreases in the transverse direction). This result was obtained experimentally for the first time and is fully consistent with the results of numerical modeling of the behavior of systems of magnetic particles in an elastic two-dimensional array under magnetization, which point to the positive magnetostriction of structural systems with clusters.

The comparison and analysis of the results describing the glass transition of polymers in the framework of modern theoretical methods were continued. The comparison with the experiment was made on the basis of the data of differential scanning calorimetry for polystyrene at cooling rates in the range from $5 \cdot 10^{-6}$ K/s to 2 K/s. The cooling rate range covered exceeds the available and described in the literature results by three orders of magnitude. It was shown that the use of conventional theoretical methods (TNM, Adam-Gibbs and others) leads to a significant discrepancy with the experiment. A new expression for the relaxation time to describe the experimental data in the framework of the approach with a single order parameter was proposed. The used approaches were compared, and prospects for their further development were analyzed. As additional parameters for comparison, the limiting fictitious temperature of the system, characteristics of the C_p peaks (height and angle) and produced enthalpy were used (**Fig. 10**). The predictive ability of the models was checked using the linear extrapolation of their parameters as a function of the cooling rate. It has been shown that the Adam-Gibbs models give better results [12, 13]. The work was performed in collaboration with the University of Rostock (Rostock, Germany).

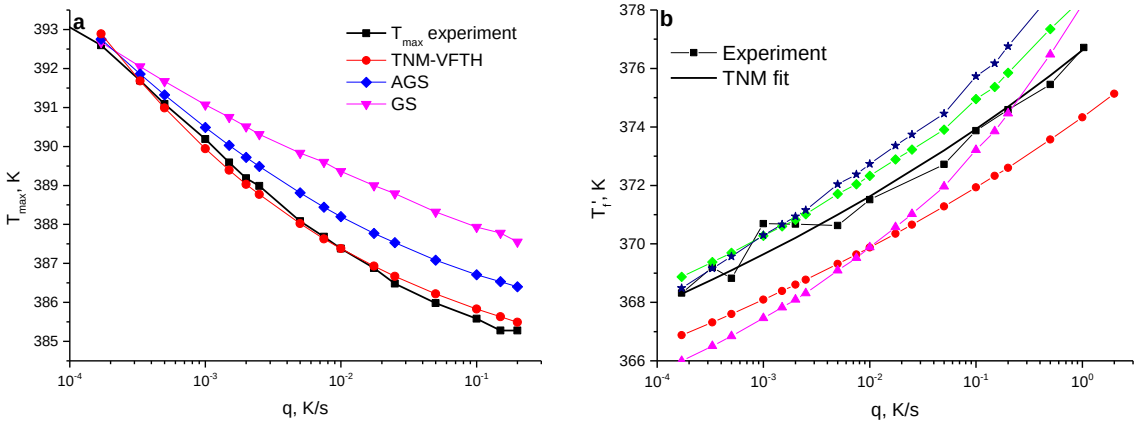

Fig. 10. At the left: Dependence of C_p peak positions on the cooling rate. At the right: Dependence of the experimental and model T_f on the cooling rate. Comparison of different models.

Atomic and molecular dynamics

The vibrational dynamics of water retained in graphene oxide was experimentally and theoretically studied [14]. Nowadays it is generally accepted that graphene oxide (GO) mostly contains hydroxyl (-OH) and epoxy (-O-) groups spread over its basal planes. The presence of hydrogen atoms on the basal planes of freshly synthesized GO sheets points to its metastability. As a

result, it transforms into a stable form by a recombination of hydrogen atoms with neighbouring epoxy and hydroxyl groups and produces water, which is always present in graphene oxide materials. The neutron scattering measurements of GO were performed at 20 K on the NERA time-of-flight inverted-geometry spectrometer. The GO sample was synthesized by a modified Hummers method at the Institute of General and Inorganic Chemistry RAS (Moscow). Because of the lack of information on the inelastic scattering spectra for GO we performed the atomistic simulations of the low-temperature spectrum based on the Lerf-Klinowski model with a variable number of water molecules in the interlayer space (with a distance of 7 Å as was revealed in simultaneous measurements by neutron diffraction). In an attempt to simulate the short-range order a systematic periodic model was proposed. Also the calculations using the density functional theory (DFT) were performed. The experimental one-phonon INS spectrum of GO obtained on the NERA spectrometer is compared with the theoretical results and the representative periodic models in **Fig. 11**. There are usually six bands resolved in the experimental spectrum, which were found at about 1500, 1000, 500, 250, 100, and 25 cm^{-1}, respectively. The theoretical calculations allowed us to analyze the specific features of the spectrum. The band in the range of about 1500-1200 cm^{-1} can be accurately attributed to the set of δC-O-H modes. The dominant and pronounced feature covering the range of ~ 700-300 cm^{-1} may be linked with the set of libration modes of water. The general shape and position of this band were properly restored. The libration modes are widely distributed below 700 cm^{-1} in the following order: $\omega H^{\cdot}O\text{-}H > \tau H^{\cdot}O\text{-}H > \rho H^{\cdot}O\text{-}H$.

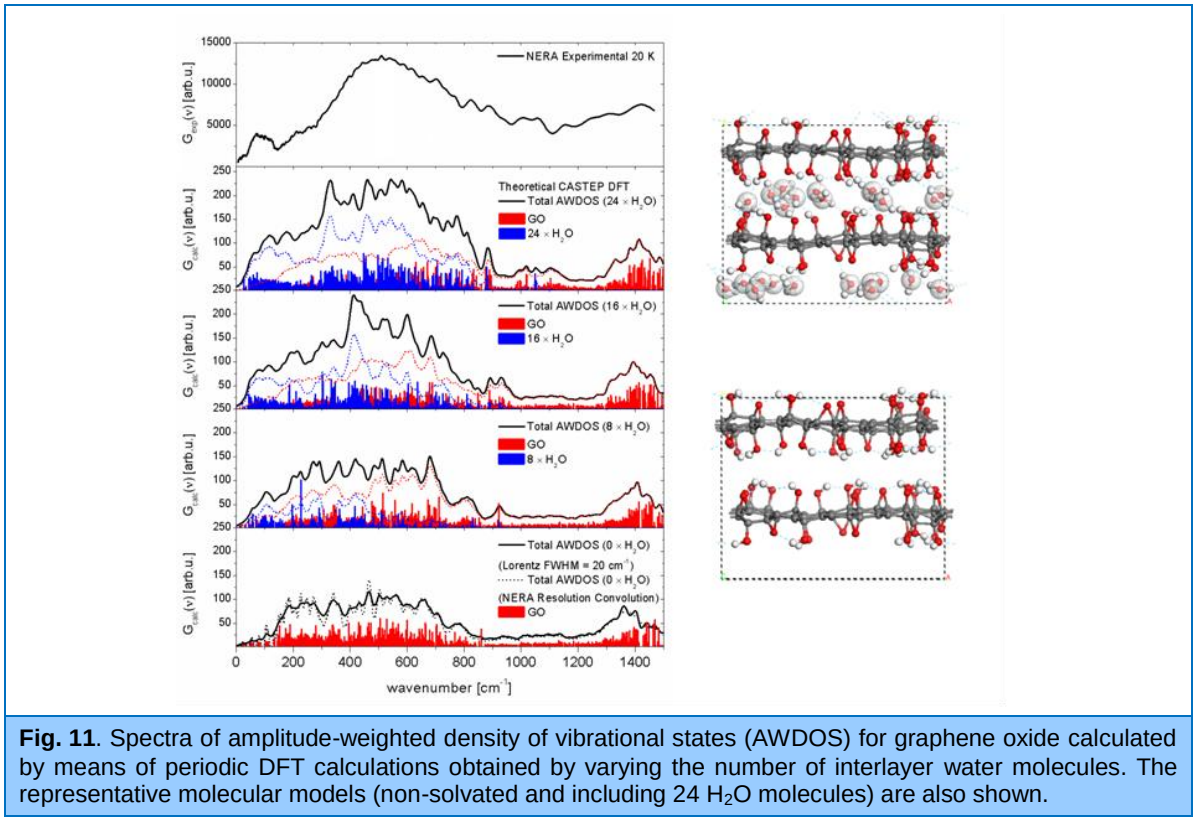

Fig. 11. Spectra of amplitude-weighted density of vibrational states (AWDOS) for graphene oxide calculated by means of periodic DFT calculations obtained by varying the number of interlayer water molecules. The representative molecular models (non-solvated and including 24 H_2O molecules) are also shown.

The wagging modes, as a rule, manifest themselves in the range of > 600 cm^{-1}, whereas the twisting modes are located at < 600 cm^{-1}. The vibrational modes are widely spread below 500 cm^{-1}. The experimental bands arising at ~250 cm^{-1} and ~50-150 cm^{-1}, respectively, can be associated with the translational modes of coordinated water. According to the calculations, the upper band can be attributed mainly to $\nu O^{\cdots}O$ stretching vibrations of water molecules hydrogen-bonded with hydroxyl

groups. The band around ~ 50-150 cm^{-1} may be linked with the visible motions of the centers of masses of water, which are, in turn, strongly coupled with the deformations of the GO structure. The modes formed below 100 cm^{-1} can be attributed to the water transitional modes strongly coupled with the butterfly-like deformations of the GO layers. Finaly, the energetically lowest modes were theoretically found at about 30 and 45 cm^{-1}, respectively. The upper modes can be associated with the so-called 'breathing' motions of the GO framework; which may be described as a fluctuation of the interlayer distance. The lowest vibrations (so-called shearing modes) correspond to the parallel translations of the layers. These motions show up as a band observed experimentally at 30 cm^{-1}. The analysis allowed a satisfactory qualitative description of the corresponding inelastic scattering spectrum (determined mainly by the interlayer water molecules), which confirms the correctness of the Lerf-Klinowski model.

On the DIN-2PI spectrometer the inelastic coherent neutron scattering from liquid gallium was investigated at an initial neutron energy E_o = 28.7 meV and 7.65 meV and sample temperatures T = 333 K and 533 K (**Fig. 12**). It was found that the dispersion curve in liquid gallium splits into two branches, which is, apparently, due to the presence of two types (metallic and covalent bonding) of particle interaction in this metal. This feature of the particle interaction in gallium is also reflected in the structure of the liquid metal as the asymmetry of the main peak of its structure factor.

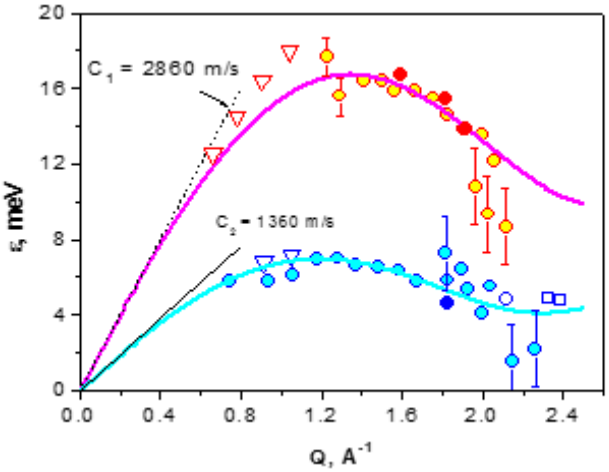

Fig. 12. Dispersion curves in liquid gallium (T = 333 K). The circles show the experimental data obtained on the DIN-2PI spectrometer (open circles – initial neutron energy E_0 = 28.7 meV, full circles – E_0 = 7.65 meV). Open squares show inelastic neutron scattering. Triangles – inelastic scattering of synchrotron radiation. C1 and C2 denote sound velocities for the top and bottom branches of the dispersion curve.

Applied research

Among traditional applied investigations in the NICM Department are the experimental studies of internal stresses and texture of rocks and minerals, determination of internal stresses in bulk materials and products, including engineering materials and components of machines and devices. For the most part, these investigations are carried out using neutron diffraction.

On the FSD diffractometer the experiments on investigations of residual stress distributions in welded joints obtained by various methods of beam welding were continued [15] (**Fig. 13**). Samples for measurements were produced in the Institute of Electronics, BAS (Sofia, Bulgaria) in the form of plates welded by electron-beam (EBW) and laser-beam (LBW) welding. It was found that the residual stress maxima are located not in the centers of the welds, but in a heat-affected zone (HAZ), and the residual stress level decreases rather sharply in regions remote from HAZ. Maximum-largest in both samples is the component of the stress tensor σ_x directed along the weld line and having mainly stretching character. For EBW and LBW samples maximum levels of residual stresses are comparable in magnitude and reach values of 460 and 530 MPa, respectively. Basing on the results of the previous experiments at FSD on residual stresses in witness specimens from nuclear power

plants, it may be noted that the stress level in the specimen LBW is typically high for this type of welding. At the same time, the EBW sample demonstrates a substantially greater level of stresses in comparison with that achieved for witness specimens with electron-beam welding (~ 200 MPa). The results of these measurements point to non-optimal parameters of the electron-beam welding, and, thus, there is a possibility for their improvement and residual stress reduction. Along with it, the results of neutron measurements can serve as a reliable method for diagnostics of the residual stress level.

In addition to the study of residual stresses in these samples, the residual microstrains (**Fig. 13**) were investigated as well. They were derived from the broadening of the diffraction peaks against the instrumental resolution function. The analysis of the behavior of the widths as a function of the interplanar spacing d_{hkl} has shown that the peak broadening is anisotropic and depends on the direction [hkl] in the crystal. This behavior is a typical manifestation of the orientation factor of dislocations in respect to the scattering vector, which allows one to quantitatively assess the density of dislocations in a material under study. In the EBW sample the maximum level of microstrains in the material reaches $2.5 \cdot 10^{-3}$, and the positions of the maxima in the microstrain distribution are in good agreement with the locations of the weld centers. In the LBW sample the maximum level of microstrains is almost twice as high, $4.5 \cdot 10^{-3}$. The obtained experimental data will be used for further model calculations by the finite element method (group of Prof. V.Mikhailov, Brandenburg University of Technology, Germany) and compared with the results of mechanical tests by drilling holes, microhardness measurements and optical studies of the microstructure (group of Prof. P.Petrov, Institute of Electronics BAS, Bulgaria).

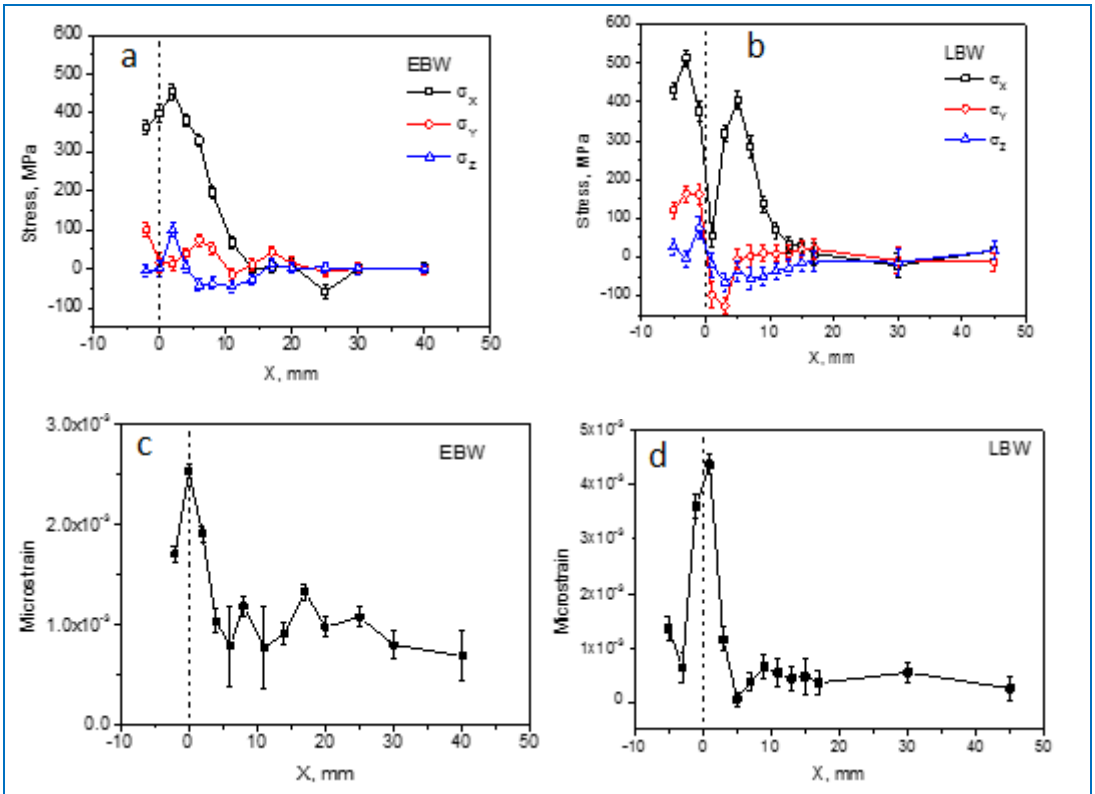

Fig. 13. Residual stress distribution in an S355J2+N steel plate welded by EBW (a) and LBW (b) welding. Residual microstrain distribution in an S355J2+N steel plate welded by EBW (c) and LBW (d) welding.

This will make it possible to study systematically the dependence of the residual stress distribution on the used technology in the welding process and on its parameters for the most widely used engineering materials. Thus, this information can serve as a basis for developing specific technical recommendations to achieve the desired level and profile of residual stresses.

The texture, inner stresses, and stresses under applied load in multiphase polycrystalline samples of granite [16] were studied at diffractometers SKAT and Epsilon (**Fig. 14**). The experiments to study mechanical properties under uniaxial cyclic deformation were carried out in a load range up to 100 kN (150 MPa) and supplemented by a simultaneous acoustic emission analysis.

The obtained values for the inner stresses ranged from -1×10^{-3} to 1.2×10^{-3}. When measuring stresses under the applied load, the z-axis of the cylindrical sample was oriented at an angle of 45° relative to the neutron beam, allowing the simultaneous measurement of components σ_1 and σ_3. The negative stresses along the z-axis are consistent with the Hooke's law, the positive stresses along the x-axis oriented perpendicular to σ_3 are smaller and determined by the Poisson's ratio.

In cooperation with the O.Honchar Dnepropetrovsk National University (Ukraine) a number of samples of ferrite-pearlite wheel steel R7 were studied to determine the effect of modification and thermo-mechanical treatment on the crystallographic texture [17]. The samples were cut out of the rail wheel rims and the transitional zone (between the wheel hub and disk). The texture measurements were carried out using the thermal neutron diffraction technique on the SKAT diffractometer. Three complete pole figures (PF) (200), (110), (211) for α-Fe phase in 5˚×5˚grid were extracted from a set of 1368 (19×72) measured spectra for each sample.

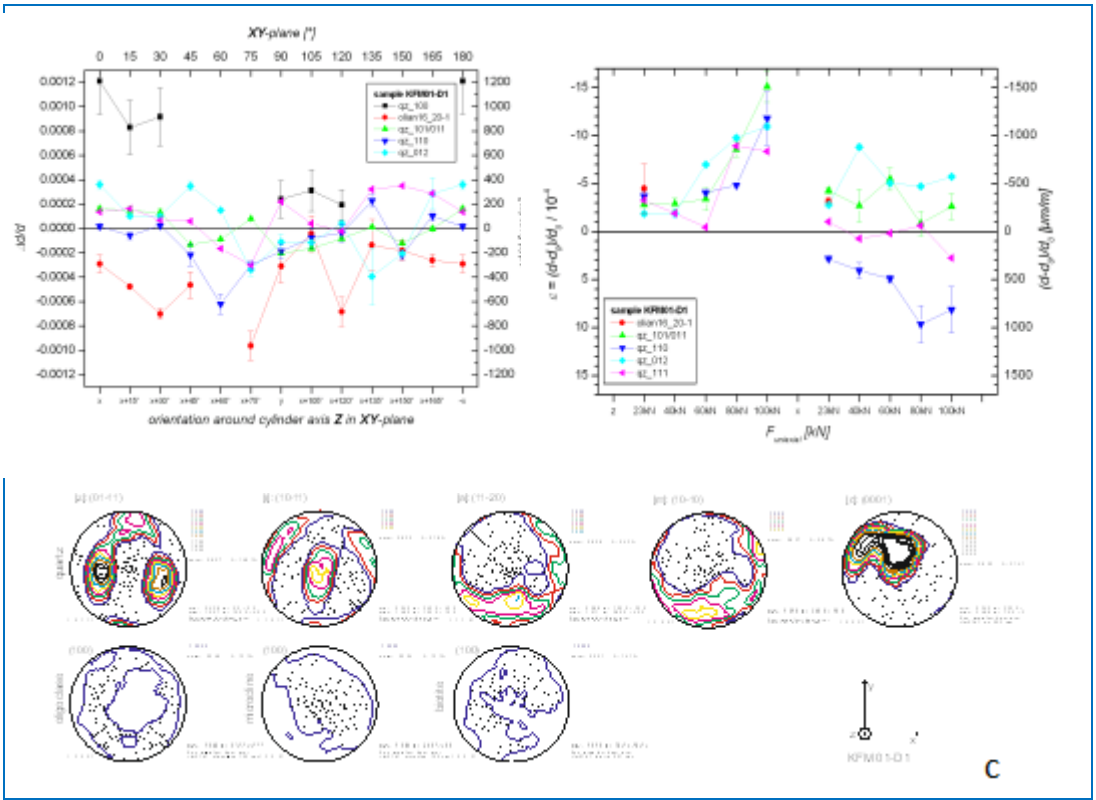

Fig. 14. a) Inner stresses for crystallographic planes of quartz (10-10), (10-11)/(01-11), (11-20), (01-12), 11-21) and oligoclase (20-1). b) Stresses under the action of the applied load for crystallographic planes of quartz (10-10), (10-11)/(01-11), (11-20), (01-12), 11-21) and oligoclase (20-1). c) Pole figures characterizing the texture of quartz, oligoclase, microcline and biotite.

1. SCIENTIFIC RESEARCH

Using the measurement data, the texture components of the deformation and recrystallization corresponding to the technological procedures in the wheel manufacturing process were determined even for very weak textures. It has been concluded that for the samples from the rim the introduction of a modifier in the alloy causes a change in the weak preferred orientation. The reorientation of the texture component during annealing can be explained by secondary recrystallization processes and phase transitions in steel. The changes in the scattering of the texture components in the modified samples are associated with the introduction of the modifier as well as with some differences in the heat treatment modes that were applied to the experimental and conventional steels. Despite the weak character of the texture, the rolling texture components (Δ symbols in Fig. 15) and recrystallization components (• symbols in Fig. 15), characteristic for bcc structure materials, were determined, which confirms the high potential of the SKAT diffractometer (**Fig. 15).**

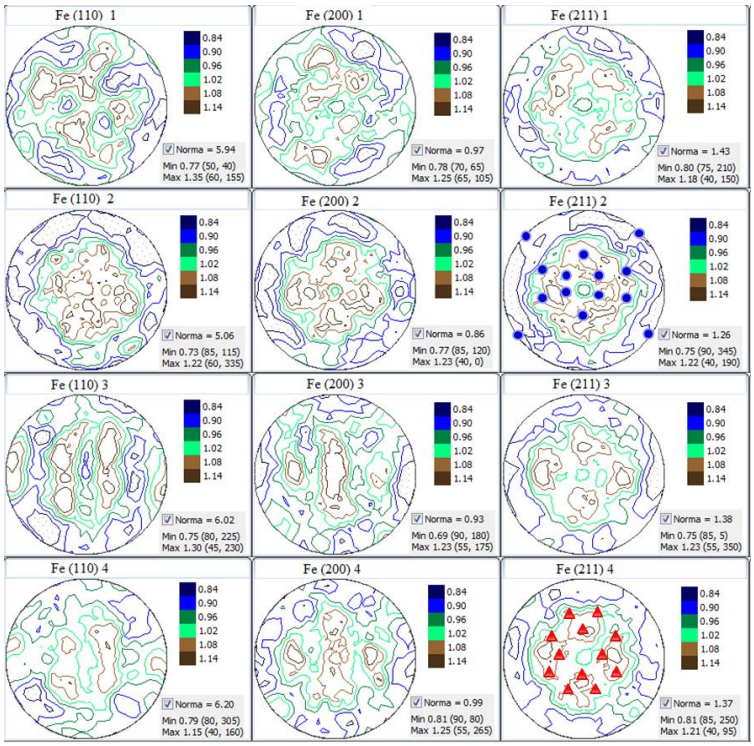

Fig. 15. Changes in the crystallographic texture in the modified samples of wheel steel after heat treatment. Pole figures for α-Fe (110), α-Fe (200) and α-Fe (211) are shown.

II. Instrument development

Work to develop the final configuration of the new DN-6 diffractometer was carried out. In cooperation with the SC Department the construction of a second ring-shaped detector consisting of 96 independent helium counters is in progress. The first successful methodological experiments on neutron diffraction in diamond anvil cells with Fe_3O_4 magnetite samples were conducted at pressures of up to 23 GPa (**Fig. 16**). Also, work was carried out on further development of the technique of the neutron experiment using high-pressure sapphire anvil cells. The accessible pressure range was extended up to 12 GPa by reducing the working area of the anvils down to 1 mm.

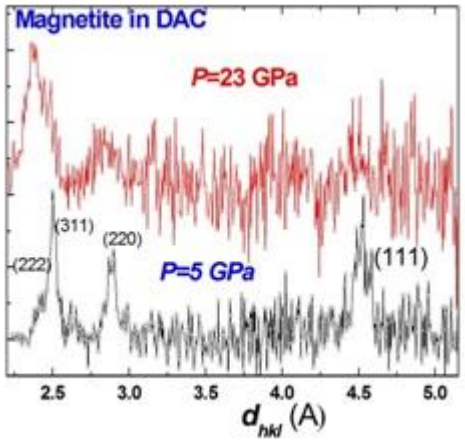

Fig. 16. Neutron diffraction spectra of Fe_3O_4 magnetite obtained using diamond anvil cells at the DN-6 diffractometer at pressures of 5 and 23 GPa.

In 2014, work was carried out on the preparation of the GRAINS reflectometer for operation within the framework of the user policy program. The GRAINS reflectometer was included in the list of facilities available to the IBR-2 users, and the description of the setup was posted on the FLNP website. Specialized liquid cells (**Fig. 17**) were developed and tested for studying liquid/air and liquid/solid interfaces. A universal holder for performing measurements with solid samples was created. An automatic movable platform for the detector (**Fig. 17**) was installed in its working place and tested. In the framework of the development of new coatings for neutron optical devices the experiments were performed to study the oxidation effect on the structure of thin films on glass substrates.

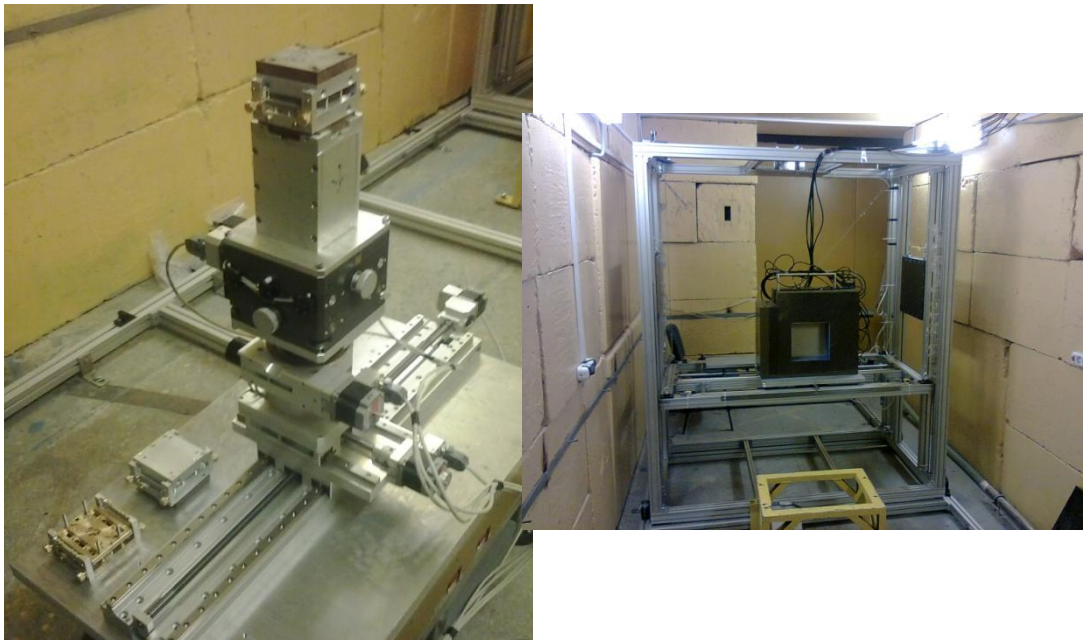

Fig. 17. Sample table with a liquid cell (left) and automatic movable platform for the detector (right).

The implementation of the project aimed at constructing a new diffractometer on beamline 6a for neutron diffraction studies of transition processes in real time was continued. A background shield was manufactured and installed for the diffractometer detector system (ring-shaped detector in the

axial geometry for backscattering angles, two modules comprising eight point counters for medium scattering angles and a module consisting of eight counters for small scattering angles). New preamplifiers were installed on the point detectors. A thermostat covering a temperature range from –40°C to +100°C was put into service and first measurements with model biological membranes were carried out.

The development of a prototype of the spectrometer for neutron radiography and tomography on beamline 14 (**Fig. 18**) continued. A HUBER goniometer with translational and rotational degrees of freedom was installed in working position. First tomography experiments with different types of objects were conducted (**Fig. 19**). The procedure of 3D-reconstruction of the internal structure of objects using a variety of software packages was optimized. The obtained results showed a good quality of the acquired data which is comparable to that achieved in other world neutron centers.

Fig. 18. Spectrometer for neutron radiography and tomography on IBR-2 beamline 14.

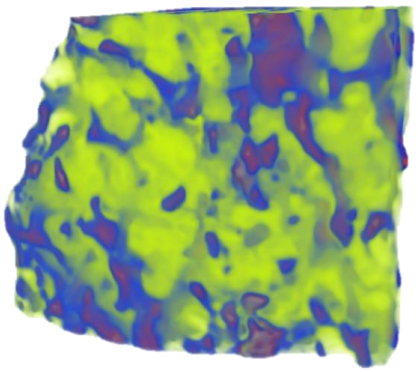

Fig. 19. Neutron tomographic image of the meteorite Seymchan showing the distribution of Fe-Ni alloy and fraction of rocks (mainly olivine).

In 2014, the 4-th element (out of 7 planned) of ZnS-based 90°-detector ASTRA_Right with wavelength-shifting optical fiber readout was installed on FSD in cooperation with the specialists from the SC Department. By the end of 2014 the final geometric alignment of this element on FSD and adjustment of operating parameters of the detector are to be performed. Thus, the continuation of work on the extension of the multi-element detector system of FSD will significantly enhance the detector solid angle.

The work was continued on the introduction of list-mode data acquisition electronics into regular operation. In 2014, at the FSD diffractometer during the experiments in cycles №6 (October, water moderator mode) and №7 (November, cryogenic moderator mode) the list-mode analyzer was tested in the regime of real continuous operation. The comparative analysis of spectra recorded in parallel by the "old" and new list-mode analyzer has shown their identity. In addition, the acquisition of data from all elements of 90°-detectors ASTRA with the subsequent application of electron focusing made it possible to enhance the efficiency of the experiment by a factor of 3.

A new analyzer was also installed on HRFD and first experiments were conducted with comparative simultaneous measurement of diffraction spectra using the existing DSP-based analyzer and the new list-mode analyzer. High-resolution spectra were extracted from the list-mode data using the developed algorithm and compared with the DSP-spectra. The comparison has shown that the spectra are identical (**Fig. 20**), which is indicative of the correct operation of the new electronics and

the developed algorithms for obtaining diffraction spectra from "raw" data. The problem that needs to be solved is insufficient data processing speed at the available computation power. At present, the equipment is being purchased and algorithms are being developed, which will allow an increase in the processing speed of at least ~100 times.

On IBR-2 beamline 13 the development of the Fourier diffractometer FSS was continued in cooperation with the SC Department. In 2014, the design study for the installation of the diffractometer was completed. At present, the construction of biological shielding and installation of necessary technological equipment have mainly been completed. In addition, on FSS a steel collimator was installed in the embedded tube of the beamline to reduce the radiation load on the neutron guide; 1st section of the mirror neutron guide and a Fourier-chopper with a table were assembled and installed.

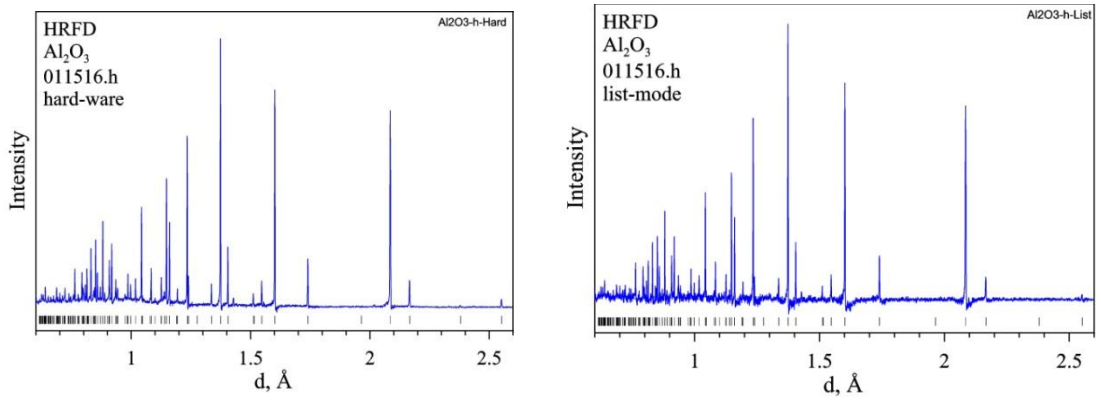

Fig. 20. Comparison of the diffraction spectra measured on HRFD using DSP-analyzer (left) and list-mode-analyzer (right). One can see the similarity of the spectra and identical relative intensities of the diffraction peaks. Slightly enhanced background in the case of the list-mode analyzer is connected with non-optimal (increased) strobe pulse width.

For the REMUR reflectometer a sample module for experiments in an alternating magnetic field with a frequency of 10-60 MHz and a magnetic system of a wide-aperture polarization analyzer designed for operating with a two-dimensional PSD (**Fig. 21**) were manufactured.

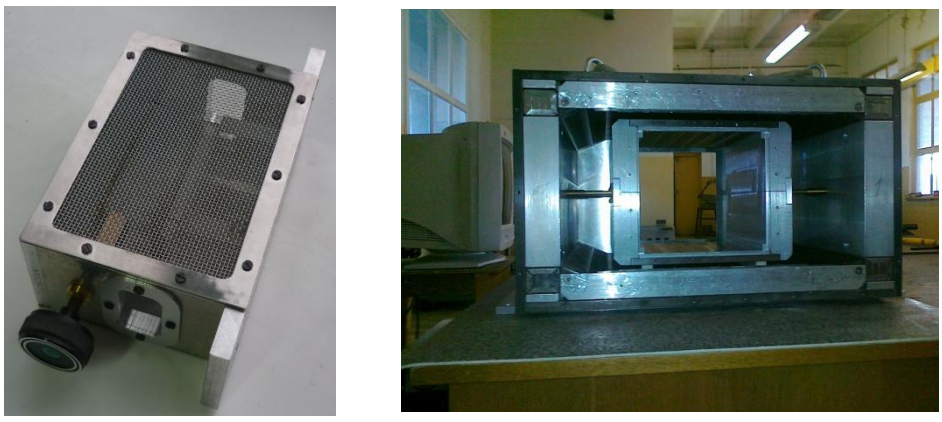

Fig. 21. A sample module for experiments in an alternating magnetic field with a frequency of 10-60 MHz (left) and a magnetic system of a wide-aperture polarization analyzer (right) of the REMUR reflectometer.

1. SCIENTIFIC RESEARCH

In order to evaluate the possibilities of different methods of microstructural characterization based on the analysis of data obtained at the HRFD TOF-diffractometer, the experiments with a set of niobium carbide NbC_y powders, y ≈ 0.93 (cubic lattice), with various mean crystallite sizes in a range of 100-2500 Å, were performed [18]. The additional experiments were carried out on the HRPT high-resolution diffractometer with a monochromatic neutron beam in PSI (Switzerland). The combined data analysis was performed using the classical Rietveld and Williamson-Hall methods and with the application of the Whole Powder Pattern Modeling (WPPM) technique. The samples of niobium carbide $NbC_{0.93}$ with different mean crystallite sizes were obtained by high-energy milling of an initial coarse grain powder during various periods of time, which are indicated in the sample names as NbC-n, where n = 0, 1, 5, 10, 15 is the milling time in hours. Some powder diffraction spectra of NbC-n measured on HRFD are shown in **Fig. 22**. The treatment of the diffraction spectra of the milled samples by the Rietveld method revealed the presence of two fractions with very different widths of the peaks and biased peak maxima. In the analysis of the widths of the diffraction peaks the classical Williamson-Hall method was used which implies the analysis of the dependence of "half-width" (full width at half maximum, FWHM) or integral peak widths as a function of a scanned variable in the diffraction spectra.

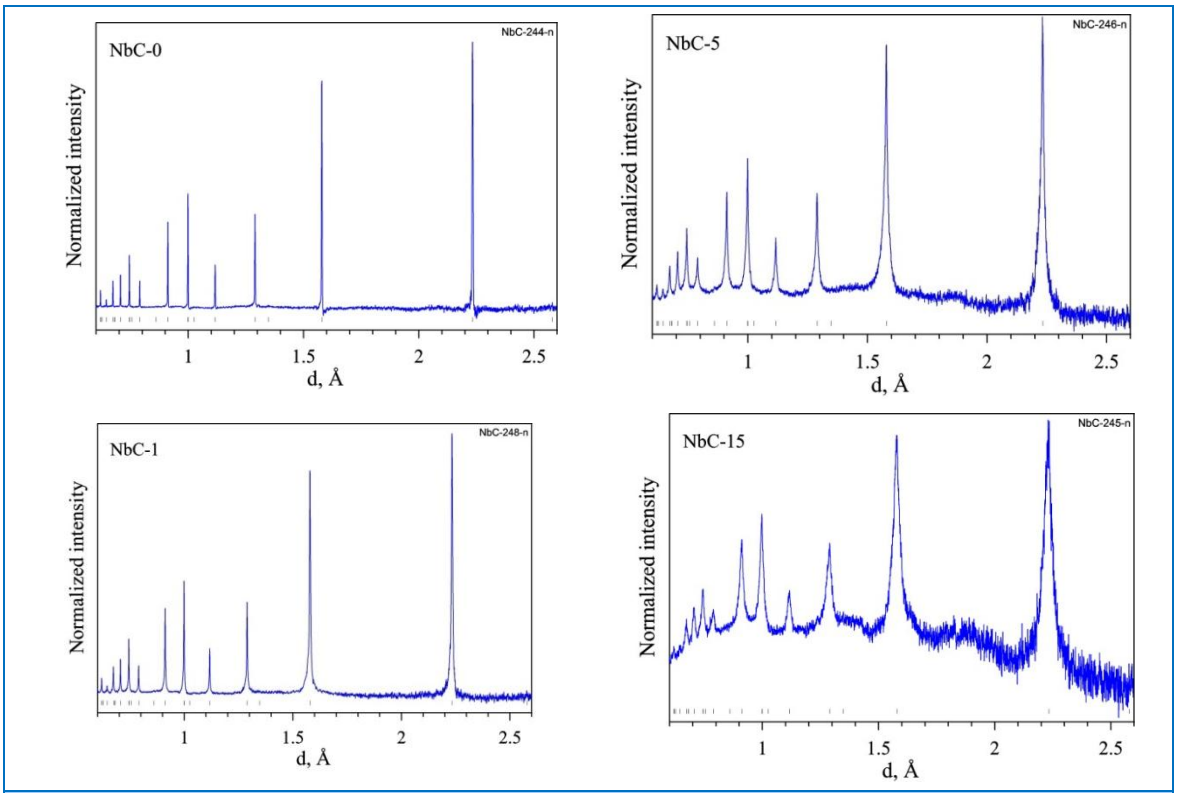

Fig. 22. Normalized powder diffraction spectra of NbC-n, n = 0, 1, 5, 15 measured at HRFD. The peak width and the incoherent background increase with increasing milling time. After 5- and 15-hour milling a broad peak at d ≈ 1.9 Å appears, which is associated with the formation of an amorphous phase and the formation of a low order in it. The vertical lines show the calculated peak positions.

The dependence $W^2(d^2)$ for the initial powder NbC-0 is shown in **Fig. 23**, where the contribution of the HRFD resolution function to the peak width is given as well. For polycrystalline powders NAC and Al_2O_3 this dependence is linear, whereas the experimental points for NbC-0 is better described by a parabola, which corresponds to L ≈ 2550 Å. The main difference of this depenedence for NbC-0 from the resolution function is associated with the presence in the powder of

microstrains at a level of $\varepsilon \approx 1 \cdot 10^{-3}$. The same dependence for the milled powders showed that the experimental data cannot be described by a single curve, since there is a significant scatter of the experimental points. This effect can be attributed to the manifestation of the strong microstrain anisotropy, i.e. the dependence of the peak broadening on a specific set of Miller indices.

The implementation of the WPPM method in the PM2K software package allows one to process neutron data from a diffractometer with a monochromatic beam. Spectra obtained on a TOF-diffractometer including HRFD can be processed but without regard for correct weights of experimental intensities. Nevertheless, PM2K was probed in the analysis of the data for powders NbC-0 and NbC-10 which were obtained on HRFD and HRPT. When calculating the profiles of the diffraction peaks the crystallite size distribution and the presence of some dislocation density were taken into account in addition to the resolution function effect. The size distribution of the lognormal type was used. For NbC-0 the calculated mean crystallite size, $\langle L \rangle_V$ = 2230 Å, is close to the value of L = 2550 Å determined by the Williamson-Hall method. For the NbC-10 powder the values $\langle L \rangle_V$ = 169 Å and 142 Å were obtained according to the HRPT and HRFD data, respectively; the corresponding lognormal distributions are shown in **Fig. 22**. This means that the processing of HRFD data even without considering correct weights allows one to obtain reasonable results.

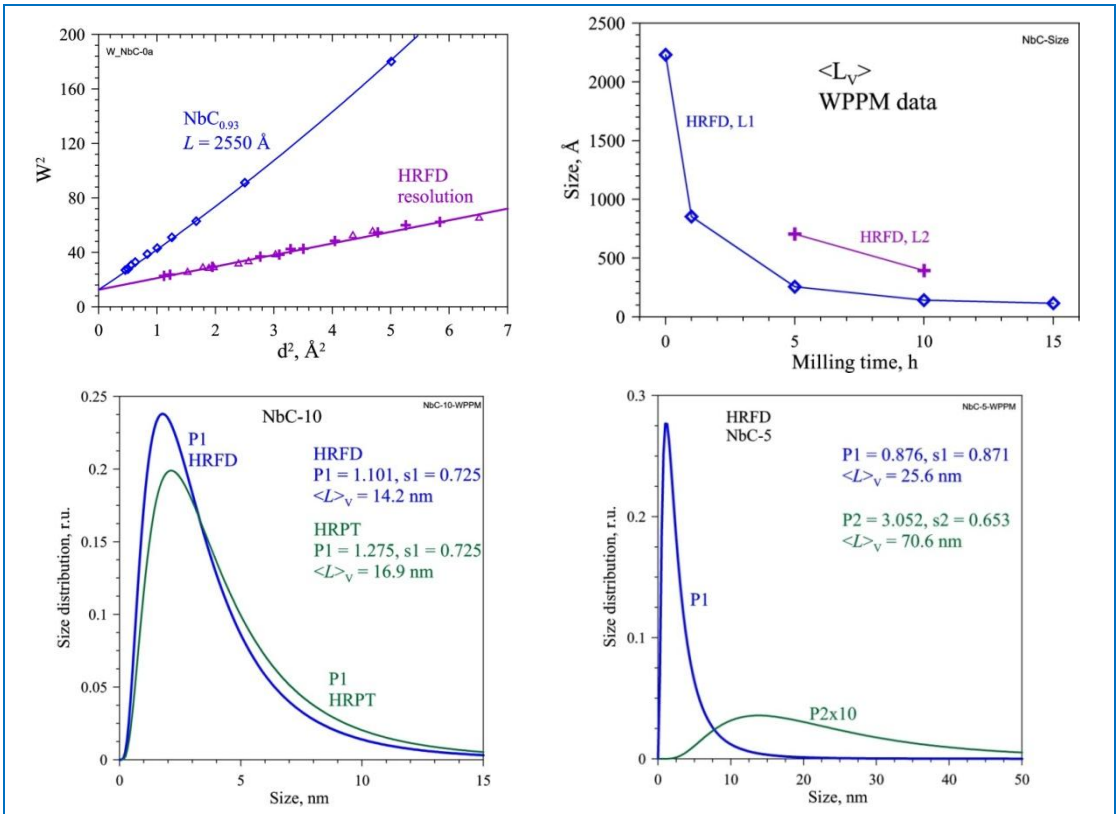

Fig. 23. (a). Dependence $W^2(d^2)$ for the initial powder NbC-0 (blue diamonds) and contribution to the peak width of the resolution function of HRFD (bottom line) determined from the spectra of standard powders NAC and Al_2O_3 (crosses and triangles). Dependences $W^2(d^2)$ for NAC and Al_2O_3 are linear, which is indicative of the fact that there is no size effect. The size effect (L ≈ 2550 Å) manisfests itself in the dependence for NbC-0. (b) The milling time dependence for characteristic crystallite sizes (regions of coherent scattering) obtained by the WPPM method for the F1 fraction (all samples) and F2 fraction (NbC-5 and NbC-10). (c) The log-normal size distribution of crystallites in the main phase for NbC-10, calculated from the diffraction data obtained on HRFD and HRPT. The diffraction sizes are 14 and 17 nm, respectively. (d) The log-normal size distribution of crystallites in NbC-5 obtained from the diffraction data measured on HRFD. Two fractions with different distribution parameters corresponding to the diffraction sizes of 256 Å and 706 Å are determined

1. SCIENTIFIC RESEARCH

On the REFLEX reflectometer the influence of an oxide layer in titanium films covering polarizing supermirrors on their polarizing efficiency was investigated (**Fig. 24**)**.** The top layer of titanium is designed to protect the layers of cobalt and iron (the basis of supermirrors) from oxidation. Along with it, an oxide layer with an approximately zero SLD forms on the very titanium film. Thus, the titanium oxide layer has not only a protective function, but becomes practically transparent to thermal neutrons without impairing the reflective properties of the supermirror. On the REFLEX reflectometer the reflection coefficients for two neutron spin states were measured for a series of samples with different thicknesses of the oxide layer. The experimental results are currently being processed; the corresponding publication is under preparation.

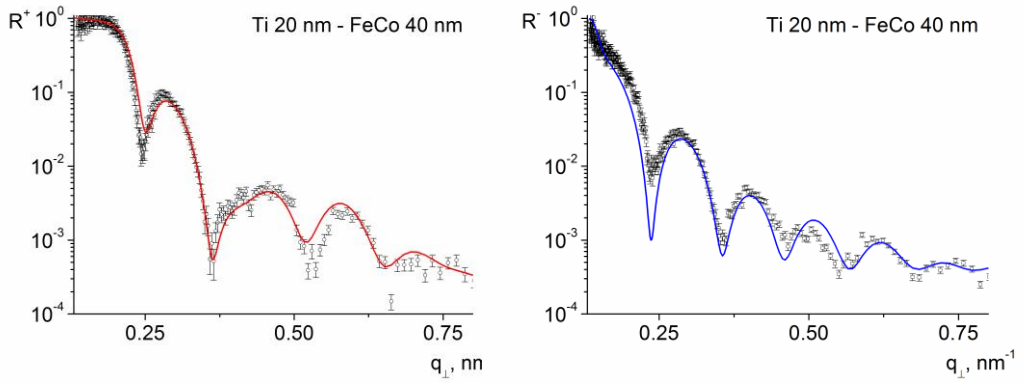

Fig. 24. Reflection coefficients of polarizing films coated with a titanium oxide layer for two neutron spin components.

The simulation of experiments on spin-echo small-angle scattering from perfect uniform spheres a few tens of nanometers in diameter was performed using the VITESS software package. The scheme of the spin-echo spectrometer implemented in the VITESS package corresponded to the spin-echo instrument on beamline 9 of the IBR-2 reactor. The scattering curves obtained from the Monte Carlo simulations are in satisfactory agreement with the theoretical calculations (**Fig. 25**).

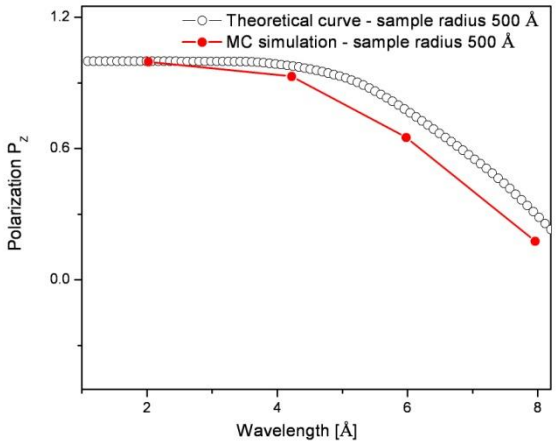

Fig. 25. Dependence of the neutron beam polarization after passing the second arm of the spin-echo spectrometer in scattering by perfect spheres 50 nm in diameter. The red curve corresponds to theoretical calculations, the black one shows the results of the Monte Carlo simulation of the experiment in the VITESS package.

On the REMUR reflectometer the experiments to obtain a set of neutron microbeams with different wavelengths and intensity distribution over the scattering angle for the resonances n = 0, 1, 2 at the grazing angles of the incident beam of 2.55, 3.27, 5.82 and 6.92 mrad were performed

(**Fig. 26**). A three-layer structure (planar waveguide) converts a conventional collimated neutron beam about 0.1 mm into a narrow divergent neutron microbeam about 0.1 μm wide. Such a narrow probe makes it possible to scan local microstructures with high spatial resolution. Neutrons fall on to the surface of the film, penetrate the waveguide layer, propagate along the film in the waveguide layer (channelling) and come out of the end side as a narrow strip. The divergence of the microbeam in this case is determined by the conditions of Fraunhofer diffraction from a narrow slit. Inside the waveguide one can observe the phenomenon of resonant amplification of neutron density followed by the generation of neutron standing waves. Therefore, the microbeam at the output of the waveguide has a narrow wavelength distribution around the resonant wavelength. At steady-state neutron sources the wavelength is fixed and limited to the value of about 4 Å, and at pulsed sources the wavelength of the microbeam can be changed by varying the grazing angle of the incident beam. The obtained experimental data are in agreement with the theoretical predictions. Using the time-of-flight method the waveguide can be easily tuned to any required wavelength of the microbeam including wavelengths above 4 Å. And by selecting certain intervals of the scattering angle one can simultaneously register several microbeams.

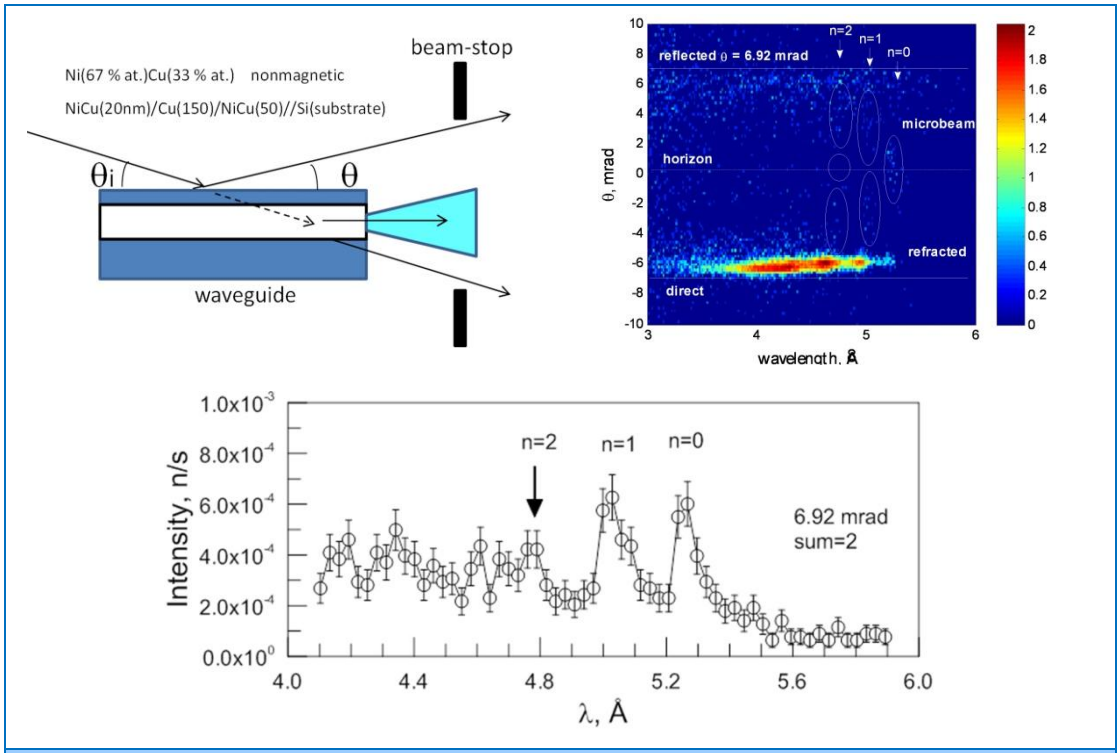

Fig. 26. Scheme of the experiment to obtain neutron microbeams (a). Distribution of scattered neutron intensity over the scattering angle and wavelength (b, c).

References

1. Kozlenko D.P., Kichanov S. E., Lukin E. V., Dang N. T., Dubrovinsky L. S., Liermann H.-P., Morgenroth W., Kamynin A. A., Gridnev S. A., Savenko B. N., Pressure-induced polar phases in relaxor multiferroic $PbFe_{0.5}Nb_{0.5}O_3$. (2014) Physical Review B, v. 89, p. 174107 (1-7).
2. Burzo E., Vlaic P., Kozlenko D.P., Kichanov S.E., Dang N.T., Rutkauskas A.V., Savenko B.N., Magnetic properties, electronic structures and pressure effects of $Ho_xY_{1-x}Co_2$ compounds. (2014) Journal of Alloys and Compounds, v. 584, pp. 393–401.

1. SCIENTIFIC RESEARCH

3. Kozlenko D.P., Burzo E., Vlaic P., Kichanov S.E., Rutkauskas A.V., Savenko B.N., Sequential Cobalt Magnetization Collapse in $ErCo_2$: Beyond the Limits of Itinerant Electron Metamagnetism. (2014) Scientific Reports, in consideration.
4. Melníková L. , Petrenko V.I. , Avdeev M.V. , Garamus V.M. , Almásy L., Ivankov O.I. , Bulavin L.A. , Mitróová Z., Kopčanský P., Effect of iron oxide loading on magnetoferritin structure in solution as revealed by SAXS and SANS. (2014) Colloids and Surfaces B, in press.
5. Kopcansky P., Siposova K., Melnikova L., Bednarikova Z., Timko M., Mitroova Z., Antosova A., Garamus V.M., Petrenko V.I., Avdeev M.V., Gazova Z., Destroying activity of magnetoferritin on lysozyme amyloid fibrils. (2014) Journal of Magnetism and Magnetic Materials, in press.
6. Melnikova L., Petrenko V.I., Avdeev M.V., Ivankov O.I., Bulavin L.A., Garamus V.M., Almásy L., Mitroova Z., Kopcansky P., SANS contrast variation study of magnetoferritin structure at various iron loading. (2014), Journal of Magnetism and Magnetic Materials in press.
7. Petrenko V.I., Avdeev M.V., Garamus V.M., Bulavin L.A., Kopcansky P., Impact of polyethylene glycol on aqueous micellar solutions of sodium oleate studied by small-angle neutron scattering. (2014) Colloids and Surfaces A, accepted.
8. Prylutskyy Yu.I., Petrenko V.I., Ivankov O.I., Kyzyma O.A., Bulavin L.A., Litsis O.O., Evstigneev M.P., Cherepanov V.V., Naumovets A.G., Ritter U.. On the origin of C60 fullerene solubility in aqueous solution. (2014) Langmuir v.30, p. 3967−3970.
9. Tomchuk O.V., Bulavin L.A., Aksenov V.L., Garamus V.M., Ivankov O.I., Vul' A.Ya., Dideikin A.T., Avdeev M.V., Small-angle scattering from polydisperse particles with a diffusive surface.(2014) Journal of Applied Crystallography, v.47, p.642–653.
10. Tatarskiy D.A., Petrenko A.V., Vdovichev S.N., Udalov O.G., Nikitenko Yu.V., Fraerman A.A., Nonreciprocal transmission of neutrons through the noncoplanar magnetic system. (2014) Physical Review Letter, submitted.
11. Киселев М.А., Земляная Е.В., Жабицкая Е.И., Аксенов В.Л., Исследование однослойных везикул ДМФХ в водных растворах сахарозы методами малоуглового рассеяния нейтронов и рентгеновских лучей. (2015) Кристаллография, т. 60, №1, с.140-150.
12. Schmelzer J.W.P., Tropin T.V., Kinetic criteria of glass-formation, pressure dependence of the glass-transition temperature, and the Prigogine-Defay ratio. (2014)Journal of Non-Crystalline Solids, (in press).
13. Tropin T.V., Schulz G., Schmelzer J.W.P., Schick C., Heat ca pacity measurements and modeling of polystyrene glass transition in a wide range of cooling rates. (2014) Journal of Non-Crystalline Solids, (in press).
14. Drużbicki K., Natkaniec I., Vibrational Properties of Water Retained in Graphene Oxide. (2014) Chemical Physics Letters, v. 600, p.106–111.
15. Bokuchava G.D., Papushkin I.V., Petrov P.I., Residual Stress Study by Neutron Diffraction in the Charpy Specimens Reconstructed by Various Welding Methods. (2014) Comptes rendus de l'Académie Bulgare des Sciences, v. 67, p. 763-768.
16. Scheffzuek C., Ullemeyer K., Vasin R., Naumann R., Schilling F.R. Strain and texture investigations by means of neutron time-of-flight diffraction: application to polyphase gneisses. (2014) In: Holden T.M., Muránsky O. & Hamelin C.J. (Eds.): Mechanical Stress Evaluation by

Neutrons and Synchrotron Radiation VII. Materials Science Forum v. 777, p. 136-141.

17. Lychagina T., Nikolayev D., Sanin A., Tatarko J., Ullemeyer K., Investigation of wheel steel crystallographic texture changes due to modification and thermo-mechanical treatment. (2014) Materials Science and Engineering, Dresden.

18. Курлов А.С., Бобриков И.А., Балагуров А.М., Гусев А.И., Анизотропия деформационных искажений в нанокристаллических порошках нестехиометрического карбида ниобия $NbC_{0.93.}$ (2014) Письма в ЖЭТФ, т. 100,(в печати).

1. SCIENTIFIC RESEARCH

NEUTRON NUCLEAR PHYSICS

In 2014, in FLNP the scientific activity in the field of neutron nuclear physics was carried out in the following traditional directions: investigations of time and space parity violation processes in neutron-nuclear interactions; studies of the fission process; experimental and theoretical investigations of fundamental properties of the neutron; gamma-spectroscopy of neutron-nuclear interactions; atomic nuclear structure, obtaining of new data for reactor applications and for nuclear astrophysics; experiments with ultracold neutrons. The greater part of the fundamental investigations was conducted on the modernized IBR-2 reactor, IREN pulsed resonance neutron source and EG-5 electrostatic generator. Of particular note is the wide range of applied research using NAA. A number of investigations in the field of fundamental physics and ultracold neutron physics were performed on the neutron beams of nuclear research centers in Germany, China, USA, France, Switzerland.

Modernization of the IREN facility

In 2014, the modernization of the IREN facility was continued (**Fig. 27**). Its purpose is the achievement of design parameters of the neutron source (intensity of the order of 10^{13} n/s) by 2016. The project involves the assembling of the second accelerating section, installation of new modulators and replacement of klystrons. By now, two new modulators producing high-voltage pulses with 180 MW pulse power at a repetition rate of up to 120 Hz and two E3730A Toshiba 50MW klystrons have been purchased. The implementation of the project will allow working with a repetition rate of 50 Hz at an electron energy of ~170 MeV, thus providing an average beam power of ~1.5 kW. An additional increase in the neutron yield can be achieved by replacing the tungsten neutron production target with a U-238 target. The installation of the second accelerating section, new RF-power sources and a uranium target calls for a thorough modernization of the engineering infrastructure of the IREN facility, which is currently underway. In 2014 an air-conditioning and ventilation system was installed in the accelerator halls; also, work began on upgrading the power supply system of building 43. Along with these activities in 2014 the IREN facility operated for 1,360 hours for physics experiments.

Fig. 27. Lifting of modulators to the accelerator hall through a specially made opening.

I. Experimental and methodological investigations

Modernization of multi-detector system “Romashka-INRNE”

The multidetector system “Romashka-INRNE” consists of 12 NaI(Tl) detector modules and is designed for measuring neutron cross sections at the IREN facility. The detector system was assembled and installed on IREN beamline №4. Twelve emitter repeaters of signals from photomultipliers of γ-ray NaI(Tl) detectors were manufactured, tested and installed. A series of measurements was performed using standard spectrometric gamma sources SSGS (Cs-137 and Co-60) for different source-detector geometries for experimental and model (analytical) determination of gamma-radiation detection efficiency of non-point sources. The experimental values of the efficiencies were obtained; the determination of the model ones is in progress. Using the computer program FLUKA the (neutron, gamma)-field intensity distribution was calculated in the area of the gamma-spectrometer “Romashka-INRNE” on IREN beamline №4 (**Fig. 28**)

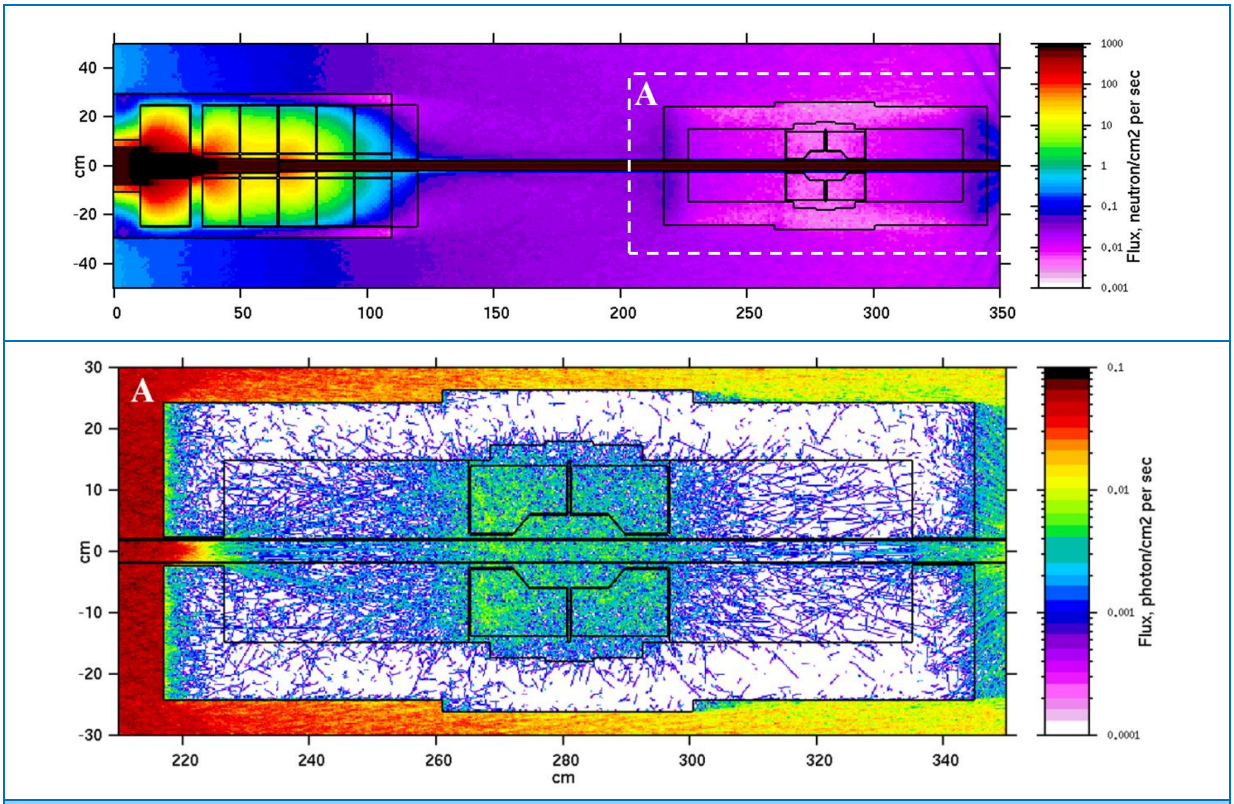

Fig. 28. Intensity of the neutron field in the area of a shielding collimator (SC) of the 12-detector gamma spectrometer “Romashka-INRNE” (top) and of γ-rays in it when a beam of neutrons and γ-rays from the IREN facility falls on the SC input.

Project TANGRA: Development and optimization of the tagged neutron method for elemental analysis and nuclear reaction studies

The multidetector system "Romashka" consisting of 24 hexagonal NaI(Tl) crystals was tested using γ-rays from inelastic scattering of 14-MeV neutrons by carbon, $^{12}C(n,n'\gamma)^{12}C$. A neutron generator ING-27 was used as a source of tagged neutrons. Neutrons are produced in the reaction d + 3H → 4He(3.5MeV) + n(14.1MeV) in which α-particles and neutrons fly apart in almost opposite directions, and therefore, with a knowledge of α-particle momentum direction, the neutron momentum direction can be determined with high accuracy. Thus, neutrons can be tagged using a multichannel

α-detector built into a portable neutron generator, which accelerates deuterons up to energies of 80-100 keV and focuses them on a tritium target. A 64-pixel silicon detector built into ING-27 was used to detect α-particles. The measurement of the time interval between the signals from α- and γ-detectors allows one to determine the distance from the point of neutron emission in the d-t reaction to the point of interaction between the tagged neutron and the nucleus of the substance under study (velocity of 14.1-MeV neutron is 5 cm/ns). Thus, it is possible to determine all three coordinates of the point where characteristic γ-radiation is generated. In the experiment, time and amplitude spectra were measured in coincidence with the signals from the central silicon pixel which corresponds to the neutron cone directed at a graphite target positioned in the center of the detector system "Romashka" (**Fig. 29**).

Fig. 29. Experiment to study inelastic scattering of 14-MeV tagged neutrons by ^{12}C nuclei: 1 - tagged neutron generator ING-27, 2 - polyethylene, 3 - lead, 4 – gamma-detection system "Romashka", 5 - graphite cube.

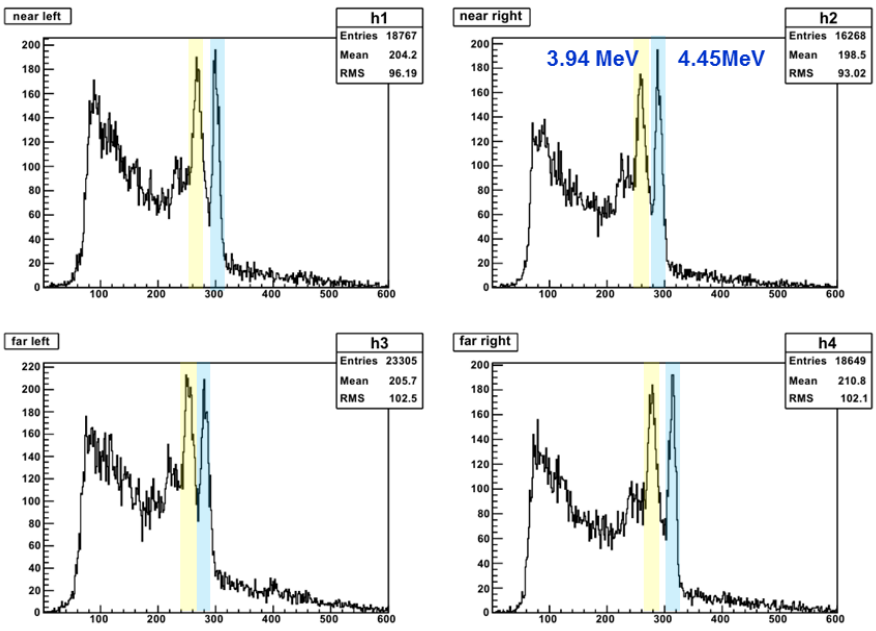

Fig. 30. Amplitude spectra of γ-rays from 4 sections of the "Romashka" setup.

The detectors were shielded from exposure to the direct neutron beam from the generator using a combined collimator made of polyethylene and lead. The experiment has shown that the obtained time and amplitude resolution is sufficient for conducting measurements with the tagged neutron method using the combination of ING-27 + "Romashka". The amplitude spectra of γ-rays from 4 NaI(Tl) sections are presented in **Fig. 30.**

The experimental studies and simulation of the most effective shielding were carried out to reduce the direct neutron flux coming from the generator to gamma- or neutron detectors. An experimental stand was constructed which allows measuring the efficiency of detector shielding using different shielding materials with thicknesses varying from 0 to 50 cm. NaI(Tl), BGO, stilbene crystal and BC-501 liquid scintillators were used as detectors. The last two scintillators allow neutron/gamma pulse shape discrimination. Different combinations of lead, iron and borated polyethylene were tested as shielding materials. The most suitable compositions of the combined shield for the projected experiments were experimentally found to be: 30 cm (Fe) + 10 cm (BPE) + 10 cm (Pb) and 20 cm (Fe) + 10 cm (BPE) + 20 cm (Pb). More detailed results will be published in the journal *Physics of Elementary Particles and Atomic Nuclei, Letters* (in Russian) and an abridged version of the paper will be submitted to *Nucl. Instr. and Methods* (in English). **Figure 31** presents the layout of the experiment and one of the graphs showing the degree of attenuation of 14-MeV neutrons from the generator ING-27 by the combined shield consisting of Fe and Pb layers of different thicknesses.

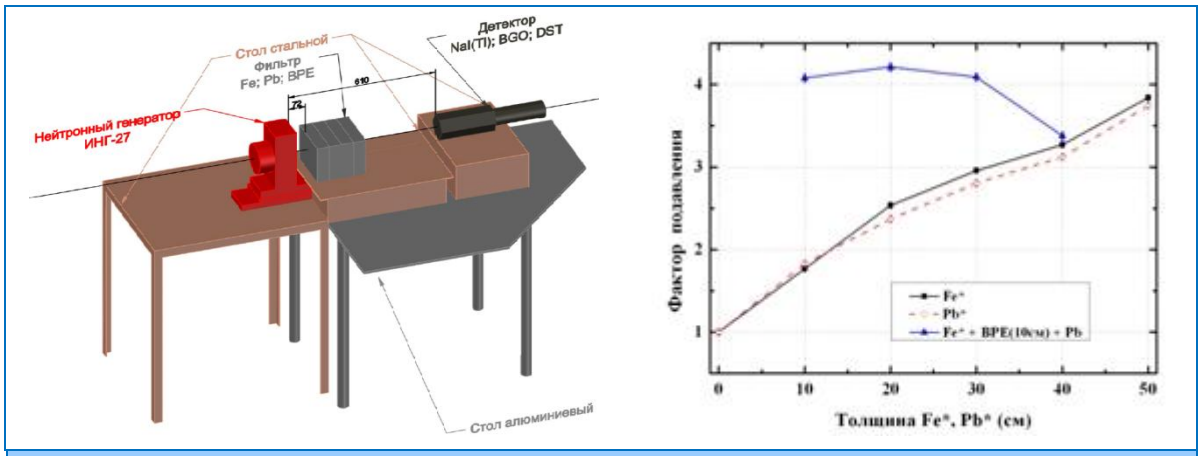

Fig. 31 Left: Layout of the experiment to optimize shielding against 14-MeV neutrons. Right: neutron (and γ-ray) attenuation factor measured with a hexagonal NaI(Tl) detector as a function of the thickness of Fe and Pb layers.

A setup was designed and constructed for measuring the angular distribution of γ-quanta emitted in the inelastic scattering of 14-MeV neutrons by carbon (**Fig. 32**). NaI(Tl) γ-detectors are arranged in the horizontal plane at different angles with respect to the direction of the neutron beam hitting the target. A collimator, which provides maximum shielding of detectors from exposure to the direct neutron beam from the generator was manufactured. The collimator dimensions are minimized to reduce the background from fast neutrons scattered by it. The experiments are planned to be conducted at the end of 2014 - the beginning of 2015.

1. SCIENTIFIC RESEARCH

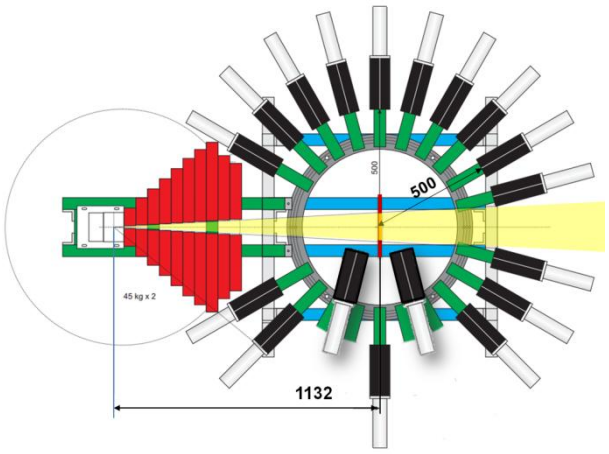

Fig. 32. Layout of the setup for measuring the angular distribution of γ-quanta emitted in the inelastic scattering of 14-MeV neutrons: tagged neutron generator ING-27; combined shield; set of neutron and γ-ray detectors.

Activities on the preparation of the (n,e) scattering experiment

In 2014, the debugging of programs for the 8-channel time encoder and PC-based measuring module of the AURA setup was continued. At the IREN neutron facility the hours-long testing of the operation of the setup (including the control of the turntable and collection of spectra) was carried out [3]. In the course of further testing of the AURA setup four week-long measurement cycles were conducted to measure the anisotropy of slow neutrons with energies in the range of 0.005-10 eV scattered by metallic vanadium, which is used as a calibration sample in condensed matter physics experiments. Each measurement cycle consisted of a series of hour-long exposures with recording of spectra measured by the detectors upon completion of each of them. Since there are four detectors on the turntable and each of them alternately measures the neutron scattering in forward and backward directions (positions of the detectors with respect to the neutron beam change with the turntable rotating through 180° upon completion of each exposure), the anisotropy is calculated as the geometric mean of the ratio of forward/backward counts from all the detectors:

$$R = \sqrt[4]{\frac{(N_s - N_{bg})_{2f}(N_s - N_{bg})_{3f}(N_s - N_{bg})_{1f}(N_s - N_{bg})_{4f}}{(N_s - N_{bg})_{1b}(N_s - N_{bg})_{4b}(N_s - N_{bg})_{2b}(N_s - N_{bg})_{3b}}},$$

where under the radical sign the numerator is the total counts with the subtraction of the background recorded by the detectors in the neutron forward scattering position, and the denominator is the sum of detector counts in the backscattering position. The relative error of the ratio was calculated as

$$\delta R = \sqrt{\sum_1^8 \delta^2 (N_s - N_{bg})}, \text{ where } \delta(N_s - N_{bg}) = \frac{\sqrt{(N_s + c^2 N_{bg})}}{N_s - cN_{bg}} \text{ and } c = \frac{M_s}{M_{bg}}.$$

M_s and M_{bg} – monitor counts with and without a sample, respectively. The results are presented in **Fig. 33**.

The data of [4] are in good agreement with the R(E) relations obtained earlier in the experiments at the IBR-2 reactor and suggest that at neutron energies below 0.1 eV the scattering by vanadium has an anisotropic behavior different from purely kinematic anisotropy of neutron scattering by a free nucleus.

The Monte Carlo calculations are being continued to refine the kinematic correction for the asymmetry of thermal neutron scattering by krypton, which is required for the experiment on the

extraction of a precise n,e-scattering length value from the angular anisotropy of slow neutrons scattered by an inert gas at atmospheric pressure.

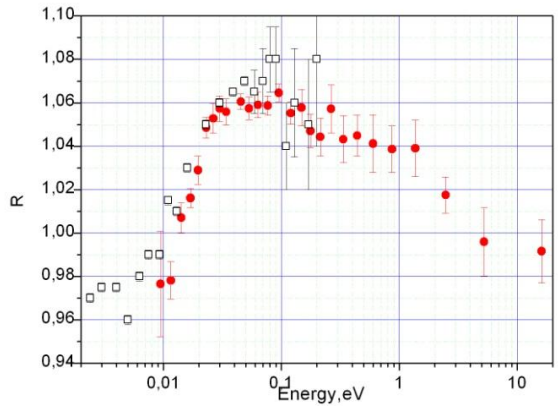

Fig. 33. Averaged R(E) relations from [3] (points) and data obtained in 2004 on IBR-2 beamline 11b (open squares).

Measurement of parameters of polarized neutron beam at the KOLKHIDA setup

In 2014, on IBR-2 beamline №1 on the polarized neutron spectrometer after repeated refitting of in-channel collimators the work was carried out to determine parameters of the polarized neutron beam. The parameters were determined in the neutron energy range of 0.062-2.3 eV using the two-converter method. A polarized neutron beam with polarization P_n = 0.98 was obtained. The layout of the polarized neutron setup is shown in **Fig. 34**. The primary-neutron spectrum is formed in the moderator of the reactor. The neutrons emerging from the moderator go through the channel in the biological shield and pass through primary collimator 1. Prior to entering the analyzer, the neutrons go through Soller collimator *2*. In order to polarize neutrons and to analyze their polarization, we use Co-Fe single crystals.

The intensity and energy spectrum of the primary neutron beam incident on the polarizer were measured using the RM-70 fission chamber. The chamber was placed at a flight distance of 13.5 m. As a result, we obtained data on the neutron intensity and spectrum in an energy range of 10-200 meV (**Fig. 35**). The neutron flux in the specified energy range was $1.0 \cdot 10^6$ n/cm^{2}s.

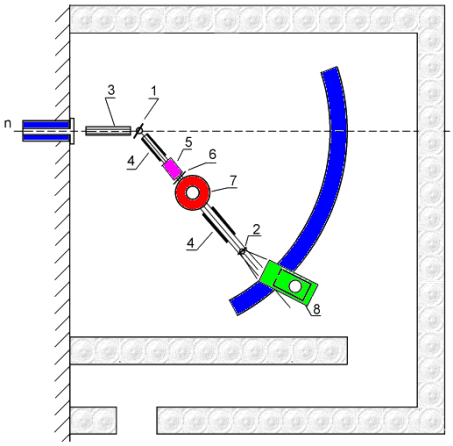

Fig. 34. 1 – primary collimator; 2 – Soller collimator; 3 – polarizer crystal; 4 – guiding field electromagnets; 5 – Mezei flipper; 6 – shim; 7 – cryostat; 8 – analyzer crystal; 9 – detector.

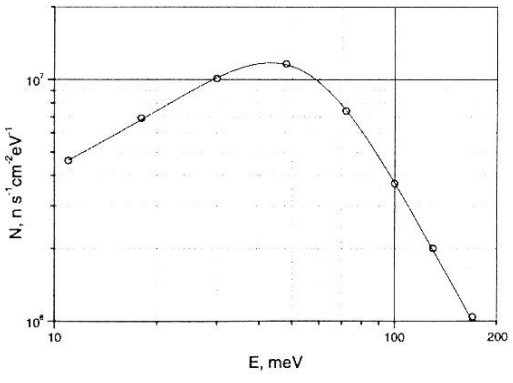

Fig. 35. Dependence of the neutron flux density on the energy of neutrons incident on the polarizer.

1. SCIENTIFIC RESEARCH

For the Co-Fe single crystal, the neutron diffraction was measured in the Laue geometry for different angles θ in a range of 3°-19° at which the incident neutrons hit the (200) surface (**Fig. 36, 37**). The measured values of the neutron wavelengths and energies for the listed angles θ are presented in Table 1. The reflected beam maximum was determined by varying the θ angle. The detector counting rate n_1 and the intensity I_1, which takes into account the detector efficiency and the reflected beam area ($s \cong 4$ cm^2), are given in **Table 1**.

Table 1. Parameters of the polarized neutron beam**.**

Angle θ (deg)	19	12	6	4	3
Wavelength λ (Å)	1,15	0,74	0,37	0,25	0,19
Energy En (eV)	0,062	0,15	0,6	1,3	2,3
Detector counting rate	800	270	65	33	22
after the polarizer n_1 (s^{-1})	430	200	80	60	50
Polarized beam intensity I_1, n/cm^{2}s	70	23	3,1	0,6	0,2
Detector counting rate after the analyzer n_2, s^{-1}	70	23	3.1	0.6	0.2

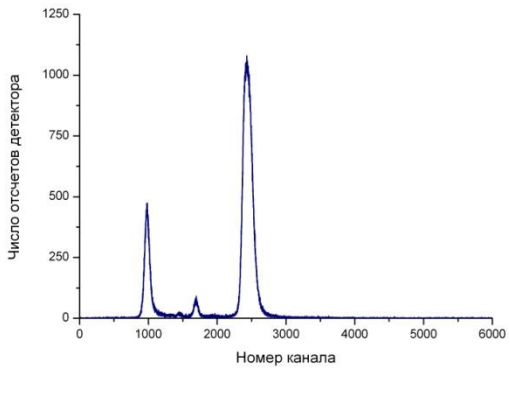

Fig. 36. Time-of-flight neutron spectra after the polarizer obtained for 3 min. θ = 19°.

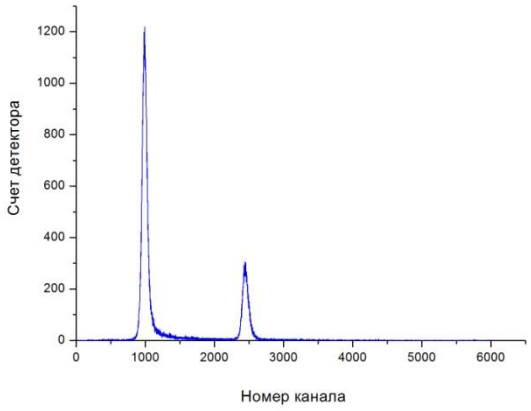

Fig. 37. Time-of-flight neutron spectra after the analyzer obtained for 10 min. θ = 19°.

Observation of transition from Laue diffraction to Bragg diffraction

In the framework of preparation of experiments to investigate the weak neutron-nucleus interaction in neutron diffraction, experimental studies of neutron diffraction by a potassium bromide single crystal were carried out on IBR-2 beamline 1. A potassium bromide single crystal was chosen due to a rather large P-odd effect in the transmission found in the p-wave resonance of bromine-81. In particular, an interesting phenomenon—transition from Laue diffraction to Bragg diffraction—was revealed.

The incident neutron beam had a cross section of 4x40 mm and divergence 4x10^{-3} rad. A plate of cadmium or borated polyethylene was placed in front of the single crystal to shield its side surface from the neutron beam. The similar plate was placed behind the single crystal and covered either its side surface in the Laue neutron diffraction geometry or the end surface when observing the transition

from Laue diffraction to Bragg diffraction. **Figure 38** presents the TOF spectra obtained in two geometries. The simplest explanation for the observed effect is the crystal twinning. To test this hypothesis, the single crystal was rotated through 180 degrees around the scattering vector. **Figure 39** shows the TOF spectra of these measurements.

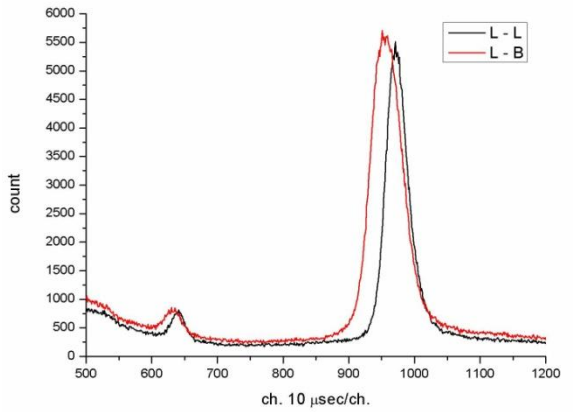

Fig. 38. Black line corresponds to neutron diffraction in the Laue geometry, the red line – transition from Laue diffraction to Bragg diffraction.

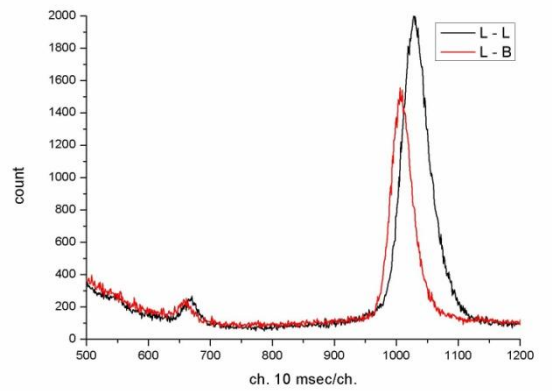

Fig. 39. Single crystal is rotated through 180° around the scattering vector. The black line corresponds to neutron diffraction in the Laue geometry, the red line – transition from Laue diffraction to Bragg diffraction.

One can see that the spectrum character is unchanged. In principle, such an effect can be observed in a deformed single crystal or due to the weak neutron-nucleus interaction. If the single crystal is deformed, by rotating it through 180 degrees around the axis perpendicular to the scattering vector one should expect the opposite peak distribution. The results of these measurements presented in **Fig. 40** support the hypothesis about a deformed single crystal. The same effect is observed in three potassium bromide single crystals produced at different times.

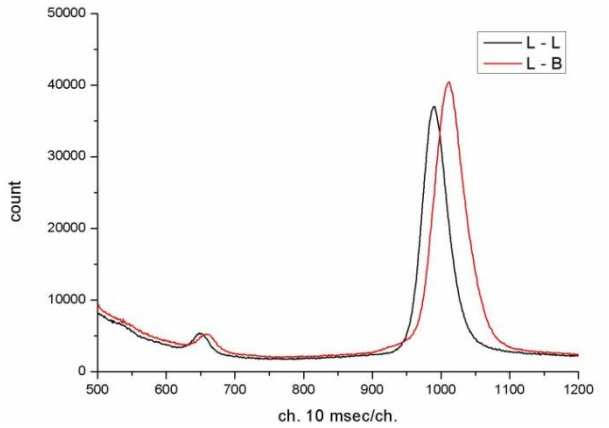

Fig. 40. Single crystal is rotated through 180° around the axis perpendicular to the scattering vector. The black line corresponds to neutron diffraction in the Laue geometry, the red line – transition from Laue diffraction to Bragg diffraction.

Development of techniques for fission physics investigations

Detection of ternary and quaternary spontaneous fission of ^{252}Cf using ΔE-E telescopes based on silicon pixel detector TimePix

In 2014, in cooperation with TU Prague the measurements of ternary and quaternary spontaneous fission of ^{252}Cf were carried out using Timepix detectors. To identify ternary particles, the ΔE-E method was used to separate light charged particles by charge. A thin (12 μm) silicon detector

was used as a ΔE-detector and a TimePix pixel detector with a 300 μm-thick sensor layer – as an E-detector.

The layout of the experimental setup is shown in **Fig. 41**. A spontaneous fission source ^{252}Cf and two assemblies of ΔE-E detectors were placed in a vacuum chamber. Aluminum 31 μm-thick foil was placed between the source and the detector. The foil provided the full absorption of fission fragments and alpha particles from spontaneous alpha decay of Californium (6.2 MeV). Thus, the detectors recorded only long-range light charged particles from ternary fission.

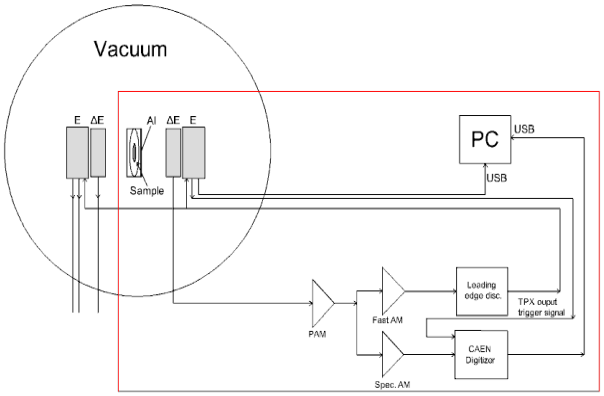

Fig. 41. Layout of the experimental setup.

Figure 42a shows the two-dimensional ΔE-E separation curves of light charged particles. In the experiment we managed to detect particles ranging from hydrogen to beryllium. One can clearly see the most intensive region of alpha particles. The energy spectra were plotted for each type of particles. The preliminary corrections for energy losses in the aluminum foil and ΔE detector were calculated using the Srim program. **Figure 42b** demonstrates the measured energy distribution of alpha particles in the ternary fission of ^{252}Cf in comparison with the published data.

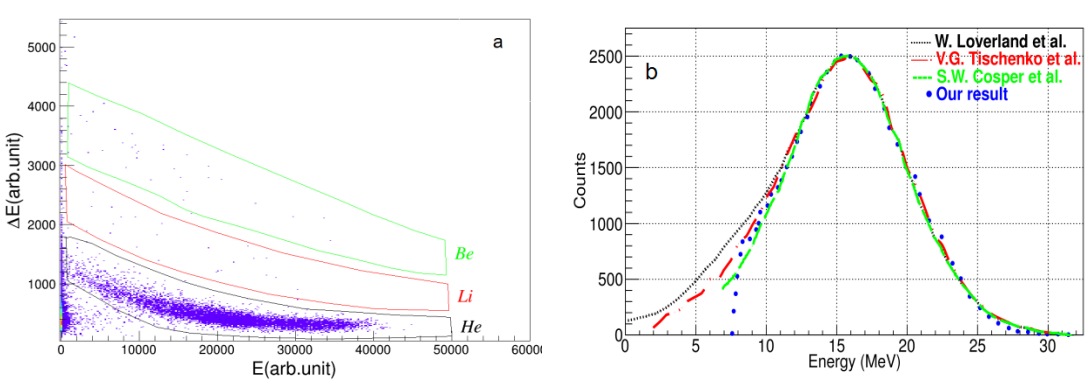

Fig. 42. (a) ΔE-E spectrum of light charged particles. (b) The energy spectrum of alpha particles.

Figure 43 (a, b, c) presents the energy spectra of helium, lithium and beryllium. Each spectrum was fitted with the Gaussian curve and the light charged particle yields were determined. The experiment was also aimed at searching for even more rare fission mode than ternary fission – quaternary fission, when in addition to two main fragments two light charged particles are emitted. The probability of this process is extremely low and reaches 10^{-6}-10^{-7} of the normal binary fission. As a rule, two alpha particles are formed in quaternary fission, and can be emitted either independently

(true quaternary fission), or as a result of decay of an unstable nucleus of ^{8}Be emitted as a third particle (pseudo-quaternary fission).

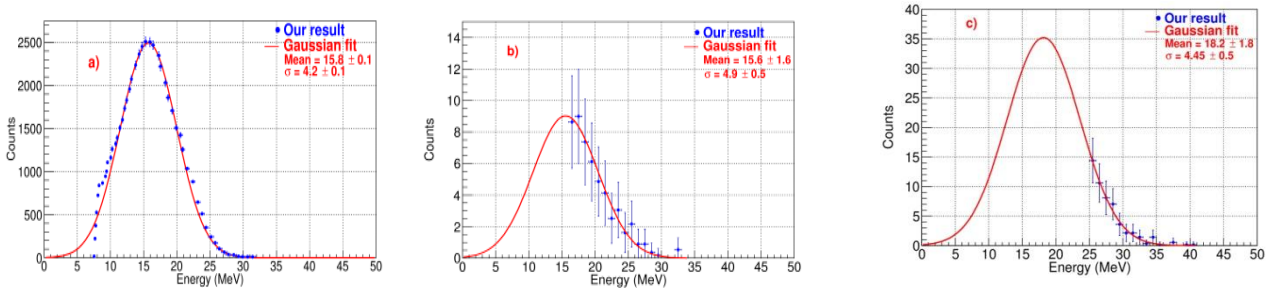

Fig. 43. The energy spectra of light charged particles: (a) He, (b) Li, (c) Be.

Seventy two events were observed, in which two particles were detected simultaneously in one or two telescopes. A symmetrical energy distribution between two particles was observed in 63 events, and an asymmetric distribution – in 9 events. The two groups of events were attributed to α-α and α-t quaternary fission, respectively (**Fig. 44a**). The events in which two α-particles were emitted at a very small angle to each other, were attributed to the pseudo-quaternary fission (decay of unstable short-lived ^{8}Be). Using the measured energies of alpha particles, the energy spectrum of emitted ^{8}Be particles was reconstructed (**Fig. 44b**). Also, the probabilities of true and pseudo-quaternary fission were determined, which are in agreement with the available experimental and theoretical estimates.

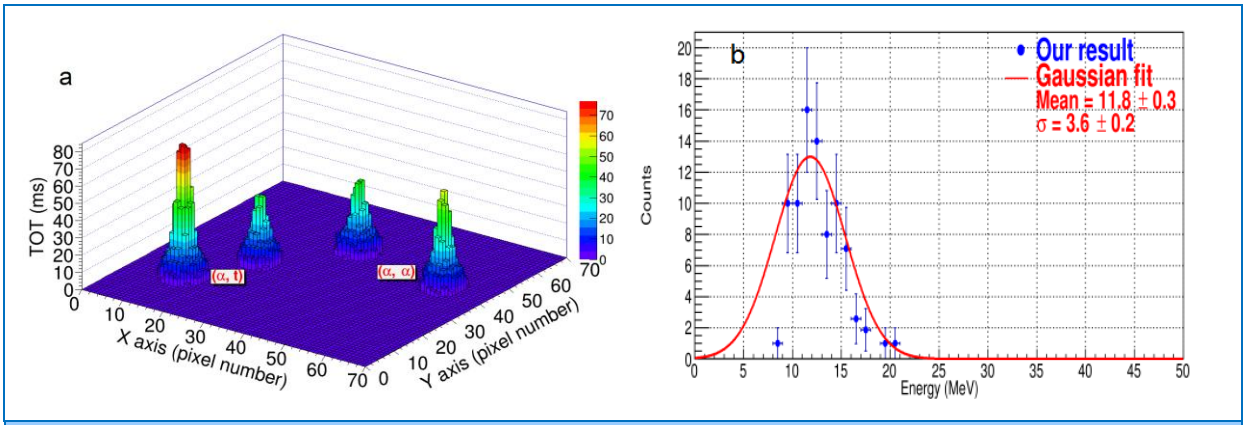

Fig. 44. (a) Examples of clusters for α-α and α-t coincidences; (b) Reconstructed energy spectrum for ^{8}Be.

Position-sensitive chamber for studying prompt fission neutrons

In connection with the development of a position-sensitive double ionization chamber a series of calculations was performed. The calculations of electrostatic fields and simulation of the detector response to fission fragments were made (**Fig. 45**). Formulas to calculate the coordinates of fission fragments in a three-dimensional Cartesian coordinate system were derived. The results of the numerical simulation of the detector have shown that due to the strip-like structure of the chamber anodes, it is possible to abandon the use of a Frisch grid. The DAQ system architecture was developed to acquire data from detectors using a 64-channel system of synchronization and digitization of detector pulses. It was demonstrated that the developed detector may be used for obtaining images of objects in neutron radiography at a pulsed neutron source.

1. SCIENTIFIC RESEARCH

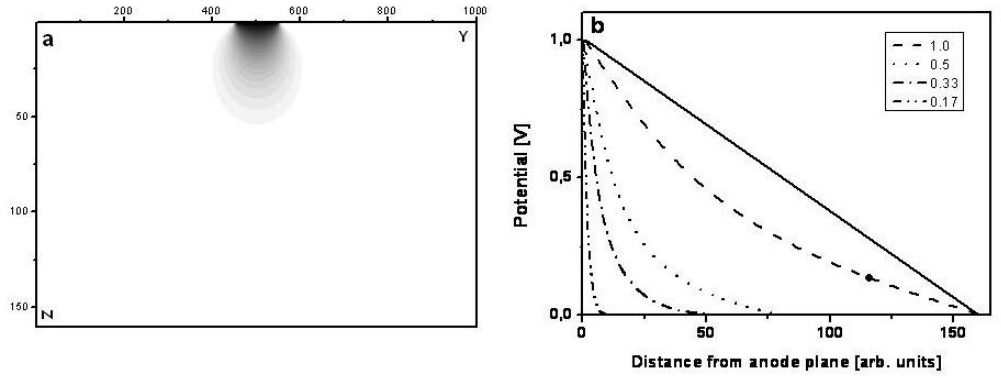

Fig. 45. Examples of calculations for weighting potentials forming signals from chamber electrodes

Investigations of (n,p), (n,α) reactions

The experimental and theoretical investigations of the (neutron, charged particle) reactions induced by fast neutrons were continued. The experiments are carried out at the Van de Graaf accelerators EG-5 in FLNP JINR and EG-4.5 of the Institute of Heavy Ion Physics of Peking University. Data on the neutron reactions with the emission of charged particles induced by fast neutrons are of much interest for studying the mechanisms of nuclear reactions and atomic nuclear structure as well as in choosing engineering materials and in performing calculations in the development of new facilities for nuclear power engineering.

The measurements of the ^{25}Mg(n,α)^{22}Ne and ^{54,56,nat}Fe(n,α) reactions were conducted. The data analysis for the measurements of the ^{57}Fe(n,α)^{54}Cr and ^{63}Cu(n,α)^{60}Co reactions at $E_n \sim 4.0$-6.5 MeV was completed; the results were published. The data treatment for the measurements of the ^{40}Ca(n,α)^{37}Ar reaction was completed; a paper was prepared for publication. For this nucleus the differential cross sections for ^{40}Ca(n,α_0), (n,$\alpha_{1,2}$), and (n,$\alpha_{3,4,5}$) reactions were measured at neutron energies of 4.0, 4.5, 5.0, 5.5, 6.0, and 6.5 MeV . The experimental values of the cross sections were compared with the calculations using the TALYS-1.6 code (**Fig. 46, 47**).

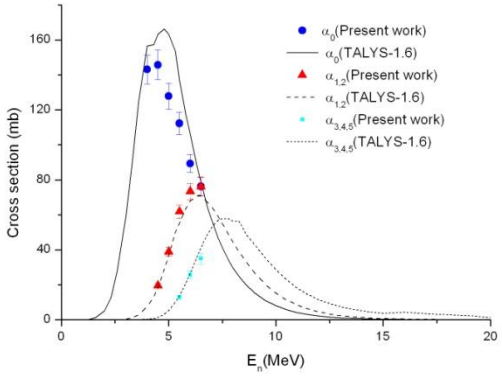

Fig. 46. The measured partial cross sections for the reactions ^{40}Ca (n,α_0), (n,$\alpha_{1,2}$) and (n,$\alpha_{3,4,5}$) compared with the calculations made by using the TALYS-1.6 code.

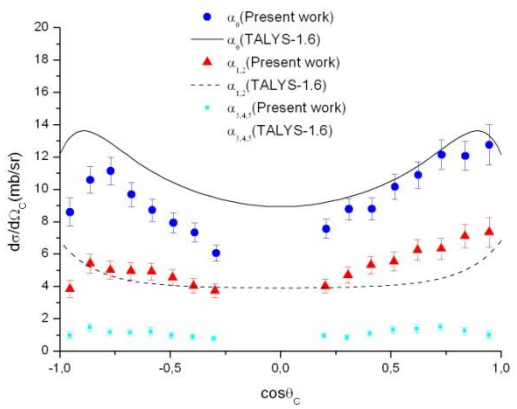

Fig. 47. Partial differential cross sections for the ^{40}Ca(n,α)^{37}Ar reaction in CMS at $E_n = 5.5$ MeV.

A systematic analysis of our experimental cross sections for the (n, α) reaction in the energy range from 4 to 6 MeV was performed. The dependence of these cross sections on the parameter (N-Z+0.5)/A in the specified energy range was observed and explained within the context of the statistical model.

Investigations of nuclear structure

A principally new variant of the practical model describing a cascade decay of an arbitrary level of a nucleus of any type with an excitation energy equal or greater than the nucleon binding energy, was proposed and fully tested. The complete absence of suitable for practical purposes theoretical models of the properties of excited levels with a structure determined by several quasiparticles and phonons called for the inclusion in this model of purely phenomenological concepts about the density of vibration-type levels and partial widths of their decay, in particular to define the shape of the energy dependence of the total density of quasiparticle and phonon levels at any nuclear excitation energies. The variation of these dependences for various functions of the excitation energy, as well as the analysis of approximated values of the parameters in the modified phenomenological representations showed that the change in the density of vibration-type levels (accurately reproducing the experimental values of the intensities of two-quantum cascades) is uniquely determined by the same parameter for nuclei with any weight and shape – the average nucleon coupling energy $\Delta = 12.8/\sqrt{A}$.

The number of broken Cooper pairs of nucleons below the coupling energy and their break-up thresholds is in agreement with the previously obtained values for the used variants of modification of the phenomenological part in the model. That is, the models that take into account the presence in the nucleus of the normal and superfluid phases and their interaction describe such parameters of the excited nucleus like the density of levels and the probability of their decay with radically better from the methodical viewpoint accuracy. Correspondingly, the statistical model of the nucleus (existing for more than fifty years), does not correspond to the present-day level in the experimental study of the nucleus.

The new experimental data on the intensities of two-quantum cascades in the nuclei of ^{52}V and ^{64}Cu obtained at the Dalat reactor (Vietnam) were analyzed in the framework of this model for gamma-decay of neutron resonances (**Fig. 48-50**). It was shown that these new data are fully reproduced by the model which takes into account the presence of a superfluid form of nuclear matter in an excited nucleus. These data do not fit to the existing representations of the nucleus as a purely fermionic system.

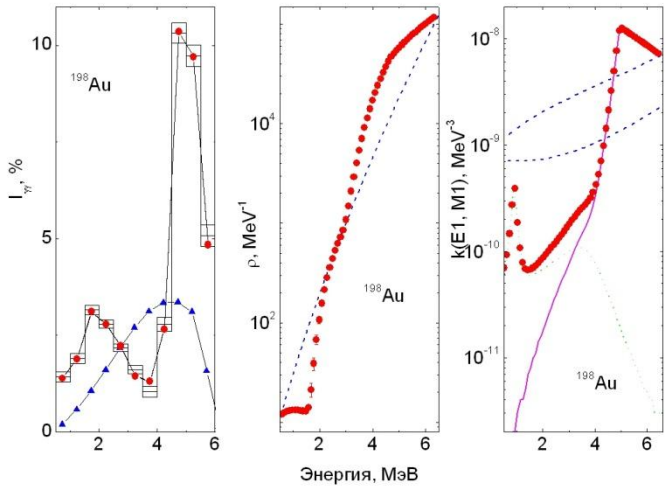

Fig. 48. Example of the resulting approximations of the modified model to the intensity of two-quantum cascades in the nucleus of ^{198}Au. Red points – approximation using the new model. Blue dots and lines – the result of calculation and model predictions of the most common functions of the level density (ρ) and radiation strength functions (k(E1) or k(M1)) of the statistical model of the nucleus.

1. SCIENTIFIC RESEARCH

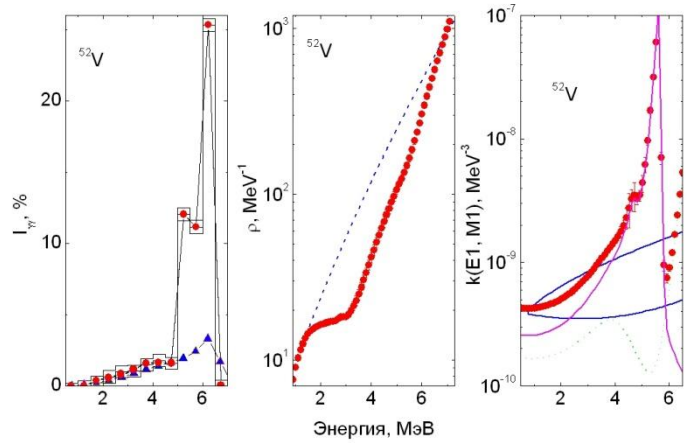

Fig. 49. Example of the resulting approximations of the modified model to the intensity of two-quantum cascades in the nucleus of ^{52}V. Red points – approximation using the new model. Blue dots and lines – the result of calculation and model predictions of the most common functions of the level density (ρ) and radiation strength functions (k(E1) or k(M1)) of the statistical model of the nucleus.

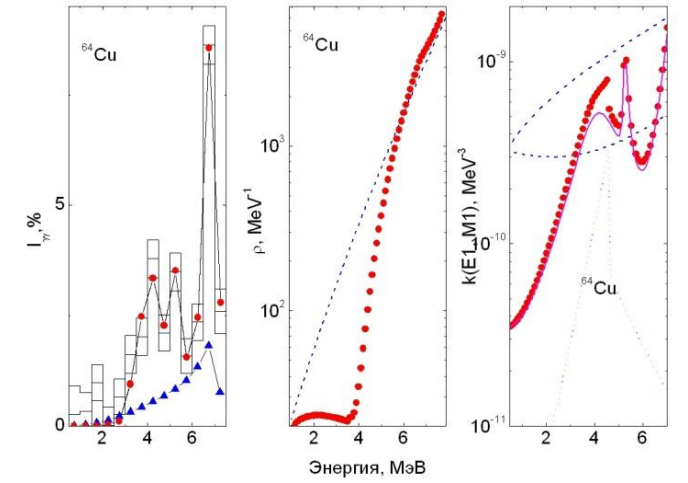

Fig. 50. Example of the resulting approximations of the modified model to the intensity of two-quantum cascades in the nucleus of ^{64}Cu. Red points – approximation using the new model. Blue dots and lines – the result of calculation and model predictions of the most common functions of the level density (ρ) and radiation strength functions (k(E1) or k(M1)) of the statistical model of the nucleus.

Design calculations of a helium UCN source at a thermal neutron beamline

At present, further progress in the physics of ultracold neutrons (UCNs) as a tool for nuclear physics research is often limited by the intensity of the available UCN sources. Therefore, in many world scientific centers projects of new advanced sources aimed at increasing the density and flux of UCN by 1-2 orders of magnitude are under development.

A helium UCN source was first proposed as early as in 1975 [6]. The principle of operation of such a source is based on the fact that neutron scattering in liquid helium ^{4}He can be accompanied by the generation of a phonon with an energy of 1.02 meV. If the neutron energy is slightly greater than 1.02 meV, the neutron is moderated down to ultracold energies. Thus, UCN can be generated from incident neutrons with energies within a very narrow range, since UCN energy is bounded from above by ~ 300 neV. The neutron could also generate two or more phonons in helium simultaneously. Both processes provide a comparable number of UCN for a wide range of incident cold neutron energies. It was also shown in the cited work that the produced UCNs could be stored in superfluid helium for a long time if the helium temperature is ~1 K or lower. This fact allows building up the UCN density in a source of this type up to very high values.

If we surround a UCN source containing liquid helium at temperatures below 1 K placed in a cold neutron beam by a cold neutron reflector producing UCN (i.e. make a trap for cold neutrons), this

makes it possible to significantly increase the cold neutron flux and, as a consequence, the UCN generation rate in the source. If as a reflector material we use a substance which is also a good thermal neutron moderator (and which is actually to be a source of cold neutrons), this allows us, first, to significantly increase the cold neutron flux and consequently the production capacity of the source, and, second, to use "cheap" thermal neutrons instead of "expensive" cold ones for producing UCN [6]. Thus, the maximum flux density in cold neutron beams at the reactor in ILL reaches ~ 10^{10} $cm^{-2}s^{-1}$, while the maximum flux density in a thermal neutron beam at the same reactor could be ~ 10^{11} $cm^{-2}s^{-1}$.

Such a UCN source surrounded by a moderator-reflector, which is a source of cold neutrons, is schematically shown in **Fig. 51**. The higher the albedo of the reflector, the higher the neutron flux density of the source (in the limit, when the albedo of the reflector is strictly equal to unity the neutron flux density accumulated in the cavity of the reflector is strictly equal to the flux density at the source — for the PIK and ILL reactors ~$10^{15}$$n{\cdot}cm^{-2}s^{-1}$).

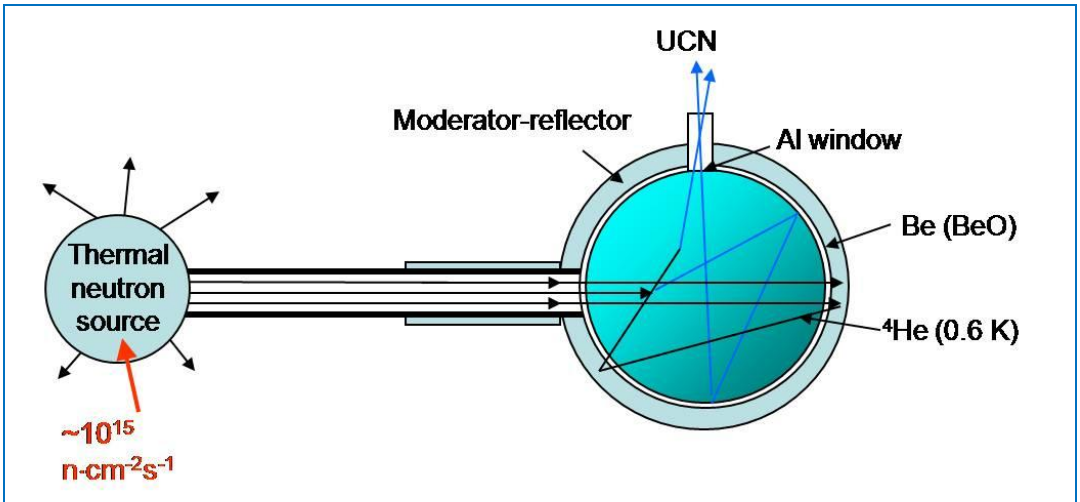

Fig. 51. Scheme of a UCN source surrounded by a moderator-reflector

A substance with the maximum albedo for cold neutrons, which we managed to find, is solid methane in phase II cooled to the temperature of ~ 4 K. Solid methane is, at the same time, one of the best cold moderators.

If a UCN source is positioned at the end of the neutron guide 20 cm in diameter directly behind the reactor biological shield, then the thermal neutron flux density at the entrance to the source is $1.2{\cdot}10^{11}$ $n/(cm^2s)$ at the rector in ILL and $3.6{\cdot}10^{11}$ $n/(cm^2s)$ at the PIK reactor. The respective integral fluxes are $3.8{\cdot}10^{13}$ n/s and $1.14{\cdot}10^{14}$ n/s.

To determine how the moderator-reflector made of solid methane operates, in 2013 the number and spectrum of neutrons accumulated inside the solid methane cavity were measured under the monochromatic neutron beam with a wavelength of 1.8 Å. In 2014 the computer simulation of the experiment was carried out using the program MCNP 4c with a special kern for solid methane. The results of the measurements and calculations are in full agreement (**Fig. 52**). This allowed us to calculate the parameters of the proposed UCN source. The results of these calculations are as follows: UCN volume density achieved in the source 40 cm in diameter installed at the reactor in ILL is $4.4{\cdot}10^4$ UCN/cm^3 at the UCN production rate of $5{\cdot}10^6$ UCN/s. The same source installed at the PIK reactor will give $1.3{\cdot}10^5$ UCN/cm^3 and $1.5{\cdot}10^7$ UCN/s, respectively. In this case, the UCN volume density in the source will be three orders of magnitude higher than that in the available UCN sources.

1. SCIENTIFIC RESEARCH

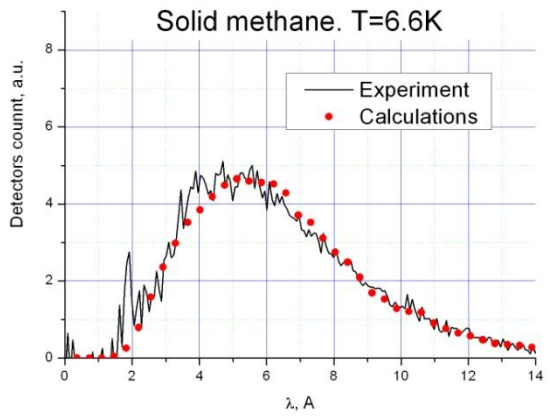

Fig. 52. Spectrum of neutrons accumulated in the methane cavity. Thin black line – results of the measurements. Points – results of numerical simulation of the experiment.

Cooperation in the framework of the GRANIT project in ILL (France)

FLNP JINR in cooperation with the P.N.Lebedev Physical Institute of RAS and Virginia State University (USA) are the members of the GRANIT collaboration. The GRANIT project aimed at designing and building a second-generation gravitational neutron spectrometer with ultra-high energy resolution GRANIT (**GRA**vitational **N**eutron **I**nduced **T**ransitions).

In 2014, in the framework of the development of the spectrometer the loss factor in the sapphire neutron guide (under construction) was measured. The measured probability of losses in the neutron guide was $3 \cdot 10^{-4}$ per reflection event. The spectral independence of the losses points to the absence of neutron gaps in the neutron guide. Upon outgassing or cooling down to liquid-nitrogen temperatures the probability of losses drops several times. This will allow one to apply a new neutron guide system with significantly improved characteristics in the coming year.

Continuation of the experiment to test the weak equivalence principle for the neutron

The experiment to verify the weak equivalence principle for the neutron was continued with the Epigraph gravitational spectrometer built in 2010 and significantly improved in 2011. The operation of the instrument is based on the combined use of Fabry-Perot neutron interferometers and a neutron flux modulator-chopper. The change in the energy of the neutron mgH falling in the gravitational field is compared with the energy transferred to the neutron diffracted into the –1 order by a moving diffraction grating.

A specific feature of the instrument is the possibility of using an original time-of-flight technique based on a periodic modulation of the neutron flux and on measurements of the oscillation phase of the detector count rate. The UCN detection is synchronized with the modulator. A high degree of beam monochromatization ($\Delta v/v < 2\%$) makes it possible to work with the times of flight, which manifold exceed the modulation period, thus ensuring a unique energy resolution of the instrument.

In 2014:

1. The results obtained in the previous measurement cycle were analyzed.
2. Possible reasons for several systematic effects revealed earlier were analyzed.
3. A new software package to control the elements of the instrument, data acquisition and primary processing was designed. Using this package the frequency of the modulator-chopper and the rotating grating can be tuned and stabilized, as well as the analyzing filter can be moved along the vertical direction. For data acquisition and primary processing a stand-alone module E 20-10 with a four-channel ADC (sampling frequency of 10 MHz, data buffering) is used. Data interchange with a PC is via a USB port. Due to specific features of the PF2 UCN

source, with which the experiments are carried out, the operation of the program is synchronized with the device distributing beams from the UCN source.

4. To better understand the operating peculiarities of the instrument and to identify systematic errors, the MC simulation of the spectrometer using the Geant4-UCN software package was started.

In the measurement cycle (started on November 3) on the UCN beam in ILL (Grenoble) at least three origins of systematic errors, which occurred in the measurements in 2012, were found.

TOF Fourier spectrometry of UCN and experimental investigation of UCN spectra at diffraction from a moving grating

When analyzing the results of the experimental data obtained in 2012, it was realized that the used phenomenon of quantization of neutron energy at diffraction from a moving grating is not well studied both theoretically and experimentally. In 2014 we made significant efforts to fill this gap. The experimental study of this phenomenon included the following activities:

1. The experimental data of test experiments in Fourier spectroscopy of ultracold neutrons were analyzed.
2. The Monte Carlo simulations of TOF Fourier spectra and their analysis were performed.
3. A new modulator of the spectrometer (**Fig. 53**) with a corresponding stator was designed and manufactured.

In the measurement cycle (started on November 3) on the UCN beam in ILL (Grenoble) the TOF Fourier spectrometry technique was successfully tested and TOF UCN spectra measured with three different types of interference filters were obtained.

A multiwave dynamic theory of neutron diffraction from a moving phase grating was developed in the framework of the approximation of slowly varying amplitudes in cooperation with V.A.Bushuyev (Moscow State University). The effect of the speed of the grating, its period and the height of grooves on a discrete energy spectrum and intensities of diffraction peaks of various orders was analyzed. As an extension of the previous studies by A.I.Frank, in which the possibility of a negative time delay in the neutron reflection from multilayer structures was predicted, the analysis of the concept of a group time delay (GTD) in the reflection of electromagnetic waves and neutrons from resonant and nonresonant media and layered structures was carried out in cooperation with V.A.Bushuyev.

Fig. 53. Multi-slit Fourier-chopper of the Epigraph spectrometer.

The relationship of GTD with a pulse time delay and spatial longitudinal beam shifts was considered. The arising pseudoparadoxes, as well as the effect of GTD on the shape of reflected pulses and beams were discussed. The calculations of quantum effects in neutron transmission through a high-frequency quartz oscillator were started. Within the context of the effective potential model this object is represented as an area of the potential with boundary and magnitude, which are

periodically dependent on time. The difficulty of these quantum calculations stems from the fact that the neutron propagation time through a medium (10^{-4} s) is much larger than the oscillation period (5×10^{-7} s) (**Fig. 54**).

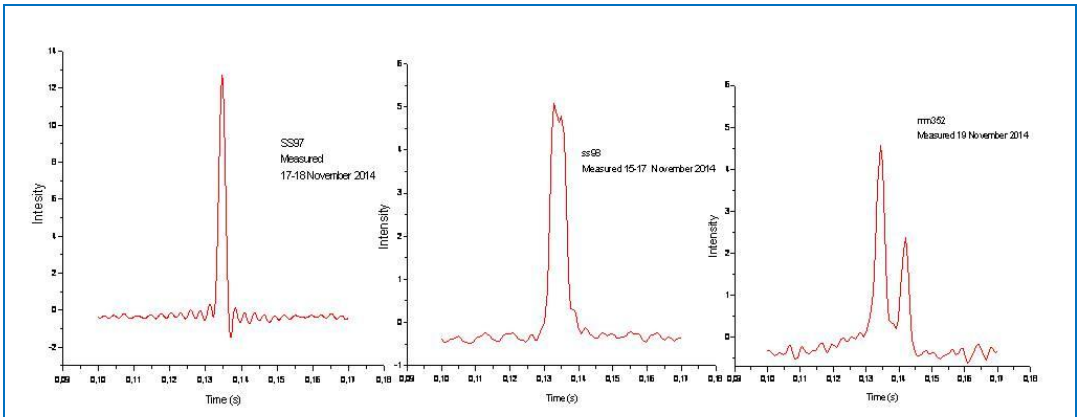

Fig. 54. Time-of-flight spectra obtained with interference filters using Fourier spectroscopy. From left to right: five-layer filter with a narrow bandwidth of about 4 neV, nine-layer filter with a wide bandwidth of about 10 neV and five-layer filter with connected resonators and a splitted band.

II. Methodological and applied research

Analytical and methodological investigations at the IREN facility

On the IREN facility the effect of neutron and gamma radiation on plastic scintillators used in the CMS experiment at CERN was investigated. Three years of operation experience with the hadron calorimeter have shown an unexpectedly large reduction in light output of plastic detectors. It was concluded that not all the factors of the radiation influence on the scintillators were taken into account. To clarify this issue, plastic scintillators of four types, namely SCSN-81, UPS-923A (manufactured in Kharkov), BC-408, LHE (manufactured in Dubna) were studied. The irradiation was carried out on the IREN resonance neutron source with the maximum exposure time of up to 30 days. The light output of the samples with different shapes before and after irradiation was compared. No significant effect of the irradiation rate on the light output was revealed. There is a large amount of bronze between the scintillators in the CMS experiment, therefore the influence of the additional induced radioactivity emitted by radioisotopes that emerged as a result of neutron irradiation of bronze was studied. For this purpose, two identical scintillators SCSN-81 were irradiated at the same distances from the target of IREN, but behind one of the scintillators a bronze disc had been placed. The measurements of light output have shown that there is a significant contribution of the induced radioactivity. The results of the measurements are confirmed by the calculations using the FLUKA program.

In 2014, the measurements and data treatment related to the search for cosmic dust in the samples provided by the Sternberg Astronomical Institute, MSU, were completed. The measurements were performed on the IREN facility. The samples from expeditions of 2010 – 2011 in the region near the Aktru glacier (North Chui Ridge of Altai) were analyzed (**Fig. 55**).

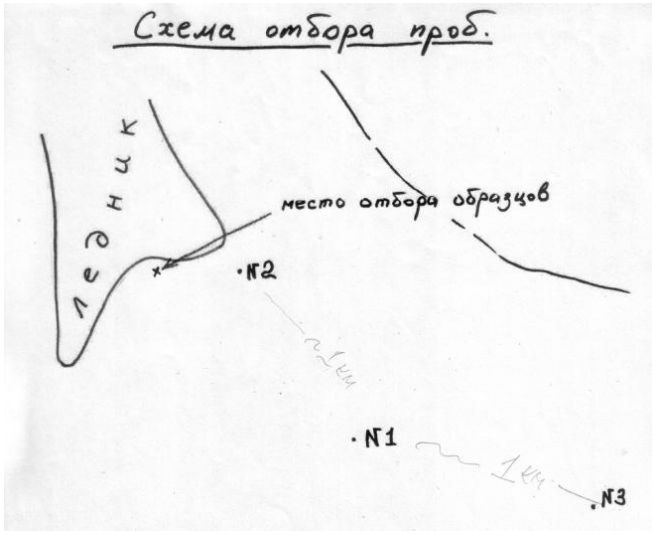

Fig. 55. Sample collection place near the glacier.

The point X denotes the place where the samples of bottom sediments accumulated in the rock cavities of the stream bed were collected. At points 1-3 control soil samples of glacial moraines were collected from several horizons: surface, at a depth of 0.3 m; 0.6 m. The distance between points 1-3 is about 1 km. The analysis was performed using the neutron spectroscopy technique. The results of the study are given in **Table 1.**

Table 1. Results of sample analysis.

Sample collection place	Depth, m	Sample weight, g	Mass of iron in sample, g	Weight fraction of iron in sample, %
Point X		270	12.6 ± 2.4	4.7± 0.9
Point №1	0.0	470	10.98±1.77	2.34±0.37
	0.3		14.05±1.6	3.0±0.34
	0.6		8.59±1.9	1.83±0.40
Point №2	0.0		14.02±4.0	3±0.9
	0.3		13.4±2.1	2.8±0.4
	0.6		11.15±2.56	2.4±0.5
Point №3	0.0		9.30±1.30	1.98±0.30
	0.3		15.8±2.37	3.36±0.5
	0.6		17.21±1.38	3.66±0.29

Analytical investigations on charged particle beams of the EG-5 accelerator

In 2014 the EG-5 accelerator was in operation for various experiments for about 495 hours. The main research area is the elemental analysis of surface layers of solids using nuclear analytical techniques: RBS (*Rutherford Backscattering Spectrometry*) and ERD (*Elastic Recoil Detection*). The experiments were conducted in cooperation with a number of Russian and foreign research institutes:

A.M.Prokhorov General Physics Institute of RAS (Moscow), B.P.Konstantinov Petersburg Nuclear Physics Institute (Gatchina), Voronezh State University, Marie Curie-Sklodowska University (Lublin, Poland), Institute of Electrical Engineering of the Slovak Academy of Sciences (Bratislava, Slovak Republic), Institute of Applied Physics of the National Academy of Sciences of Ukraine, VINCA Institute of Nuclear Sciences, University of Belgrade, Serbia. In addition, the specialists from DLNP carried out experiments to investigate the characteristics of matrix gallium-arsenide semiconductor detectors on charged particle beams of the EG-5 accelerator.

Analytical investigations at the IBR-2 reactor

Development of the NAA Sector experimental base

In the reporting period in the NAA&AR Sector a software package for complex automation of multielement neutron activation analysis (NAA) at the IBR-2 reactor (Pavlov et al., 2014) was developed and three automatic sample changers (SC) were installed to automate mass measurements of spectra of irradiated samples on three detectors. A new switch cabinet for spectrometric electronics and controllers to control the SC provided their operation at a specified temperature. After the completion of the installation work the final tuning of the program for the automation of spectrum measurements using the NAA database was made. The activities on automation of NAA are conducted in the framework of the IAEA Coordinated Research Project «Development of an Integrated Approach to Routine Automation of Neutron Activation Analysis" (F1.20.25/CRP1888, Contract No. 17363).

During the reactor maintenance shutdown in the summer the adjustment of operation of the pneumatic transport system with a new compressor as well as the installation of an air conditioner and suction-and-exhaust ventilation system in room 129a of the REGATA facility were carried out.

For the purpose of carrying out elemental analysis by atomic absorption spectrometry (AAS) a Thermo Scientific *iCE 3500 Atomic Absorption Spectrometer*, suction-and-exhaust ventilation system and an exhaust fume hood were installed in the laboratory building (room 83-3) in accordance with the requirements for laboratories working with acids used in the analysis of samples by AAS. Upon the completion of the installation work the specialists from Intertech Corporation carried out the start-up and adjustment of the atomic absorption spectrometer and issued a certificate of release to service. In the same building (room 83-2) a low-background HPGe detector with shielding was installed for conducting planned radioecological studies.

Methodological work

In connection with the beginning of joint work with the *Astrobiology Sector* of the N.M.Sissakian *Laboratory* of Radiation Biology, JINR, on the determination of the elemental composition of meteorites, as well as to assess the capabilities of automatic sample changers on the detectors the methodological studies were performed to determine the concentrations of elements for some medium- and long-lived isotopes of meteorites by means of measuring induced gamma activity spectra within a few hours after short-term irradiation. Samples were irradiated for 1-3 min with subsequent acquisition of spectra immediately after irradiation, and then with a delay ranging from a few hours up to tens of hours.

The libraries of short-lived isotopes used for standard mass measurements of element concentrations were corrected and supplemented with data for a number of medium- and long-lived isotopes. Thus, for isotopes with a half-life of several tens of hours and even years a technique was developed for determining the element concentration in some specific samples after short-term exposures. The need for using single-element standard samples with specified parameters (and consequently the necessity of their purchase) was identified.

Biomonitoring of air pollution

In 2014, in the framework of the international program "Heavy metal atmospheric deposition in Europe – estimations based on moss analysis" the work to study the environmental situation in the ferrochrome production area in the Tikhvin District of the Leningrad Region was completed. The obtained results were included in the Annual Report of the UN Commission on the long-range transport of air pollutants in Europe. In the framework of the RFBR grant (№ 14-05-31279) for young scientists “My first grant”, 170 moss and soil samples were collected on the territory of Moscow and Tver regions. A multivariate statistical analysis of NAA data was performed, and distribution maps of pollutants on the territory under study were plotted using the GIS technology.

A long-term cooperation with the Slovak specialists in biomonitoring of atmospheric depositions of trace elements found its reflection in chapter "Atmospheric pollution” (Mankovska, Frontasyeva, Ostrovnaya, 2014), as well as in the ISINN Proceedings. The study of atmospheric depositions of heavy metals and radionuclides around the Temelin nuclear power plant in Czech Republic was completed. During the reporting period two studies were made on data analysis of atmospheric depositions of heavy metals and other elements in Albania. In the framework of the Serbia-JINR Collaboration Program a comparative analysis of air pollution in the so-called "street canyons" of Moscow and Belgrade was performed. The paper was submitted to “*Environmental Monitoring and Assessment*”. The neutron activation analysis of moss samples collected by teachers and students in the national parks of Poland was done in the framework of the Program of Poland-JINR collaboration.

The study on the determination of element concentrations in moss-biomonitors collected in the area around the Kardzhali lead-zinc plant – one of the most ecologically *adverse* places in Bulgaria was completed. The obtained results were used in the bachelor's thesis work of Bulgarian student Gergana Hristozova (Plovdiv) supervised by Assoc. Prof. S.Marinova and Assoc. Prof. M.V.Frontasyeva and defended with distinction in Bulgaria in 2014. In the near future the NAA of soil samples from the same environmental "hot spots" of Bulgaria will be completed. The results will be included in the master's thesis of G.Hristozova.

Biotechnologies

In 2014, in collaboration with the E.Andronikashvili Institute of Physics, I.Javakhishvili Tbilisi State University and I.Chavchavadze State University *(*Tbilisi*,* Georgia) the studies were continued on the development of methods for synthesis of silver and gold nanoparticles by new species of microorganisms – Archaea. The strain of thermo-acidophilic crenarchaeon *Sulfolobus islandicus* LAL14/1 provided by the Pasteur Institute (Paris, France) was used to obtain silver and gold nanoparticles at high temperatures (75 °C). In combination with a number of optical and analytical methods the neutron activation analysis at the IBR-2 reactor was used to characterize the processes of synthesis of gold and silver nanoparticles by the Archaea strain, whose application for technological purposes has been very limited so far. The paper was accepted for publication in American academic journal *Advance Science, Engineering and Medicine*.

In 2014, the joint investigation carried out in cooperation with the Institute of Microbiology and Biotechnology of ASM was continued to study the process of removing toxic metals (chromium, nickel) from wastewater using microalgae *Spirulina platensis*. Also, studies were conducted to monitor changes in the content of the main components of *Spirulina* biomass (proteins, carbohydrates, and others) in the process of formation of silver nanoparticles by microalgae.

Two projects were submitted to RFBR: "Development of new biosorbents for removing heavy metals from wastewater" in cooperation with Sohag University in Egypt and “Study of physical and chemical processes of immobilization of radioactive and toxic metals by cells of bacteria and microalgae” in collaboration with the A.N.Frumkin Institute of Physical Chemistry and Electrochemistry of RAS.

1. SCIENTIFIC RESEARCH

In the framework of a pilot project in cooperation with the University of Oulu, Finland the potential of NAA for analysis of pine sawdust used in wastewater treatment as a sorbent of metals was demonstrated. In cooperation with the Institute of Environmental Engineering of Óbuda University (Budapest, Hungary) similar investigations were conducted in a model experiment on the use of *Miscanthus sinensis* plant as a sorbent of metals. The study is a part of a PhD thesis of postgraduate student of Óbuda University, Albert Szaniszló (Hungary).

In collaboration with the Institute of Water Problems of RAS the elemental composition of cyanobacterial communities (extremophiles) living in hot springs of Kamchatka at temperatures above 55 °C was determined using epithermal NAA.

Environmental assessment

In 2014, the multielement analysis of soils and bottom sediments from various regions of the Nile delta and its near-shore area was continued in the framework of the joint JINR-Egypt project «Assessment of the environmental situation in the delta of the Nile River using nuclear and related analytical techniques». The obtained results have shown that the element composition of these samples is determined mainly by geochemical features of the region under study and is not affected by the anthropogenic load.

Within the framework of the Cooperation Agreement with the Institute of Biology of the Southern Seas (Sevastopol) to assess the state of the coastal ecosystem of the Crimea, the analysis of macroalgae-biomonitor samples in the coastal zone of the Black Sea was completed. The cleanest water areas of the coastal zone of the Crimea were found and for the algae the background concentrations of about 30 macro- and microelements were determined. A technique of sampling and preparation of phytoplankton for NAA on the IBR-2 reactor was optimized and the element composition of 50 samples was determined. The concentrations of 46 elements in the phytoplankton of the Black Sea were obtained for the first time. The effect of the elemental composition on the biophysical parameters of the functional activity of phytoplankton communities in coastal areas was assessed. The obtained results have shown that phytoplankton can be successfully used as a biomonitor of water ecosystems. The study was presented at the III International Scientific Conference "Biodiversity and Sustainable Development" (Simferopol, Russia) and ISINN-22 (Dubna, Russia).

In cooperation with Moscow State University (Faculty of Biology) the investigation on the determination of the elemental composition of soil, bottom sediments, terrestrial and aquatic vegetation was started to assess the transport of pollutants in the strategically important areas of the Black Sea (coastal zone of Anapa, Novorossiysk and Tuapse) .

In collaboration with the University in Stellenbosch, South Africa, complex investigations of air pollution using mosses and lichens as well as of water ecosystem (Saldanha and Danger bays) in the Atlantic Ocean, West Coast of South Africa, were continued in the framework of the project "Mollusks as Biomonitors of Water Ecosystems in the Republic of South Africa".

Analysis of food products

The studies were completed and a joint paper (in cooperation with the analytical center of the Geological Institute of RAS) on the application of nuclear-physical analytical methods for studying the quality of foodstuffs, in particular, for the determination of Cl, Br, I and Se in the human organism was accepted for publication in the leading American academic journal *Food and Nutrition Sciences*.

The NAA was used to study the elemental composition of some agricultural crops (cereal crops and vegetables) grown using bioenergoactivator "Biorag" developed by biochemists of I.Javakhishvili Tbilisi State University, as well as to analyze the respective soil samples. The soil composition shows good agreement with the mean values characteristic for terrestrial rocks. The

results of NAA for the investigated samples revealed no toxic elements in the agricultural crops grown using the bioenergoactivator. Moreover, the content of heavy metals in all cases decreased, which is indicative of a positive effect of the innovative product on the elemental composition of the agricultural crops.

The results of NAA of edible oils (sunflower and olive oils) from Romania have revealed a significant difference in their elemental composition, which is in agreement with the published data obtained by other methods. The concentrations of heavy metals do not exceed the guideline values recommended by the World Health Organization for food products. The study was presented at ISINN-22 and accepted for publication in *Revue Roumaine de Chimie*.

Geology

In 2014, in the framework of the joint JINR-Romania project (Prof. A.Duliu, University of Bucharest) the investigation of geochemistry of the Black Sea was continued. Using NAA the elemental composition of the vertical profiles of bottom sediments was studied. The study of geochemistry of loess samples of the Quaternary Period collected in the Dobruja region (Romania) made it possible to obtain information about the climate of the Quaternary Period.

In cooperation with the Western Cape University (South Africa) the NAA study of coal fly ash from the Matla coal power station in the Mpumalanga province in South Africa was conducted. The analytical advantages of NAA using epithermal neutrons in determining the elemental composition of ash were demonstrated over such methods as inductively coupled plasma atomic emission spectroscopy (ICP-AES), laser ablation inductively coupled plasma mass spectrometry (LA ICP-MS) and X-ray fluorescence (XRF).

Analysis of materials of extraterrestrial origin

In 2014, the study aimed at searching for cosmic dust in peat columns collected in Siberia and in the meltwater from the high-mountain glacier Aktru in Altai was completed. The age determination of peat column layers was carried out at the Adam Mickiewicz University in Poland. The particles detected by means of electron microscopy along with the results of the neutron activation analysis of peat column samples (judging from the iron/nickel concentration ratio) allow us to assume that these particles could be of extraterrestrial origin. The identification of the material collected using magnetic traps in the meltwater from the glacier in Altai is more controversial. The results of the investigations were discussed at a round table meeting "Actual problems of general and space radiobiology and astrobiology" held on October 28-29, 2014 in Dubna. Studies of a peat column from the site of the Tunguska meteorite fall in 1908 have started in cooperation with the specialists from the Adam Mickiewicz University (Poland) who have extensive experience in dating (age determination) of samples and interpretation of data of the retrospective element analysis of peat columns.

Anthropological research

In the framework of the RFBR project (№12-06-00096/14 due to be completed in 2014) in cooperation with the Moscow State University (D.N.Anuchin Research Institute and Museum of Anthropology*)* the NAA of hair samples of a representative group of children from the Ongudaysk District of the Altai Republic as well as soil and plant samples from the places of their residence was continued to find possible correlations between their elemental composition and to reveal the endemic features of the effect of the geochemical environment on the human body.

Medicinal plants

The analysis of medicinal plants using NAA has become a new promising line of research in the NAA&AR Sector. These investigations are carried out in cooperation with specialists from Mongolia, Poland and Bulgaria. The study on the analysis of traditional Mongolian plants (*Carduus*

crispus L., Sanguisorba officinalis, Granium pratense, Chamaenerion angustifolium (L)Scop) used in herbal medicine won Thomas Edison Award-2014 (PHOTON Foundation «…The authors receive Thomas Edison Award-2014 in the domain of Medicinal Plants for Inspiration and Knowledge Distribution among young research scholars»).

https://sites.google.com/site/photonfoundationorganization/home/international-journal-of-medicinal-plants.

Materials science

In 2014, in the framework of the BRFBR-JINR joint grant and in cooperation with the Scientific and Practical Materials Research Center of the National Academy of Sciences of Belarus, the investigations of the crystallization processes and the characterization of artificial diamonds in the C-Mn-Ni-Fe system were conducted. In the course of the experiment diamond crystals were obtained in the Fe-Ni-C and Mn-Ni-C systems at a pressure of 5 GPa and a temperature of 1700 K. The use of NAA allowed us to study the impurity composition of the diamonds. The electronic microscopy study was performed using a scanning electron microscope Hitachi SU8000 in the N.D.Zelinsky Institute of Organic Chemistry (Moscow) under the grant for short-term scientific and educational training in the field of electron microscopy (Yu.V.Alekseenok). Electron microscopy was used to determine the size and shape of the obtained crystals. It has been found that despite the similarity in the crystal formation mechanism, their characteristics differ significantly. In the Fe-Ni-C system crystals have a more perfect geometry and larger sizes. From the impurity composition data it follows that in the Mn-Ni-C system the process of nucleation is stimulated resulting in the formation of smaller crystals with lesser hardness and imperfect shape. Thus, by using a specific catalyst system, it is possible to obtain crystals with specified characteristics. Also, a joint project was started aimed at studying phase formation processes and physical characteristics of the compounds in the Cu-Fe-S system at high pressures and temperatures. A part of the experimental material was sent to the University of Galaţi, Romania, to perform X-ray diffraction and scanning electron microscopy analyses.

Educational activities

In 2014, on the basis of the NAA&AR Sector the training courses were held for senior-year students of the University of Dubna and for students and school teachers of International Summer Schools (May-June, July and October, 2014) organized by the JINR University Center. Also, a lecture on the use of nuclear-physical analytical methods in the life sciences was delivered for teachers and students from Germany (July 2014).

In the period from April 12 to April 19, 2014 the NAA&AR Sector and JINR University Center organized a series of lectures by Professor of the University of Texas (USA) Sheldon Landsberger “Gamma-Spectrometry and Advances in Nuclear Methodologies in Low Level Gamma Ray Counting: Applications in Environmental Analysis”, which attracted a large number of scientists, post graduates and students from different laboratories of JINR, University Center and Dubna State University.

References

1 Исследования в области нейтронной ядерной физики http://wwwinfo.jinr.ru/plan/ptp-2014/r441104.htm.

2 Development of the tagged neutron method for elemental analysis and nuclear reaction studies (project TANGRA), http://indico.jinr.ru/materialDisplay.py?contribId=7&materialId=0&confId=759.

3 Enik T.L., Likhachev A.N., Mitsyna L.V., Popov A.B., Salamatin I.V., Sirotin A.P., AURA setup testing at IREN neutron beam. JINR Preprint E3-2014-13, Dubna, 2014.

4 Enik T.L., Mitsyna L.V., Popov A.B., Salamatin I.M., The Angular Anisotropy of Slow Neutrons Scattering Measured at IREN Facility with Vanadium as a Sample. JINR Preprint E3-2014-27, p. 42.

5 Golub R., Pendlebury J.M., Super-thermal sources of ultra-cold neutrons. (1975) Physic Letters A, v. 53, p. 133-135.

6 Baessler, S. et al., New methodical developments for GRANIT. (2011) Comptes Rendus Physique, v. 12, p. 729.

1. SCIENTIFIC RESEARCH

NOVEL DEVELOPMENT AND CONSTRUCTION OF EQUIPMENT FOR THE SPECTROMETER COMPLEX of the IBR-2 FACILITY

At the 40th meeting of the PAC for Condensed Matter Physics a detailed report on theme 1075 for 2009-2014 as well as the justification and proposal for opening a new first-priority theme "Development of Experimental Facilities for Condensed Matter Investigations with Beams of the IBR-2 Facility" for 2015-2017 (these materials are available at http://indico.jinr.ru) were considered and approved. Below are the results of activities carried out in 2014 in the main research areas of the theme.

Cryogenic moderators

In 2014, studies were conducted on an experimental full-scale test stand of cryogenic pelletized moderator CM-201 (**Fig. 56**).

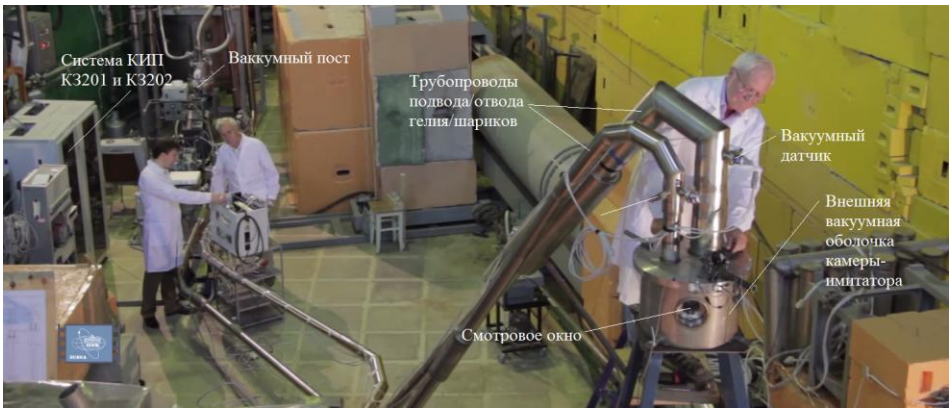

Fig. 56. Full-scale stand of CM-201 (control and measurement equipment of CM-201 and CM-202; vacuum station; helium/bead feed/discharge pipes; observation window; vacuum sensor; outer vacuum jacket of simulator chamber).

The main purpose of the experiments was to test the possibility of loading the chamber of the cryogenic moderator CM-201 with frozen beads made of a mixture of mesitylene and metaxylene by transporting them through a pipeline ascending at an angle of 50°. The experiments have shown that beads without difficulty move up the inclined section of the transport pipeline and reach the simulator chamber located inside the outer vacuum jacket (**Fig. 57**). The filling of the simulator chamber was monitored by a high-resolution camera (**Fig. 58**).

The cryogenic moderator CM-202 has been in operation since 2012. In 2014, its control systems and software were upgraded. As a result, control systems for CM-202, CM-201 and cryogenic helium facility (KGU) have been developed practically anew and accommodated in the common electronic equipment rack (**Fig. 59**). They also include the CM emergency monitoring system, which controls the circulation of helium in the system and its flow rate in the pipeline. If these parameters go beyond the allowable limits, the control electronics sends a signal to the IBR-2 control panel to reduce the reactor power. In 2014, CM-202 operated for physics experiments during two cycles (2 and 7 cycles of IBR-2 operation). At the same time, first experiments with cold neutrons were carried out at the spectrometers NERA-PR, REMUR and others. Also, important studies were conducted aimed at extending the cycle duration of IBR-2 operation in the cryogenic mode up to 11 days.

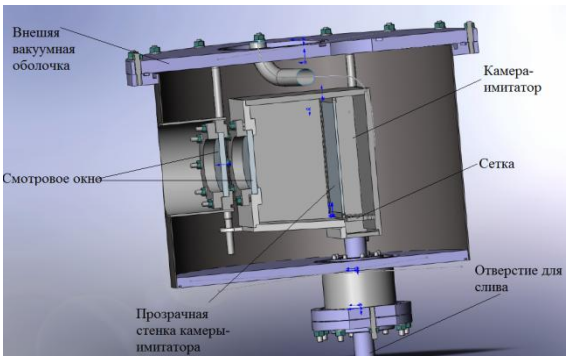

Fig. 57. Simulator chamber (observation window; outer vacuum jacket; simulator chamber; grid; discharge vent; transparent wall of simulator chamber).

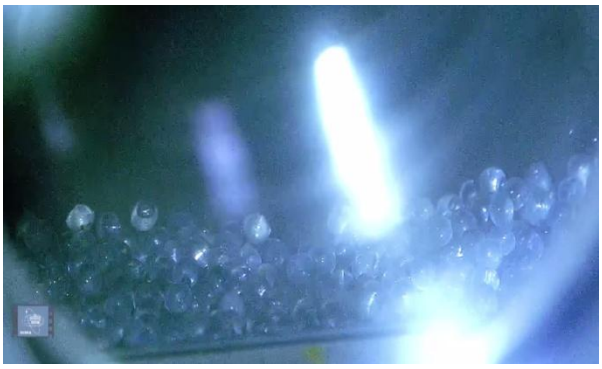

Fig. 58. Photo of frozen beads being loaded into the chamber.

At present, the maximum duration of CM-202 operation is 410 MWh (8.5 days of IBR-2 operation). The possibility of increasing the cycle duration depends on the viscosity of the irradiated working mixture (metaxylene and mesitylene) of the moderator. The viscosity of the metaxylene-mesitylene mixture after irradiation is about 12 arb. units (8.5 days, 410 MWh). This value of viscosity allows the irradiated liquid to flow freely from the chamber to a discharge tank. It is possible that higher values of viscosity can lead to the clogging of the discharge outlet and consequently result in a failure of the CM-202 operation.

In order to find a way out of this situation, a number of experiments were performed on loading the CM-202 chamber with frozen beads consisting of a solution of 55 g of naphthalene and 1 l of metaxylene-mesitylene mixture (in the ratio of 3:1). After irradiation for 374 MWh the viscosity was found to be about 6 arb. units, i.e., sufficiently low compared to the viscosity of the irradiated solution without naphthalene (**Fig. 60**).

Fig. 59. Control electronic equipment racks for CM-201, CM-202 and KGU.

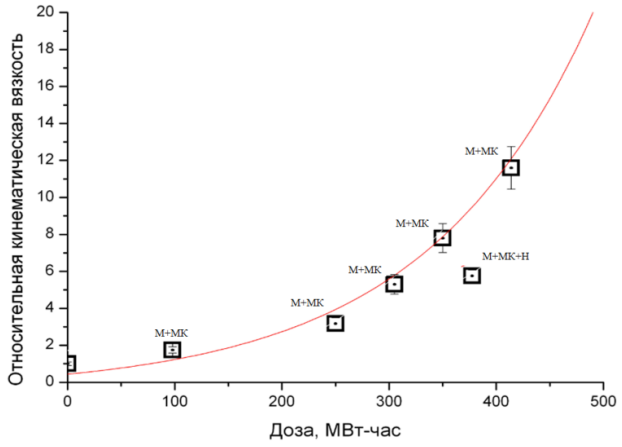

Fig. 60. Dependence of viscosity of the liquid mixture on the radiation dose liquid mixture on the radiation dose: M-MK- mesitylene-metaxylene solution (in the ration of 3:1), M-MK-H - solution of 55 g naphtalene dissolved in 1 L of mesitylene-metaxylene mixture (in the ratio of 3:1).

Thus, the solution with naphthalene can be used for longer operation time of IBR-2 and maybe even for 11 days. Experiments to extend the duration of the CM-202 operation cycle will be continued in cooperation with Moscow State University in 2015.

Calculations and simulation of spectrometers

A technique using the Reverse Monte Carlo (RMC) method to reconstruct a 3D structure of glasses (or other disordered systems) using neutron diffraction data has been developed. A special program has been developed, which allows one to determine coordination of glass atoms using Voronoi networks. If necessary, there is an option to construct a Voronoi tessellation taking into account ionic radii of particles. In this case we used some functions of the specialized software library Voro++. An example of calculations of the total scattering law S(Q) (or its analog – total structure factor F(Q)) by the RMC method for $Fe_{63}Er_2Mo_{14}C_{15}B_6$ glass in comparison with the experimental data is shown in **Fig. 61**. **Figure 62** presents a general example of a 3D Voronoi tessellation constructed with regard for ionic radii of particles (different colors represent different elements).

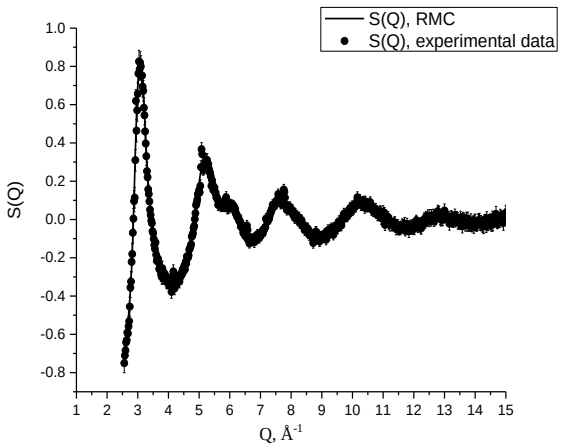

Fig. 61 Experimental total scattering law S(Q) and its calculation using RMC_POT program.

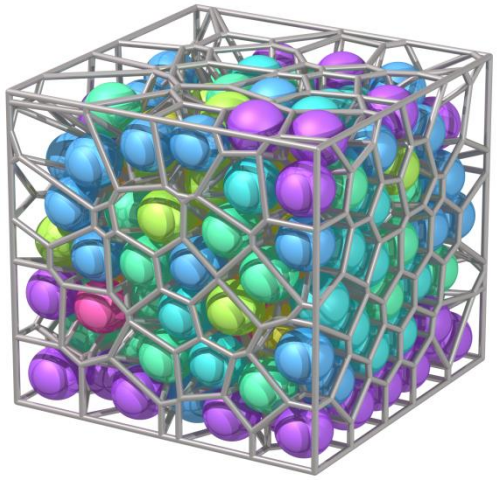

Fig. 62 Example of a constructed Voronoi tessellation.

In cooperation with the Laboratory of Information Technologies, JINR, we started the development of special mathematical models and respective programs for simulating neutron scattering in samples (including multilayer rough samples) and magnetic scattering. First results of the simulation of two-layer rough samples were obtained.

In 2014, in cooperation with the NICM Department a number of activities on the modernization and development of the Fourier diffractometer were carried out.

FSS. Work was continued on the construction of a new high-resolution Fourier diffractometer on the basis of the units of the FSS spectrometer (Geesthacht, Germany). The received equipment was inspected and design studies of its installation on IBR-2 beamline 13 were performed. The optical sections and housings of the neutron guides were cleansed and degreased. Additional sections and support posts of the neutron guides were manufactured. In order to reduce the radiation load on the neutron guide, a steel collimator was installed in the embedded tube of the beamline. The first section of the neutron guide and a Fourier-chopper were assembled and installed (**Fig. 63**). The electronics for accumulation of diffraction spectra («List Mode»-analyzer MPD-64) were designed and manufactured.

On the same beamline the infrastructure for testing spectrometer equipment is under construction. A biological shield and technological systems were installed on IBR-2 beamlines 13 and 14; the manufacturing of an experimenter's cabin, platform, adjustment tables, etc. is in progress.

Fig 63. First section of the neutron guide and Fourier-chopper on IBR-2 beamline 13.

HRFD. Control electronics of the background chopper were installed. The preventive maintenance of the background chopper and the adjustment of the control electronics in the phasing mode were performed. The operation of the control electronics of the Fourier chopper was restored due to the installation of a fast neutron background chopper in the ring corridor and reduction of the radiation background in the area of the beam outlet.

FSD. The characteristics of pickup signals from magnetic and optical sensors of the Fourier chopper were measured. The time dependence of differential nonlinearity and the duty ratio of pickup signals from magnetic and optical sensors as the speed of the Fourier chopper changes from –4000 to +4000 rev/min are shown in **Fig. 64** and **Fig. 65**, respectively. The measurements have shown that the noise of pickup signals from the optical sensor is approximately five times lower than that from the magnetic one. The activities for developing the detector system of FSD and designing algorithms and programs for extracting high-resolution spectra measured by a "list-mode" analyzer are covered in other sections of this report.

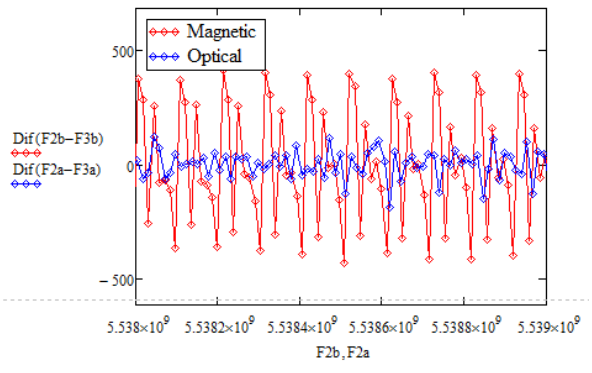

Fig. 64. Differential nonlinearity of pickup signals from magnetic and optical sensors.

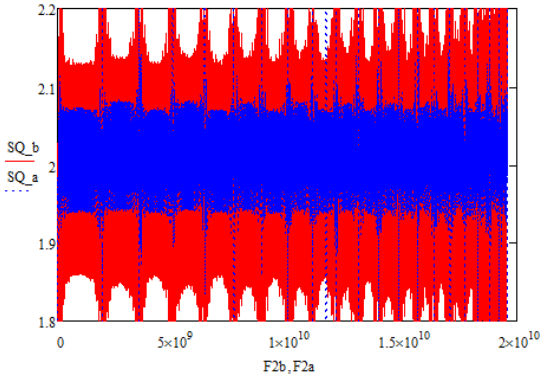

Fig. 65. Duty ratio of pickup signals from magnetic and optical sensors.

1. SCIENTIFIC RESEARCH

Detectors

Small-angle 45°- and 90°-detector systems based on 3He counters were manufactured and adjusted. These systems along with preamplifier units were installed on the RTD diffractometer and prepared for operation (Fig. 66).

Also, for the RTD diffractometer a design of a ring-shaped small-angle thermal-neutron-scattering detector was developed (**Fig. 67**). In contrast to the ring-shaped backscattering detector previously installed on RTD, the following modifications were made in the design of the small-angle detector:

- instead of stainless steel the housing is made of duralumin, which has significantly reduced its weight and the absorption of neutrons in the entrance window;
- method of fixing an anode wire was modified, which made it possible to reduce losses in the dead zones of the detector;
- all radii were made independent of each other, which allows the detector to be repaired without a complete disassembly;
- cylindrical cathodes are made of double-sided foil-clad fiberglass, which makes it possible to make 9 concentric counters instead of 8, as well as to divide the cathodes into 16 sectors and in this way to get one additional azimuthal coordinate.

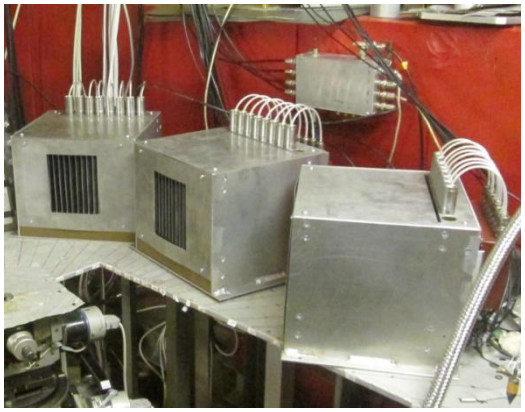

Fig. 66. Small-angle 45°- and 90°-detectors on IBR-2 beamline 6a.

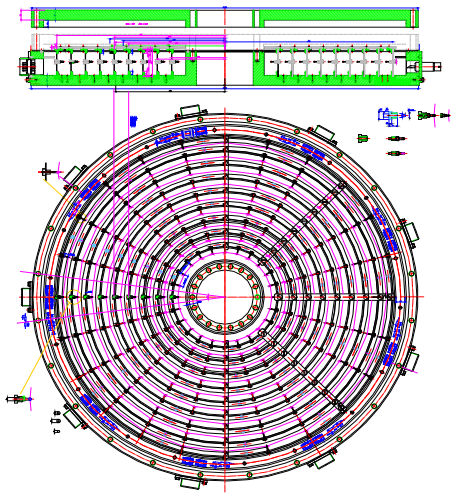

Fig. 67. Scheme of a small-angle ring-shaped detector of the RTD spectrometer.

The activities on completing the ASTRA detector system were continued. Within the framework of these activities the manufacturing of the plane comprising four scintillation counters was completed (3^{d} section, **Fig. 68**). These counters were installed on the FSD diffractometer and are being tested and adjusted in cooperation with the NICM Department. TOF spectra of both low (**Fig. 69**) and high (**Fig. 70**) resolution were obtained. In the framework of the preparation for tests a large amount of work was carried out on the adjustment of the MPD data acquisition and accumulation electronics adapted for the use with the ASTRA scintillation detectors.

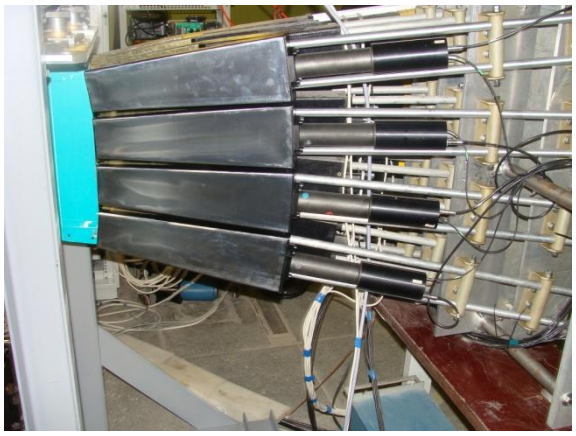

Fig. 68. Plane comprising four scintillation counters installed on the FSD diffractometer.

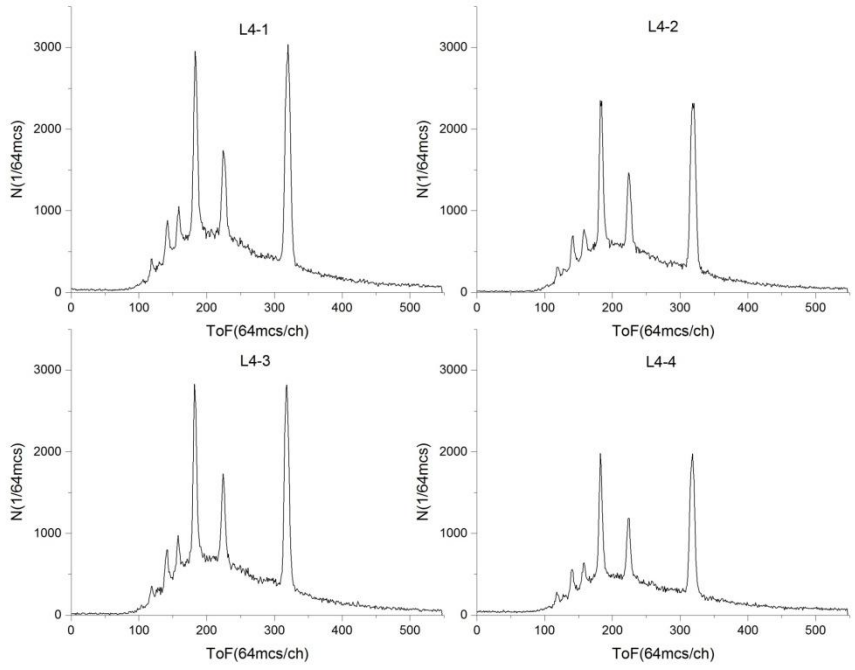

Fig. 69. TOF low-resolution spectra for four new counters.

A monitor 2D PSD was manufactured and prepared for testing. Its tests and in-service measurements of beam profiles are underway. The modernization of the PSD on the REMUR spectrometer has proved to be impossible without suspending experiments for a long time, therefore together with the physicists concerned it was decided to make a new detector. These works are included in the plan for 2015.

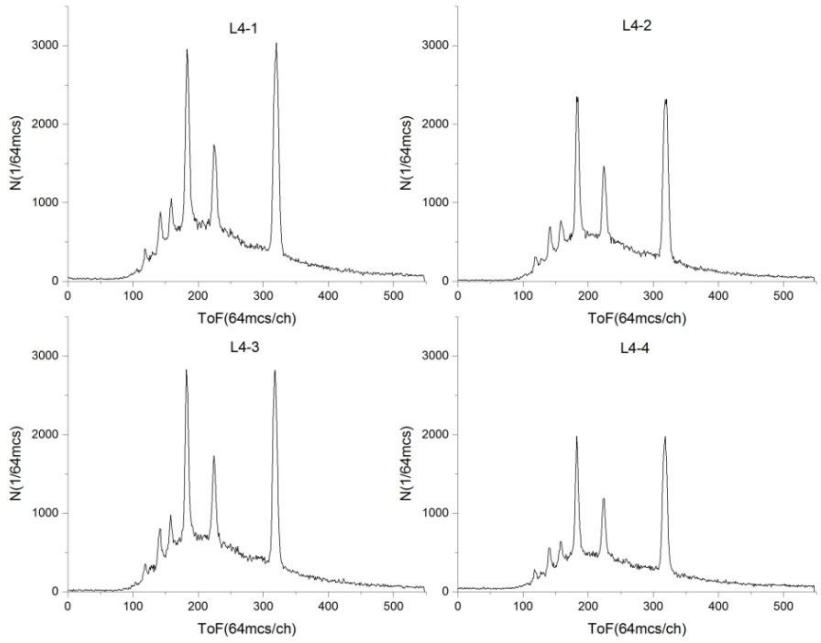

Fig. 70. TOF high-resolution spectra for four new counters.

Cryogenics

A shaft cryostat for a temperature range of 6-300 K was designed and put into operation on the NERA-PR spectrometer (**Fig. 71**). The cryostat uses a pulse tube cryocooler CRYOMECH PT405 and has a shaft 70 mm in diameter for inserting samples.

Fig. 71. Shaft cryostat for the NERA-PR spectrometer.

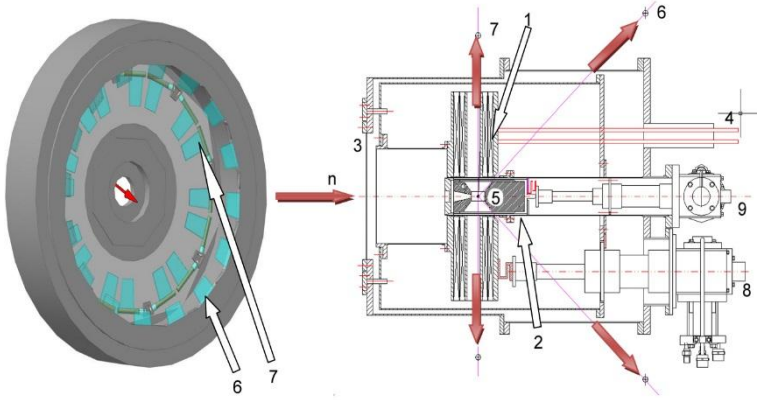

Fig. 72. Preliminary design of a cryostat with a superconducting magnet and cryostat-insert for the DN-12 diffractometer: 1 – superconducting magnet; 2 – cryostat-insert; 3 – entrance window for neutrons/window for backscattered neutrons; 4 – current lead (up to 300 A); 5 – high-pressure cell; 6 and 7 – detectors for neutrons scattered at angles of 45° and 90°; 8 – cryocooler RDK408S; 9 - cryocooler RDK101D.

The use of liquid helium and nitrogen in the conditions of a restricted access zone on DN-12 is limited for personnel safety reasons (the instrument is located in a confined space). For this reason and because of the geometrical layout of DN-12 units, obtaining low temperatures requires “cryogen-free” technologies – use of closed-cycle refrigerators without liquid cryoagents.

In order to simplify the cooling scheme of the magnet, and consequently its design, and to reduce the cost of its operation, it is considered advisable to use an HTSC tape as a superconductor of the magnet. A cooling temperature of 20 K is sufficient for operation of an HTSC-tape-based magnet and can be maintained by using liquid-helium-free cryocoolers (e.g., RDK408S).

Changing sample temperatures requires the development of a cryostat-insert for the magnet. This cryostat is planned to be equipped with holders and containers of high-pressure cells. High-pressure cells are to be made of non-magnetic materials.

Carrying out temperature measurements with the applied magnetic field requires the use of RDK101D cryocooler with a final temperature of ~ 3 K. The installation (**Fig. 72**) of the magnet on the DN-12 diffractometer will require the modernization of the housing of the diffractometer, as well as the inspection examination of the available equipment of the diffractometer in order to ensure its proper operation in magnetic fields.

Control systems of actuating mechanisms of IBR-2 spectrometers

The actuating mechanisms of the YuMO and REMUR spectrometers were upgraded and equipped with sensors. On the YuMO spectrometer, absolute multi-turn angle sensors were installed directly on the stepper motors (**Fig. 73**) for monitoring linear movement in the horizontal and vertical directions of the sample table and platforms of three detectors. The installation of sensors has , at the REMUR spectrometer an absolute multi-turn angle sensor monitors the position of the platform with a detector. At the Fourier diffractometer FSD a controller OSM88RA (current – up to 8 A, voltage – up to 72 V) was installed, thus allowing an order of magnitude (up to 1 mm/s) increase of the speed of the vertical movement of the Huber goniometer sample table.

A control system of actuating mechanisms with 4 control channels (with the possibility of further extension up to 32) was put into operation at the spectrometer of neutron radiography and tomography being constructed on IBR-2 beamline 14. The Huber goniometer head with three (two horizontal and one vertical) axes of rotation was connected to the system.

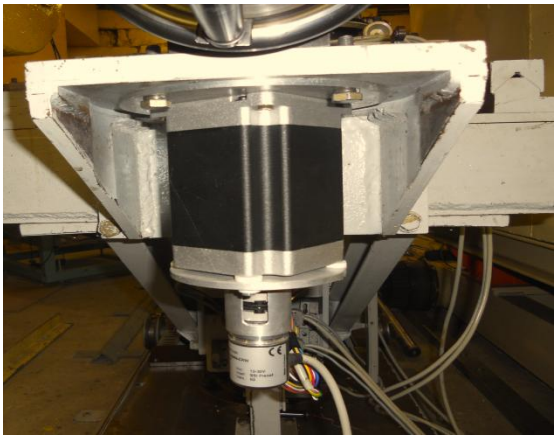

Fig. 73. Motor with angle sensor MSD1312 of the sample table for providing horizontal movement of samples at the YuMO spectrometer.

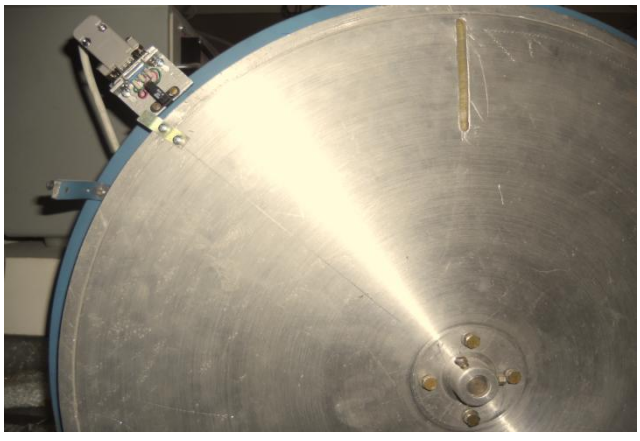

Fig. 74. Monochromator and control system on IBR-2 beamline 9.

1. SCIENTIFIC RESEARCH

Control systems of the chopper and the shutter were put into operation at the DN-6 and DN-12 diffractometers, and a DC-motor based monochromator (**Fig. 74**) with a magnetic speed sensor was put into -2 spectrometers' complex a new generation of unified data acquisition systems with world-class characteristics has been developed and constructed. These systems have been installed on all spectrometers. They are connected directly to PC and possess flexibility for fast adaptation to any changes in experimental conditions and to an increase in the number of spectrometer devices. The chosen architecture of DAQ-systems fits well into the network infrastructure and provides the ease and low cost of their regular modernization in accordance with the progress in computer engineering and communication technologies. An important distinction of this generation of electronics is the abandonment of nuclear electronics standards (CAMAC, VME, etc.), which reduce potentially achievable speed of operation because of the necessity to execute their internal protocols. Besides, the cost of "standard" electronic units is significantly higher because they, unlike computer devices and interfaces, are not mass products. The rejection of the VME standard allowed a change-over from the outdated and user-unfriendly OS-9 to the operating system Windows for the software package Sonix. And finally, new DAQ systems make it possible to accumulate raw data, which in some cases is of principal importance.

Data acquisition systems of practically all IBR-2 spectrometers consist of 1-2 basic modules, one of which processes and accumulates data from one- and two-dimensional PSD (De-Li-DAQ), and another – from an array of point detectors (MPD). From the viewpoint of hardware the basic modules are identical; and the specifying of all parameters, modes and operation algorithms specific to a concrete spectrometer, is realized on the level of microprograms, which are stored and executed in FPGA of the respective module under PC control.

An MPD module is used to acquire and store data from gas and scintillation counters. At present, all IBR-2 spectrometers are equipped with new DAQ electronics. All the above-mentioned DAQ systems consist of two types of units ─ one digital unit (its architecture is shown in **Fig. 75**) capable of registering and storing data from 1 to 240 point detector elements and several 32-channel analog units in which data acquisition, discrimination, transformation and transfer are performed from the detectors' preamplifiers to a digital unit MPD. In the analog unit the transition from LEMO connectors to a flat cable is done as well.

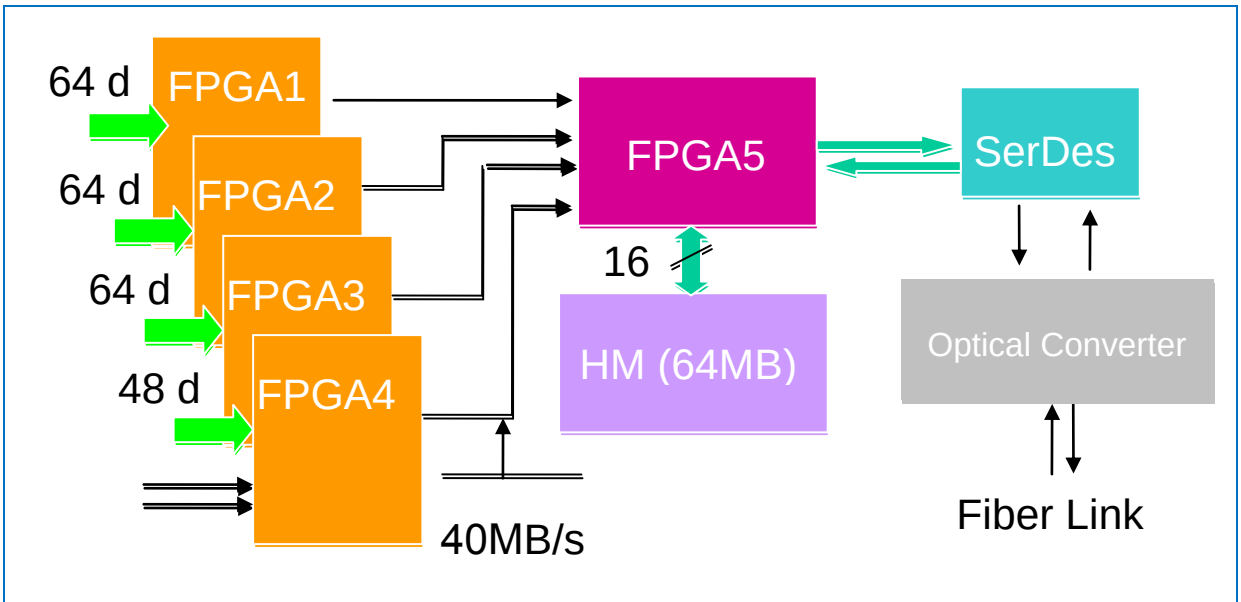

Fig. 75. Architecture of an MPD module.

These modules are also used for storing a set of histograms in short time intervals for real-time studies of transition processes in condensed matter (DN-2/RTD diffractometer).

For Fourier diffractometers HRFD and FSD a "list-mode" analyzer with a specialized software package (designed in the SC Department) has been developed and constructed on the basis of MPD modules. On these diffractometers first experiments were conducted with comparative simultaneous measurement of diffraction spectra using the existing DSP-based analyzer and the new list-mode analyzer. Using the developed algorithm high-resolution spectra were extracted from the list-mode data and compared with the DSP-spectra. The comparison has shown that the spectra are identical, which is indicative of the correct operation of the new electronics and the developed algorithms for obtaining diffraction spectra from "raw" data (for details see Section 1.1.2 of the Report).

Two types of unified new-generation electronic modules De-Li-DAQ-1 and De-Li-DAQ-2 have been designed for data acquisition and accumulation from one- and two-dimensional MWPC detectors with delay-line data readout.

The De-Li-DAQ-1 module has been developed in cooperation with HZB, Berlin. It is based on digital signal processors and field-programmable gate arrays, which has made it possible to realize wide functional possibilities and rather complex algorithms of selection and preliminary processing of events. The module has an inner histogram memory of 256 Mb and a count rate of up to 10^5 events/s. By now about fifty DAQ modules have been produced, which along with PSD developed in FLNP are used on IBR-2 spectrometers, in NRI (Řež, Czech Republic) and in a number of the Russian neutron centers (IMP UB RAS, Yekaterinburg, RRC “Kurchatov Institute”, Moscow and Branch of KIPC, Obninsk) as well as in HZB, Berlin, with detectors of other producers. The module is installed in a free slot of a personal computer, connected to PC via a PCI interface and runs under OS Windows.

The new module De-Li-DAQ-2 has 1 Gbyte histogram memory, which makes it possible to accumulate three-dimensional spectra X-Y-TOF of up to 512×512×1024 32-bit words; and high-speed interface with optical communication link to a personal computer. Connection to a PC is via USB 2.0. The De-Li-DAQ-2 module provides a count rate of more than 10^6 events/s.

As is the case with MPD, both De-Li-DAQ modules provide data acquisition and accumulation in two main modes: histogram mode (on-line sorting and accumulation of spectra in the module memory), and list mode (when raw data are accumulated directly on a PC hard disk).

It should be noted that the above-described DAQ modules are only a part of data acquisition electronics with which our physicists deal with directly. In the reporting period nearly half of analog electronics, which, as a rule, are “hidden” from them, have been modernized. These are preamplifiers, shapers, discriminators, power supplies, cables, connectors, etc. for several hundred measuring channels.

The control systems of all IBR-2 spectrometers were modernized with the replacement of the control computer in the VME standard with a PC. Along with it, the control software package Sonix used earlier was replaced with Sonix+ adapted to a new set of equipment of the IBR-2 spectrometers that had been changed during the modernization (new detectors, actuating mechanisms, sample environment systems, digital electronics, etc.).

In the course of carrying out this work the possibilities of the software package Sonix+ were significantly extended:

- New modules for controlling all controllers developed in FLNP (MPD, De-Li-DAQ-2) or purchased (to control stepper engines, goniometers, loading devices, heaters, refrigerators, high-voltage power supplies, etc.) were added. For DAQ controllers in addition to the histogram mode, the mode of raw data accumulation was implemented.
- A new, simpler and more convenient universal graphical user interface (GUI) on the basis of PyQt and matplotlib was developed and introduced, which provides both the control of the

experiment and visualization of data from all detectors being used (point detectors, 1D and 2D PSD).

- A general approach to the creation of adjustment programs for the spectrometers was proposed. On the basis of this approach the programs were developed and introduced on the IBR-2 reflectometers (REMUR, REFLEX, GRAINS) and spectrometers (YuMO, EPSILON) (**Fig. 76**). One of the versions of the program is used on the DN-6 and DN-12 spectrometers as a user interface for experiment control.
- An approach to the creation of programs for keeping a measurement log was proposed. The first variant was created and is successfully used on the YuMO spectrometer.
- A change-over of all Sonix+ components to Microsoft Visual Studio 2008 and Python 2.6 was made.

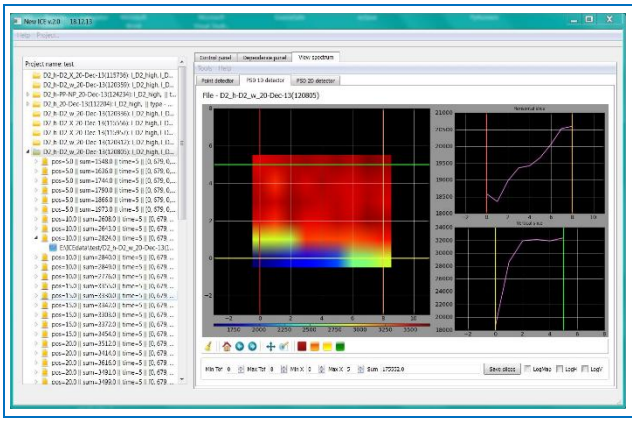

Fig. 76. Adjustment program: visualization of two-dimensional scanning data at the REMUR spectrometer.

Taking into consideration the operational experience and users' feedback, the remote experiment control system WebSonix was radically redesigned. The main results of the modernization are the improvement of the user interface, as well as higher reliability and security of the system due to the use of the latest web technologies. The help section of the system in Russian and English was significantly supplemented. A cold moderator monitoring software has been upgraded.

A regular operation of the FLNP central file-server Supermicro 6047 was started. A number of teams of physicists came up with a proposal for using it as a basis for organization of a centralized fault-free network-attached storage system for data measured on the IBR-2 spectrometers. This approach provides:

- automatic transfer of experimental data;
- continuous availability of data;
- data backup in case of a hard disk failure on the host computer of a spectrometer;
- regulation of data access rights on the server.

All services of the server are configured as a single system, which organizes network-attached storage and ensures its operation. The sftp and samba protocols allowing for the encryption of users' password have been selected to provide access to the data.

A number of requirements were put forward to the script for writing data to the server. The implementation of these requirements ensures the reliability and safety of the data storage system:

- script should be integrated into the general system for controlling experiments Sonix+;
- when writing data to the server it should copy the structure of experimental data on the host computer of the spectrometer, as well as record intermediate files if they are changed during the experiment;

- script should be maximally isolated from the general system;
- a detailed log of all processes occurring while writing data to the server should be kept in the system.

The first version was tested during a number of the reactor measurement cycles at the FSD, HRFD and SKAT spectrometers. Particular attention was paid to providing uninterrupted measurements in case of possible failures in data transfer to the server. On the whole, the tests have shown sufficient reliability of the system. In the future it is planned to provide authorization of users of the data storage system via the FLNP general authorization system, as well as to develop additional services for the convenience of working with the data storage system.

The technical specifications of the server are given in the Annual Report for 2013. An SAS2108 RAID controller and eight 4 GB RAM units, which are used as a cache, were purchased and installed in addition to the initial configuration of the server. The total usable storage capacity is 58 TB.

A new Supermicro SYS-6017R-TDAF server with two CPU Intel Xeon, 16 TB disk space and operating system Linux got its first active users.

The main tasks in the development of the FLNP network have been fulfilled (Fig. 77):

- An upgrade of the FLNP backbone network to a 10 Gbit/s rate has been done.
- The rate of up to 1 Gb/s has been provided for the end-users in the main network segments;
- The creation of a WiFi network has been completed in the FLNP main buildings and the IBR-2 experimental halls;

A trouble-free operation of all network equipment has been maintained both on the IBR-2M spectrometers and in the offices of the Laboratory.

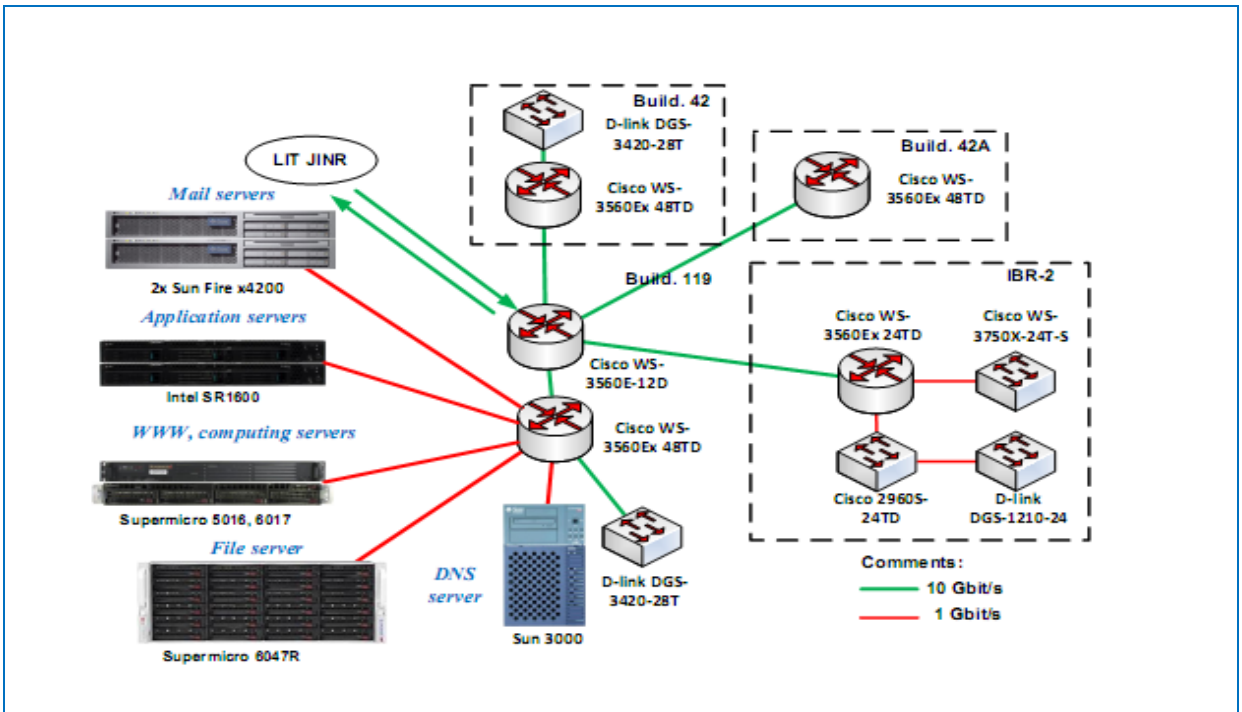

Fig. 77. Logic diagram of FLNP network (2014).

.

2. NEUTRON SOURCES

THE IBR-2 PULSED REACTOR

Information on the operation of the IBR-2 research nuclear facility

The IBR-2 research nuclear facility operated under Rostekhnadzor license № GN-03-108-2614 of 27.04.2012 and Rostekhnadzor license № GN-03-108-2871 of 30.04.2014.

On February 9, 2014 in accordance with JINR order №67 issued on 02.07.2014 the IBR-2 operation was terminated due to the expiry of the Rostekhnadzor license № GN-03-108-2614 of 27.04.2012 for operating the research nuclear facility IBR-2. On May 5, 2014 JINR obtained Rostekhnadzor license № GN-03-108-2871 issued on 30.04.2014 by the Federal Service for Ecological, Technological and Nuclear Supervision for operating the research nuclear facility IBR-2. In accordance with JINR Order of May 6, 2014, the operation of the research nuclear facility IBR-2 at a power of 2 MW was permitted to be resumed from May 12, 2014.

In 1, 3-6, 8 and 9 cycles the CM-202 moderator operated in a water moderator mode; in 2, 7 cycles – in a cryogenic mode.

The table presents data on the IBR-2 operation for physics experiments in 2014.

№ cycle	Period	Reactor operation at power, hr	Reactor operation for physics experiments, hr	Moderator type
1	13.01-24.01	284	267	water
2	30.01-08.02	213	201	cryogenic
3	13.05-29.05	405	390	water
4	03.06-11.06	172	163	water
5	22.09-06.10	334	326	water
6	13.10-27.10	332	327	water
7	31.10-09.11	193	187	cryogenic
8	21.11-08.12	404	398	water
9	15.12-26.12	239	233	water
Σ		2576	2492	

Information on the activities under the project “Complex of cryogenic moderators of the IBR-2 reactor”

In 2014, in accordance with the IBR-2 operation schedule two cycles of CM-202 operation in a cryogenic moderator mode were conducted.

The main activities carried out in the framework of theme 1105 “Development of the IBR-2 Facility with a Complex of Cryogenic Neutron Moderators” were:

- A contract for the purchase of a refrigerator by Linde AG 1200W 10K was concluded.
- A technical proposal for designing the refrigerator equipment layout in bldg. 117 was developed.
- A contract with JSC SSDI for designing the refrigerator equipment layout in bldg. 117 was concluded.

- A cryostat KV6640.00 with two gas blowers was installed on IBR-2 beamline № 3 in accordance with the plan of construction of cryogenic moderator complex. In-service thermophysical tests of the cryostat were performed.
- A test stand of CM-201 was assembled in accordance with the project design of the FLNP Design Bureau.
- Experiments on loading mesitylene beads into the test stand chamber were carried out. Studies on filling the cryogenic moderator chamber with beads of mesitylene-naphthalene mixture to determine the neutron-physical characteristics and to test the radiation resistance of the mixture.

IREN FACILITY

Throughout almost the entire first half of 2014, from January 17 to May 23 (1358 hours) IREN operated for the program of irradiation of scintillator samples of the hadron calorimeter CMS, which was drawn up by the specialists from VBLHEP. Over one hundred samples of scintillators were irradiated; their radiation characteristics were studied and relevant data were obtained that can be used to increase their radiation resistance.

In the second half of 2014 the IREN personnel carried out a large-scale modernization of technological and electrical systems of the facility. The ventilation and air-conditioning systems of the IREN accelerator halls were upgraded, the old klystron modulators were dismantled and replaced with new high-power pulsed klystron modulators of South Korean company DAWONSYS. A representative competition was held to select a contractor for implementing the project and performing work on the modernization of the IREN power supply system. Technical specifications were developed for modernization of the power supply system as well as water cooling and temperature stabilization systems of the LUE-200 accelerator. All efforts were aimed at achieving in 2016 the design parameters of the IREN facility specified in the "road map”

EG-5 ACCELERATOR

In 2014, the EG-5 accelerator operated for experiments for 665 hours. A large number of analytical studies were carried out with various samples. The samples were provided by the JINR Laboratories (FLNP, DLNP, FLNR), institutes of Russia (A.M.Prokhorov General Physics Institute, St.Petersburg Nuclear Physics Institute, Voronezh State University), institutions from JINR Member States (Maria Curie-Skłodowska University, Lublin, Poland, Institute of Electrical Engineering SAS, Bratislava, Slovakia; Institute of Physics, Belgrade, Serbia) and by students from South Africa. As a result of the studies depth profiles of various elements in near-surface layers of the samples were obtained with a depth resolution of about 5 nm. A.P.Kobzev published in the journal Physics of Elementary Particles and Atomic Nuclei, 2014, vol.45, N3 his work "On the radiation mechanism of a uniformly moving charge", suggesting a detailed explanation of the mechanism for the Vavilov-Cherenkov radiation and the transition radiation, which does not require violation of fundamental laws of physics. It is shown that the erroneous "mechanism of radiation during uniform motion of a charge" has given rise to a great number of unreal effects becoming widespread in the publications of many contemporary authors.

3. PUBLICATIONS

PUBLISHED PAPERS

DEPARTMENT OF NEUTRON INVESTIGATION OF CONDENSED MATTER

Atomic and magnetic structures (diffraction)

1. Alekseev P.A., Nemkovski K.S., Kozlenko D.P., Menushenkov A.P., Yaroslavtsev A.A., Gribanov A.V., Clementyev E.S., Pantalei C., Klobes B., Hermann R.P., "Coexistence of long range magnetic order and intervalent state of Eu in $EuCu_2(Si_xGe_{1-x})_2$: evidence from neutron diffraction and spectroscopic studies", **JETP Letters,** 2014, v. 99, p 185-189.
2. Bobrikov I.A., Balagurov A.M., Chih-Wei Hu, Chih-Hao Lee, Sangaa Deleg, Balagurov D.A., Structural evolution in $LiFePO_4$-based battery materials: *in-situ* and *ex-situ* time-of-flight neutron diffraction study. **Journal of Power Sources**, 2014, v. 258, p. 356-364.
3. Burzo E., Vlaic P., Kozlenko D.P., Kichanov S.E., Dang N.T., Rutkauskas A.V., Savenko B.N., Magnetic properties, electronic structures and pressure effects of $Ho_xY_{1-x}Co_2$ compounds. **Journal of Alloys and Compounds**, 2014, v. 584, p.393-401.
4. Craus M.L, Islamov A.Kh., Anitas E.M., Cornei N., Luca D., Microstructural, magnetic and transport properties of $La_{0.5}Pr_{0.2}Pb_{0.3-x}Sr_xMnO_3$ manganites. **Journal of Alloys and Compounds**, 2014, v. 592, p. 121–126.
5. Jabarov S.H., Kichanov S.E., Kozlenko D.P., Mehdiyeva R.Z., Lathe C., Mammadov A.I., Lukin E.V., Savenko B.N., The pressure effect on crystal structure of complex ferroelectrics $Ba_4Sm_2Fe_2Nb_8O_{30}$ and $Ba_4Gd_2Fe_2Nb_8O_{30}$. **Zeitschrift fur Kristallographie**, 2014, DOI:0.1515/zkri-2014-1753.
6. Jabarov S.H., Trukhanov A.V., Korneeva E.A., Mehdiyeva R. Z., Kichanov S. E., Mammadov A. I., Lukin E. V., Huseynov R. E., Effect of Concentration Substitution on the Size Factor in $Li_{1-x}Na_xNbO_3$ Solid Solutions. **Journal of Surface Investigation. X-ray, Synchrotron and Neutron Techniques**, 2014, v. 8, №. 6, p. 1198–1200.
7. Karpinsky D.V., Troyanchuk I.O., Mantyckaya O.S., Chobot G.M., Sikolenko V.V., Efimov V., Tovar M., Магнитные и пьезоэлектрические свойства системы $Bi_{1-x}La_xFeO_3$ вблизи перехода из полярной в антиполярную фазу. **Физика твёрдого тела**, 2014, v. 56, p. 674-678.
8. Karpinsky D., Troyanchuk I., Sikolenko V., Efimov V., Efimova E., Willinger M., Salak A.N., Kholkin A., Phase coexistence in $Bi_{1-x}Pr_xFeO_3$ ceramics. **Journal of Material Science**, 2014, v.49, p. 6937-6943.
9. Karpinsky, D., I.O. Troyanchuk, M. Tovar, V. Sikolenko, V. Efimov, V. Efimova, V. Shur, A. Kholkin Temperature and Composition-Induced Structural Transitions in $Bi_{1-x}La(Pr)_xFeO_3$ ceramics. **Journal of the American Ceramic Society**, 2014, v. 97, p. 2631-2638.
10. Karpinsky, D.V., Troyanchuk I.O., Sikolenko V.V., Efimov V., Efimova E., Silibin M.V., Chobot G.M., Willinger E., Temperature evolution of the crystal structure of $Bi_{1-x}Pr_xFeO_3$ solid solutions. **Physics of the Solid State**, 2014, v. 56, p. 2263-2268.
11. Kichanov S.E., Kozlenko D.P., Wąsicki J., Nawrocik W., Dubrovinsky L. S., Liermann H.-P., Morgenroth W., Savenko B.N., The polymorphic phase transformations in the chlorpropamide under pressure. **Journal of Pharmaceutical Science**, 2014, DOI 10.1002/jps.24241.
12. Kozlenko D.P., Rutkauskas A.V., Dang N.T., Golosova N.O., Kichanov S.E., Dubrovinsky L.S., Liermann H.-P., Morgenroth W., Savenko B.N., Pressure-induced antiferromagnet-ferromagnet transition and a change in the spin state of Co in $La_{0.5}Ca_{0.5}CoO_{2.8}$. **JETP Letters**, 2014, v. 100, p. 380-384.
13. Kozlenko D. P., Kichanov S. E., Lukin E. V., Dang N. T., Dubrovinsky L. S., Liermann H.-P., Morgenroth W., Kamynin A. A., Gridnev S. A., Savenko B. N., Pressure-induced polar phases in relaxor multiferroic PbFe0.5Nb0.5O3. **Physical Review B**, 2014, v. 89, p.1-7.
14. Kozlenko D.P., Dang N.T., Jabarov S.H., Belik A.A., Kichanov S.E., Lukin E.V., Lathe C., Dubrovinsky L.S., Kazimirov V.Yu., Smirnov M.B., Savenko B.N., Mammadov A.I., Takayama-Muromachi E., Khiem L.H., Structural polymorphism in multiferroic $BiMnO_3$ at high pressures and temperatures. **Journal of Alloys and Compounds,** 2014, v. 585, p. 741.
15. Sikolenko, V.V., Efimov V.V., Schorr S., Ritter C., Troyanchuk I.O., Neutron Diffraction Studies of the Structure of Substituted Complex Cobalt Oxides. **Physics of the Solid State, 2014,** v. 56, p. 77-80.
16. Troyanchuk, I.O., Karpinsky D., Efimov V., Sikolenko V., Prokhnenko O., Bartkowiak M., Ferromagnetic Interaction in Mn^{3+} based perovskites. **Journal of Physics: Condensed Matter**, 2014, v. 26, p. 396002.
17. Yartys V.A., Antonov V.E., Beskrovnyy A.I., Crivello J.-C., Denys R.V., Fedotov V.K., Gupta M., Kulakov V.I., Kuzovnikov M.A., Latroche M., Morozov Yu.G., Sheverev S.G., Tarasov B.P., Hydrogen-assisted phase transition in a trigydride $MgNi_2H_3$ syntehesized at high H_2 pressures: Thermodynamics, crystallographic and electronic structures. **Acta Mater**, (2014), http://dx.doi.org/10.1016/j.actamat.2014.09.012
18. Аскеров Э.Б., Мададзада А.И., Бескровный А.И., Исмаилов Д.И., Мехдиева Р.Н., Джабаров С.Г., Керимова Э.М., Неов Д., Нейтронографическое исследование $TlFeS_2$ и $TlFeSe_2$ при низких температурах. **Поверхность. Рентгеновские, синхротронные и нейтронные исследования**, 2014б № 12, с. 5-10.
19. Балагуров А.М., Бобриков И.А., Самойлова Н.Ю., Дрожжин О.А., Антипов Е.В. Применение рассеяния нейтронов для анализа процессов в литий-ионнных аккумуляторах, **Успехи Химии**, 2014, т. 83, № 12.
20. Мехдиева Р.З., Лукин Е.В., Кичанов С.Е., Козленко Д.П., Джабаров С.Г., Данг Т.Н., Мамедов А.И., Савенко Б.Н., Исследование структурных аспектов фазового перехода антисегнетоэлектрик – параэлектрик в двойном перовските Pb_2MgWO_6 при высоких давлениях и температурах, **Физика твердого тела**, 2014, т. 56, № 4, с.735-740.

Nanostructured materials (small-angle scattering and diffraction)

21. Kichanov S.E., Shevchenko G.P., Tretyak E.V., Kozlenko D.P., Malashkevich G.E., Belushkin A.V., Savenko B.N., The structural and luminescent properties of $Lu_3Al_5O_{12}:Ce^{3+}$ + Lu_2O_3 crystal phosphors prepared by colloid chemical synthesis. **Journal of Alloys and Compounds**, 2014, v. 613, p. 238-243.
22. Кичанов С.Е., Исламов А.Х., Самойленко С.А., Козленко Д.П., Белушкин А.В., Гурин В.С., Шевченко

Г.П., Трусова Е.Е., Булавин Л.А., Савенко Б.Н., Исследование особенностей структуры оксидных нанокластеров церия и титана в силикатном стекле методом малоуглового рассеяния нейтронов. **Поверхность. Рентгеновские, синхротронные и нейтронные исследования**, 2014, № 2, с. 5–10.

23. Самойленко С.А., Третьяк Е.В., Шевченко Г.П., Кичанов С.Е., Козленко Д.П., Малашкевич Г.Е., Ступак А.П., Савенко Б.Н., Особенности кристаллической структуры и оптических свойств $Lu_3Al_5O_{12}:Ce^{3+}$, полученного коллоидно-химическим методом синтеза. **Журнал прикладной спектроскопии**, 2014, т. 81, № 6, с. 958-965.
24. Самойленко С.А., Третьяк Е.В., Кичанов С.Е., Шевченко Г.П., Козленко Д.П., Булавин Л.А., Савенко Б.Н., Нейтронные и оптические исследования многокомпонентных кристаллических люминофоров $Y_3Al_5O_{12}:Ce^{3+}/ Lu_2O_3$ и $Lu_3Al_5O_{12}:Ce^{3+}/ Lu_2O_3$. **Украинский физический журнал**, 2014, т. 59, № 9, с. 901-905.

Soft matter, liquids (small angle scattering and diffraction)

25. Avdeev M.V., Particle interaction in polydisperse magnetic fluids: Experimental aspects of small-angle neutron scattering applications. **Journal of Molecular Liquids**, 2014, v. 189, p. 68-73.
26. Anitas E. M., Cherny A. Yu, Osipov V. A., Kuklin A. I., Small-angle scattering from three-phase systems: Investigation of the crossover between mass fractal regimes. **Journal of Physics: Conference Series**. 2014, v. 490. № 1, p.1-3.
27. Arzumanyan G, Vartic V, Kuklin A, Soloviov D, Rachkovskaya G, Zacharevich G, Trusova E., Skoptsov N., Yumashev K., Upconversion Luminescence of Er^{3+} and Co-Doped Er^{3+}/Yb^{3+} Novel Transparent Oxyfluoride Glasses and Glass Ceramics: Spectral and Structural Properties. **Journal of Physical Science and Application**, 2014, v. 4, № 3, p. 150-158.
28. Cherny A. Yu., Anitas E. M., Osipov V. A., Kuklin A. I., Small-angle scattering from multiphase fractal. **Journal of Applied Crystallography**, 2014, v.4, p. 198-206.
29. Belicka M., Kucerka N., Uhríková D., Islamov A.Kh., Kuklin A.I., Devínsky F., Balgavý P., Effects of N, N-dimethyl-N-alkylamine-N-oxides on DOPC bilayers in unilamellar vesicles: small-angle neutron scattering study. **European Biophysics Journal**, 2014, v. 43, p. 179–189.
30. Belushkin A.V., Kazimirov V.Yu., Manoshin S., Reverse Monte Carlo and Voronoi analysis of the local atomic structure of metallic glasses $Fe_{63}Er_2Mo_{14}C_{15}B_6$ and $Fe_{75}Y_5B_{20}$". **Journal of Non-Crystalline Solids**, 2014, v. 402, p. 210.
31. Byvshev I., Murugova T. N., Ivankov O. O., Vangeli I. M., Kuklin A. I., Yaguzhinskiy L. S., Respiration chain and ATP-synthesis system function as tightly-bounded supercomplex**. Biochimica et Biophysica Acta (BBA)-Bioenergetics**, 2014, v.1837, p. e25-e26.
32. Gibhardt H., Haramagatti C. R., Islamov A. K., Ivankov O. I., Kuklin A. I., Eckold G., Universal Behaviour of the Structure and Dynamics of Micelles Formed from Cationic Surfactants. **Zeitschrift für Physikalische Chemie**, 2014, v. 228, p.769–791.
33. Eremin R.A., Kholmurodov Kh., Petrenko V.I., Rosta L., Avdeev M.V., Molecular dynamics simulation analysis of small-angle neutron scattering by a solution of stearic acid in benzene. **Physics of the Solid State**, 2014, v. 56, № 1, p. 81-85.
34. Kiselev M.A., Zemlyanaya E.V., Ryabova N.Y., Hauss T., Almasy L., Funari S.S., Zbytovska J., Lombardo D. Influence of ceramide on the internal structure and hydration of the phospholipid bilayer studied by neutron and X-ray scattering. **Applied Physics A**, 2014, v. 116, p. 319-325.
35. Melnikova L., Mitroova Z., Timko M., Kovac J., Avdeev M.V., Petrenko V.I., Garamus V.M., Almasy L., Kopcansky P., Structural characterization of magnetoferritin. **Mendeleev Communications,** 2014, v**.** 24, p. 80-81.
36. Murugova T. N., Balgavý P., Molecular volumes of DOPC and DOPS in mixed bilayers of multilamellar vesicles. **Physical Chemistry Chemical Physics**, 2014, v.16, p. 18211-18216.
37. Nagornyi A.V., Bulavin L.A., Petrenko V.I., Ivankov O.I., Tomchuk O.V., Avdeev M.V., Vékás L., Determination of the structure factor of interparticle interactions in the ferrofluid by small-angle neutron scattering. **Nuclear Physics and Atomic Energy**, 2014, v.15, p. 59-65.
38. Nagornyi A.V., Petrenko V.I., Bulavin L.A., Almasy L., Kovalchuk V.I., Moroz K.O., Nedyak S.P., Neutron and thermodynamic studies of magnetic fluids stabilized by monocarboxylic acids. **Journal of Physical Studies** 18(2/3) (2014) 2401(6 p.)
39. Petrenko V.I., Avdeev M.V., Garamus V.M., Kubovcikova M., Gazova Z., Siposova K., Bulavin L.A., Almasy L., Aksenov V.L., Kopcansky P., Structure of amyloid aggregates of lysozyme from small-angle X-ray scattering data. **Physics of the Solid State**, 2014, v. 56, p. 129-133.
40. Petrenko V.I., Bulavin L.A., Avdeev M.V., Garamus V.M., Koneracka M., Kopcansky P., Structure and interaction of poly(ethylene glycol) in aqueous solutions. Small-angle neutron scattering data. **Macromolecular Symposia**, 2014, v. 335, p. 20-23.
41. Polovinkin V., Gushchin I, Sintsov M, Round E, Balandin T, Chervakov P, Schevchenko V, Utrobin P, Popov A, Borshchevskiy V, Mishin A, Kuklin A, Willbold D, Chupin V, Popot J.-L., Gordeliy V., High-resolution structure of a membrane protein transferred from amphipol to a lipidic mesophase. **The Journal of membrane biology**, 2014, p.1-8.
42. Prylutskyy Yu.I., Petrenko V.I., Ivankov O.I., Kyzyma O.A., Bulavin L.A., Litsis O.O., Evstigneev M.P., Cherepanov V.V., Naumovets A.G., Ritter U., On the origin of C60 fullerene solubility in aqueous solution. **Langmuir**, 2014, v. 30, p. 3967−3970.
43. Rajewska A., Medrzycka K., Hallmann E., Small-angle neutron scattering study of the structure of mixed micellar solutions based on nonionic and two cationic surfactants**. Physics of the Solid State**, 2014, v.56, p. 125-128.
44. Ryabova N.Yu., Gruzinov A.Yu., Zabelin A.V., Synchrotron X-Ray Diffraction Study of the Structure of *Oral Stratum Corneum* Model Lipid Membranes. **Crystallography Reports**, 2014, v.59, № 1, p.117–124
45. Shibaev A. V., Tamm M., Molchanov V. S., Rogachev A. V., Kuklin A. I., Dormidontova E. E., Philippova O. E., How Viscoelastic Solution of Wormlike Micelles Transforms into Microemulsion upon Absorption of Hydrocarbon: A New Insight. **Langmuir, 2014, v.** 30 № 13, p. 3705-3714.
46. Shvetsov A. V., Lebedev D.V., Chervyakova D. B., Bakhlanova I.V., Yung I.A., Radulescu A., Kuklin A.I., Baitin D.M., Isaev-Ivanov V.V., Structure of RecX protein complex with the presynaptic RecA filament: Molecular dynamics simulations and small angle neutron scattering. **FEBS Letters**, 2014, v. 588, № 6, p. 948–955.

3. PUBLICATIONS

47. Soloviov D., Zabashta Y., Bulavin L., Olexandr I., Gordeliy V., Kuklin, A., Changes in the Area per Lipid Molecule by P–V–T and SANS Investigations. **Macromolecular Symposia**, 2014, v. 335, № 1, p. 58-61.
48. Tomchuk O.V., Bulavin L.A., Aksenov V.L., Garamus V.M., Ivankov O.I., Vul' A.Ya., Dideikin A.T., Avdeev M.V., Small-angle scattering from polydisperse particles with a diffusive surface, **Journal of Applied Crystallography**, 2014, v.47, p. 642–653
49. Vlasov A., Murugova T., Grudinin S., Ivankov O., Soloviov D., Rogachev A., Round A., Ryzhykau Y., Mishin A., Balandin T., Borshchevskiy V., Gordeliy V., Kuklin A., Protein structure and structural ordering versus concentration dependence. **FEBS Journal**, 2014, v. 281, p. 539 – 540.
50. Еремин Р.А., Холмуродов Х.Т., Петренко В.И., Рошта Л., Авдеев М.В., Молекулярно-динамическое моделирование в анализе малоуглового рассеяния нейтронов органическими растворами. Труды XVIII-ой научной конференции молодых учёных и специалистов ОИЯИ (**ОМУС-2014**), 2014, с. 217-220.

Thin films (reflectometry, polarized neutrons)

51. Asgerov E. B., Madadzada A. I., Ismayilov D. I., Mehdiyeva R.N., Interaction of Heterogeneous Thin Films and Phase Formation in the Tl–Fe–S System. **Semiconductors**, 2014, v. 48, № 9, p. 1233–1236.
52. Asgerov E.B., Madadzada A.I., Ismayilov D.I., Mehdiyeva R.N., Electron Diffraction Study of the Phase Formation of Tl–Fe–Se and Kinetics of Phase Transformations of Films $TlFeSe_2$. **Semiconductors**, 2014, v. 48, № 11, p. 1449–1451
53. Ignatovich V.K., Nikitenko Yu.V., Radu F., Reflection of neutrons from fan-like magnetic systems, **American Journal of Modern Physics and Appllications**, 2014, v.1, № 1, p. 7-14.
54. Nikitenko Yu.V., Proglyado V.V., Aksenov V.L., Neutron Channeling in Layered Cu/TiCu structures, **Journal of Surface Investigation**, 2014, v. 8, № 5, p. 961-966.
55. Uyanga E., Gibaud A., Daniel P., Sangaa D., Sevjidsuren G., Altantsog P., Beuvier T., Chih Hao Lee, Balagurov A.M., Structural and vibrational investigations of Nb-doped TiO_2 thin films. **Materials Research Bulletin,** 2014, v. 60, e222-e231.
56. Боднарчук И.А., В.И. Боднарчук, С.П. Ярадайкин, Оценка сечения рассеяния нейтронов на спиновых волнах в тонких ферромагнитных слоях**, Физика твердого тела**, 2014, т. 56, № 1, с. 138-141.

Atomic and magnetic dynamics (inelastic neutron scattering)

57. Drużbicki K., Natkaniec I., Vibrational Properties of Water Retained in Graphene Oxide, **Chemical Physics Letters,** 2014, v.600, p.106–111.
58. Furrer A., Podlesnyak A., Frontzek M., Sashin I., Embs J.P., Mitberg E., Pomjakushina E., Crystal-field interaction and oxygen stoichiometry effects in strontium-doped rare-earth cobaltates. **Physical Review B**, 2014, v.90, 064426.
59. Górska N., Szostak E., Drużbicki K., Mikuli E., Inaba A., Hirao Y., A Comprehensive Study on Crystal Structure, Thermal Behavior, and Molecular Dynamics of $[Sr(DMSO)_4(NO_3)_2]$. **Journal of Coordination Chemistry**, 2014, v.67, p.3135–3154.
60. Hetmańczyk J., Hetmańczyk Ł., Migdał-Mikuli A., Mikuli E., Florek-Wojciechowska M., Harańczyk H., Vibrations and reorientations of H_2O molecules in $[Sr(H_2O)_6]Cl_2$ studied by Raman light scattering, incoherent inelastic neutron scattering and proton magnetic resonance. **Spectrochimica Acta A**, 2014, v.124, p. 429–440.
61. Hetmańczyk J., Hetmańczyk Ł., Migdał-Mikuli A., Mikuli E., Thermal properties of polycrystalline [Mn(NH3)6](ClO4)2. Crystal structure and phase transitions. **Journal of Thermal Analysis and Calorimetry**, 2014, v. 118, p. 1049–1056.
62. Hetmańczyk J., Hetmańczyk Ł., Migdał-Mikuli A., Mikuli E. "Vibrations and reorientations of NH_3 molecules in $[Mn(NH_3)_6](ClO4)_2$ studied by Infrared spectroscopy and theoretical (DFT) calculations. **Spectrochimica Acta A,** 2014, DOI: 10.1016/j.saa.2014.10.044.
63. Kwocz A., Kochel A., Chudoba D., Filarowski A., Tautomeric design of ortho-hydroxyheterocyclic Schiff bases. **Journal of Molecular Structure**, 2014, v. 1080, p. 52-56.
64. Лисичкин Ю.В., Л.А. Сахарова, А.А. Туманов, Динамика молекулы воды, адсорбированной кремнеземом и смолой SGK-7. **Физика твердого тела**, 2014, т. 56, № 1, с.99-106.
65. Łuczyńska K., Drużbicki K., Łyczko K., Starosta W., Complementary Optical and Neutron Vibrational Spectroscopy Study of Bromanilic Acid: 2,3,5,6-Tetramethylpyrazine (1:1) Cocrystal. **Vibrational Spectroscopy**, 2014, v. 75, p. 26–38.
66. Majerz I., Natkaniec I., Proton vibrations in 2,4,6-trimethylpyridinium pentachlorophenolate. **Chemical Physics Letters,** 2014, v. 608, p. 289–294.
67. Natkaniec I., Chudoba D., Hetmańczyk Ł., Kazimirov V.Yu., Krawczyk J., Sashin I.L., Zalewski S., Parameters of the NERA spectrometer for cold and thermal moderators of the IBR-2 pulsed reactor. **Journal of Physics: Conference Series**, 2014, v. 554, 012002.
68. Ozeryanskii V.A., Pozharskii A.F., Antonov A.S., Filarowski A., Out-Basicity of 1,8-bis(dimethylamino)naphthalene: The experimental and theoretical challenge. **Organic & Biomolecular Chemistry**, 2014, v.12, p. 2360-2369.
69. Panek J.J., Jezierska-Mazzarello A.B., Lipkowski P., Martyniak A., Filarowski A., Comparison of resonance assisted and charge assisted effects in strengthening of hydrogen bonds in dipyrrins. **Journal of Chemical Information and Modeling**, 2014, v.54, p.86-95.
70. Pajzderska A., Drużbicki K., Gonzalez M. A., Jenczyk J., Peplińska B., Jarek M., Mielcarek J., Wąsicki J., Experimental and Solid-State Computational Study of Structural and Dynamic Properties in the Equilibrium Form of Temazepam. **Journal of Physical Chemistry B**, 2014, v. 118, p. 6670−6679.
71. Pawlukojć A., Hetmańczyk Ł., IR, INS and DFT investigations on dynamical properties of low temperature phase of choline chloride. **Chemical Physics**, 2014, v.445, p. 31–37.
72. Pawlukojć A., Hołderna-Natkaniec K., Bator G., Natkaniec I., INS, IR, RAMAN, ^{1}H NMR and DFT investigations of dynamical properties in L-asparagine. **Vibrational Spectroscopy**, 2014, v.72, p. 1-7.
73. Pawlukojć A., Hołderna-Natkaniec K., Bator G., Natkaniec I., L-glutamine: dynamical properties investigation by

means of INS, IR, RAMAN, ^{1}H NMR and DFT techniques. **Chemical Physics**, 2014, v.443, p. 17-25.

74. Rachwalska M., Natkaniec I., Zborowski K., Hetmańczyk Ł., Urbanek Z., Inelastic Neutron Scattering (INS) Study of Low Frequency Vibrations and Hydrogen Bonding of (E)-Benzil Monoxime". **Zeitschrift für Physikalische Chemie**, 2014, v. 228, № 1, p. 63–97.
75. Sheka E.F., Natkaniec I., Rozhkova N.N., Hołderna-Natkaniec K., Neutron scattering study of reduced graphene oxide of natural origin", Pis'ma v ZhETF. 2014, v. 99, № 11, p. 754 – 759.
76. Sheka E.F., Rozhkova N.N., Hołderna-Natkaniec K., Natkaniec I, Nanoscale reduced-graphene-oxide origin of shungite in light of neutron scattering. **Nanosystems: physics, chemistry, mathematics**, 2014, v. 5, № 5, p. 659–676.
77. Smirnov M. B., Kazimirov V. Yu., Baddour-Hadjean R., Pereira-Ramos J.-P., Smirnov K.S. Atomistic mechanism of alpha-beta phase transition in vanadium pentoxide. **Journal of Physics and Chemistry of Solids**, 2014, v.75, p. 115.
78. Szostak M.M., Piela K., Hołderna-Natkaniec K., Natkaniec I., Bidzińska E., Optical nonlinearity and electric conductivity origin study on sucrose crystal by using IR, Raman, INS, NMR, and EPR spectroscopies. **Carbohydrate Research**, 2014, v.395, p. 29–37.
79. Благовещенский Н.М., Новиков А.Г., Савостин В.В., Самодиффузия в жидких литии и свинце из данных по когерентному квазиупругому рассеянию нейтронов», **Физика твердого тела**, 2014, т. 56, № 1, с.122-125.
80. Благовещенский Н.М., Новиков А.Г., Рожкова Н.Н., Анализ квазиупругого рассеяния нейтронов концентрированной водной дисперсией наноалмазов, **Физика твердого тела**, 2014, т.56, № 1, с.116-118.
81. Благовещенский Н.М., Г.Новиков А., Пучков А. В., Савостин В. В., Микроскопические свойства жидкого галлия из экспериментов по квазиупругому рассеянию нейтронов, **Письма в ЖЭТФ**, 2014, т. 100, №. 5, с. 379-384.
82. Дубовский О.А., Орлов А.В., Перспективы нейтронной спектрометрии генерируемых ультразвуком и гиперзвуком связанных мультифононных солитонов и бисолитонов нового типа, **Физика твердого тела**, 2014, т.56, № 1, с.45-49.
83. Дубовский О.А., Семенов В.А., Орлов А.В., Солитонная и мультифононная микродинамика теплопроводности плутония и урана в области температур мартенситных фазовых переходов, **Физика твердого тела**, 2014, т.56, №1, с.31-35.
84. Новиков А.Г., Топология и водородная связанность в сверхкритической воде. **Физика твердого тела**, 2014, т. 56, № 1, с.119-121.
85. Семенов В.А., Дубовский О.А., Орлов А.В., Савостин Д.В, Сударев В.В., Спектр частот вольфрама при температурах 293 и 2400 К. **Физика твердого тела**, 2014, т.56, № 1, с.36-40.

Applied studies (texture, stresses, geological materials)

86. Bokuchava G.D., Papushkin I.V., Sumin V.V., Balagurov A.M., Sheptyakov D.V., Investigation of microstrain in dispersion-strengthened steels, **Physics of Solid State**, 2014, v. 56, p. 166-170.
87. Bokuchava G.D., Papushkin I.V., Venter A.M., Petrov P.I., Residual stress studies in electron beam welding using neutron diffraction, **Journal of Materials Science and Technology**, 2014, v. 22, № 1, p. 3-11.
88. Bokuchava G.D., Papushkin I.V., Petrov P.I., Residual Stress Study by Neutron Diffraction in the Charpy Specimens Reconstructed by Various Welding Methods. **Comptes rendus de l'Académie bulgare des Sciences**, 2014, v. 67, № 6, p. 763-768.
89. Lutterotti L., Vasin R.N., Wenk H.-R. Rietveld texture analysis from synchrotron diffraction images. I. Calibration and basic analysis, **Powder Diffraction**, 2014, v. 29. № 1, p. 76-84.
90. Santisteban J.R., Malamud F., Vizcaino P., Li M.J., Vogel S., Liaw P., Carr D.G., Sumin V.V., Vasin R.N., Ridikas D. Preliminary round robin on the determination of crystallographic texture of Zr components by neutron diffraction, **IAEA report**, Vienna 2014. p. 1-8.
91. Scheffzuk Ch., Ullemeyer K., Vasin R.N., Naumann R., Schilling F.R. Strain and texture investigations by means of neutron time-of-flight diffraction: application to polyphase gneisses, **Materials Science Forum**, 2014, v. 777, p. 136-141.
92. Taran Yu., Balagurov A., Sabirov B., Davydov V., Venter A., Neutron Diffraction Investigation of Residual Stresses Induced in Niobium-Steel Bilayer Pipe Manufactured by Explosive Welding. **Material Science Forum**, 2014, v. 768-769, p. 697-704.
93. Taran Y.V., Balagurov A.M., Venter A.M., Evans A., Martensitic transformation of austenitic stainless steel cruciform geometry sample by biaxially fatigued cycling, **Materials Science Forum**, 2014, v. 772, p. 109-115.
94. Vasin R.N., Lebensohn R.A., Matthies S., Tome C.N., Wenk H.-R., The influence of grain shape and volume fraction of sheet silicates on elastic properties of aggregates: biotite platelets in an isotropic matrix. **Geophysics**, 2014, v. 79. №6, p. D433-D441.
95. Wenk H.-R., Lutterotti L., Kaercher L., Kanitpanyacharoen W., Miyagi L., Vasin R.N., Rietveld texture analysis from synchrotron diffraction images. II. Complex multiphase materials and diamond anvil cell experiments. **Powder Diffraction**, 2014, v. 29. № 3, p. 220-232.

Instruments and Methods

96. Keppler R., Ullemeyer K., Behrmann J.H., Stipp M., Potential of full pattern fit methods for the texture analysis of geological materials: implications from texture measurements at the recently upgraded neutron time-of-flight diffractometer SKAT. **Journal of Applied Crystallography**, 2014, v.47, p. 1520-1534.
97. Кожевников С.В., F. Ott, J. Torrejón, M. Vázquez, A. Thiaville, Применение поляризованного микропучка нейтронов для исследования магнитной микроструктуры, **Физика твёрдого тела,** 2014, v.56, p.63-67.
98. Калинин И.В, Морозов В.М., Новиков А.Г., Пучков А.В., Савостин В.В., Сударев В.В., Булкин А.П., Калинин С.И., Пусенков В.М., Ульянов В.А., Характеристики спектрометра ДИН-2ПИ с нейтронным концентратором, **Журнал технической физики**, 2014. т. 84, № .2, p.155-158

3. PUBLICATIONS

DEPARTMENT OF IBR-2 SPECTROMETERS COMPLEX

99. Ananiev V., Belyakov A., Bulavin M., Kulagin E., Kulikov S., Mukhin K., T. Petukhova T., Sirotin A., Shabalin D., Shabalin E., Shirokov V., Verhoglyadov A., The world's first pelletized cold neutron moderator at a neutron scattering facility. **Nuclear Instruments and Methods in Physics Research Section B,** 2014, v. 320, p. 70-74.
100. Belushkin A.V., Kazimirov V.Yu., Manoshin S. Reverse Monte Carlo and Voronoi analysis of the local atomic structure of metallic glasses $Fe_6 3Er_2Mo_{14}C_{15}B_6$ and $Fe_{75}Y_5B_{20}$, **Journal of Non-Crystalline Solids**, 2015, v. 402, p. 210-213.
101. Chernikov A.N. Trofimov V.N. Helium-3 adsorption refrigerator cooled with a closed-cycle cryocooler. **Journal of Surface Investigation. X-ray, Synchrotron and Neutron Techniques**, 2014, v. 8, № 5, p. 952–956.
102. Lieutenant K., Zendler C., Manoshin S., Fromme M., Houben A., Nekrassov D. VITESS 2.10 - Virtual instrumentation tool for the European Spallation Source. **Journal of Neutron Research,** 2014, v.17, p. 45-51.
103. Manoshin S., Rubtsov A., Bodnarchuk V., Mattauch S., Ioffe A. Extension of the VITESS polarized neutron suite towards the use of imported magnetic field distributions, **Journal of Neutron Research**, 2014 v. 17, p. 19-26.
104. Ананьев В.Д., Беляков А.А., Булавин М.В., Верхоглядов А.Е., Куликов С.А., Мухин К.А., Шабалин Е.П., Холодный замедлитель нейтронов на модернизированном реакторе ИБР-2. **Журнал технической физики**, 2014, т. 84, № 2, с. 131-134.

NUCLEAR PHYSICS DEPARTMENT

Experimental investigations

105. Badawi M. S., Ruskov I., Gouda M. M., El-Khatib A. M., Alotiby M.F., Mohamed M.M., Thabet A.A., Abbas M.I., A numerical approach to calculate the full-energy peak efficiency of HPGe well-type detectors using the effective solid angle ratio. **IOP Journal of Instrumentation**, 2014, DOI:10.1088/1748-0221/9/07/P07030.
106. Bevilacqua R., Hambsch F.-J., Bencardino R., Giorginis G., Vidali M., Lamia L., and Ruskov I., ^{10}B and ^{6}Li Nuclear Data Measurements for Incident Neutron Energies up to 3 MeV. **Nuclear Data Sheets**, 2014, v. 119, p. 104-106.
107. Bystritsky V.M., Kobzev A.P., Krylov A.R., Parzhitskii S.S., Philippov A.V., Dudkin G.N., Nechaev B.A., Padalko V.N., Pen'kov P.M., Tuleushev Y.Z., Filipowicz M., Bystritskii Vit.M., Gazi S., Huran J., Study of the d(p, gamma)He-3 reaction at ultralow energies using a zirconium deuteride target. **Nuclear instruments & methods in physics research**, 2014, v.737, p. 248-252.
108. Enik T.L., Mitsyna L.V., Popov A.B., Salamatin I.M., The Angular Anisotropy of Slow Neutrons Scattering. 2014, **JINR Preprint E3-2014-27**, 2014.
109. Frank A.I. Goos-Hänken Effect in Neutron Optics. **JINR Preprint** E3-2014-13, 2014.
110. Frank A.I. On the Goos-Hänken Effect in Neutron Optics. **Journal of Physics: Conference Series, 2014,** v. 528 012029.
111. Gledenov Yu. M., Nesvizhevsky V.V., Sedyshev P.V., Shulgina E.V., Vesna V.A., Search for P-ODD Asymmetry in the Radiative Cross-Section of the Interaction of Neutrons with Lead Nuclei. **Physics of Atomic Nucle**i, 2014, v. 77, № 3, p.316-320
112. Gledenov Yu. M., Sedysheva M. V., Stolupin V. A., Guohui Zhang, Jinhua Han, Zhimin Wang, Xiao Fan, Xiang Liu, Jinxiang Chen, Khuukhenkhuu G., Szalanski P. J., Cross sections of the $^{57}Fe(n,\alpha)^{54}Cr$ and $^{63}Cu(n,\alpha)^{60}Co$ reactions in the MeV region. **Physical Review C**, 2014, v. 89, 064607 (2014)
113. Gledenov Yu. M., Sedysheva M. V., Stolupin V. A., Guohui Zhang, Jinhua Han, Xiang Liu, Xiao Fan, Jinxiang Chen, Khuukhenkhuu G., Szalanski P. J., $^{57}Fe(n,\alpha)^{54}Cr$ cross sections in the MeV region. **ISINN-21 Proceedings**, 2014, p. 330-335.
114. Khuukhenkhuu G., Gledenov Yu.M., Sedysheva M.V., Odsuren M. and Munkhsaikhan J., Statistical model analysis of (n,α) and (n,p) cross sections averaged over the fission neutron spectrum". **ISINN-21 Proceedings**, 2014, p. 336-341..
115. Khuukhenkhuu G., Gledenov Yu.M., Sedysheva M.V., Odsuren M., Munkhsaikhan J., Delgersaikhan T., Systematical Analysis of (n,α) Reaction Cross Sections for 6-20 MeV Neutrons. **Письма в ЭЧАЯ**, 2014, т.11, №6.
116. Kulin G.V, Strepetov A.N., Frank A.I., Geltenbort P., Goryunov S.V, Jentschel M., Kustov D.V. New experimental test of dispersion law for very slow neutrons. **Physics Letters A**, 378, 2553-2556 (2014)
117. Tsulaia M.I., Neutron nuclear Precession - Nuclear Pseudomagnetizm. **Physics of Atomic Nuclear**, 2014, v.77, p1386-1398.
118. Vesna V.A., Gledenov Yu.M., Nesvizhevsky V.V., Sedyshev P.V., Shulgina E.V., Measurement of the left-right asymmetry in integral spectra of γ-quanta in the interaction of nuclei with polarized thermal neutrons. **ISINN-21 Proceedings**, 2014, p. 26-29.
119. Zeynalov SH., Zeynalova O., Hambsch F.J., Sedyshev P., Shvetsov V. Ionization chamber for prompt fission neutron investigations**. Physics Procedia,** 2014, p. 160-166.
120. Бушуев В.А., Франк А.И. Групповое время задержки при отражении волн от многослойных структур и мнимые парадоксы в нейтронной и рентгеновской оптике. **Рентгеновская оптика,** 2014, с. 31-33.
121. Бушуев В.А., Франк А.И., Кулин Г.В. Динамическая теория дифракции нейтронов на движущейся решетке. **Рентгеновская оптика**, 2014, с. 40-42.
122. Игнатович В.К., Саламатин И.М., Саламатин К.М., Сеннер А.Е Автоматизация экспериментов в области спектрометрии нейтронов с использованием сетевых технологий, **Препринт ОИЯИ**, 2014, Р13-2014-33.
123. Франк А. И., Гелтенборт П., Ентшель М., Кустов Д.В., Кулин Г.В., Стрепетов А.Н., Оптический эффект ускоряющегося вещества и длинноволновые нейтроны. **Труды XVIII Международного симпозиума**, 2014, т. 1, с. 349-353.
124. Франк А.И., О законе дисперсии в ускоряющемся веществе. **Письма в ЖЭТФ**, 2014, т. 100, с. 696-697.

Theoretical investigations

125. Ignatovich V.K., A Missed Solution for an Atom: A Gate Toward Cold Nuclear Fusion. **Infinite Energy Magazine**, 2014, № 117, p. 33-36.
126. Ignatovich V.K., Comment on Can Quantum-Mechanical Description of Physical Reality be Considered Complete?, **American Journal of Modern Physics and Application**, v 1, № 1, p. 1-6.
127. Ignatovich V., Nikitenko Yu., Florin R., Reflection of Neutrons from Fan-Like Magnetic Systems. **American Journal of Modern Physics and Application**, 2014, v.1, № 1, p 7-14.
128. Ignatovich V.K., .A Model Of Violation And Superviolation Of Bell's Inequality In Local Quantum Mechanics. **Journal of Physics & Astronomy**, 2014, v.3, №. 3, p. 1-7.
129. Игнатович В.К., Несвижевский В.В., Отражение медленных нейтронов от порошка из нано-стержней. **Атомная энергия**, 2014, т. 116, № 2, с. 100-107.
130. Kobzev A.P. On the radiation mechanism of a uniformly moving charge. **Physics Particles and Nuclei**, 2014, v. 45, № 3, p. 628-653.

Applied research

131. Afanasiev S.V., Borzakov S.B., Egorov V.A., Golutvin I.A., Igamkulov Z.A., Malakhov A.I., Moisenz P.V., Pyataev V.G., Sedyshev P.V., Shvetsov V.N., Smirnov V.A., Zontikov A.O., Experimental study of plastic scintillator damage caused by radiation on IREN at JINR. **CERN-CMS-NOTE-2014-003**, 17 p.
132. Afanasiev S., de Barbaro P. J., Borzakov S.B, Golutvin I., Igamkulov Z.A., Malakhov A., Moisenz P., Pogodaev, G.N., Pyataev V.G., Sedyshev P.V., Shvetsov V.N., Smirnov V. Measuring of induced radioactivity of the HE megatile on IREN at JINR. **CERN-CMS-NOTE-2014-002**, 13 p.
133. Baljinnyam N., Frontasyeva M.V., Aleksiayenak Yu.V., INAA for determination of trace elements in bottom ,sediments of the Selenga River basin in Mongolia. **Physics of Elementary Particles and Atomic Nuclei, 2014, v.** 11, № 2, p. 199–208.
134. Baljinnyam N., Tsevegsuren N., Jugder B., Frontasyeva M.V., Pavlov S.S., Investigation of elemental content of some Mongolian medicinal plants. **International Journal of Medicinal Plants,** 2014, v. 106, p. 481-492.
135. Cepoi L., Rudi L., Chiriac T., Valuta A., Zinicovscaia I., Duca Gh., Kirkesali E., Frontasyeva M.V., Culicov O., Pavlov S.S., Bobrikov I., Biochemical changes in some cultures of cyanobacteria at the synthesis of silver nanoparticles. **Canadian Journal of Microbiology**, 2014, DOI: 10.1139/cjm-2014-0450.
136. Eze Ch.P., Fatoba O., Madzivire G., Ostrovnaya T.M., Petrik L.F., Frontasyeva M.V., Nechaev A.N., Elemental composition of coal fly ash: Matla Coal Power Station in the Mpumalanga Province in South Africa case study using nuclear and related analytical techniques. **JINR Preprint**, E14-2013-131, 2014, p. 17.
137. Frontasyeva M.V., Pavlov S.S., Zinicovscaia I.I., Bagdavadze N. V., Kirkesali E.I., Gakhokidze R., Neutron activation analysis of agricultural crops exposed to bioenergoactivator. **Agricultural Chemistry**, 2014, № 6, p. 55-61.
138. Harmens H., Mills G., Hayes F., Sharps K., Frontasyeva M.V., Aleksiayenak Yu., Culicov O. A., Goryainova Z. I., Vergel K.N., Zinicovscaia I. and the participants of the ICP Vegetation. Air Pollution and Vegetation. **ICP Vegetation Annual Report, 2013/2014.** ICP Vegetation Programme Coordination Centre, CEH Bangor, UK, 2014.
139. Horodek P, Dryzek J, Kobets A.G., Kulik M, Lokhmatov V.I., Meshkov I.N., Orlov O.S., Pavlov V., Rudakov A.Yu., Sidorin A.A, Siemek K, Yakovenko S.L, Slow Positron Beam Studies of the Stainless Steel Surface Exposed to Sandblasting. Acta Physica Polonica, 2014, v. 125, № 3, p. 714-717.
140. Huran J, Balalykin NI, Feshchenko AA, Kobzev AP, Kleinova A, Sasinkova V, Hrubcin, Transmission photocathodes based on stainless steel mesh coated with deuterated diamond like carbon films. **Nuclear Instruments & Methods in Physics Research**, 2014, v. 753, p.14-18.
141. Kobzev A.P., Kulik M., Rzodkiewicz. W. Investigation of MOS Structures Using Nuclear Analytical Methods. **JINR News**, 2014, № 2, p. 16-17.
142. Kravtsova A., Milchakova N., Frontasyeva M., Accumulation of macro- and trace elements in brown algae Cystoseira studied by multielement instrumental neutron activation analysis (the Black Sea, south-western Crimea). **Ecological Chemistry and Engineering**, 2014, v. 21, № 1, p. 9-23.
143. Kravtsova A., Milchakova N., Frontasyeva M., Peculiarities of trace element accumulation by macroalgae Cystoseira from coastal aquatoria of Crimea (the Black sea). **Optimization and Protection of Ecosystems**, 2014, v.10, p. 146–158.
144. Maňkovská B., Frontasyeva M. V., Ostrovnaya T.M., Temporal and spatial trends (1990−2010) of trace element atmospheric deposition in Slovakia − assessment based on moss analysis. Chapter of a book "**Air Pollution**", INTECH, Open Access Publisher, 2014,
145. Maňkovská B., Oszlányi J., Izakovičová Z., Andráš P., Dubiel J., Florek M., Holý K., Frontasyeva M.V., Pavlov S.S., Ostrovnaya T.M., Temporal and spatial trends (1990−2010) of trace element atmospheric deposition in Slovakia: assessment based on moss analysis. **ISINN-21 Proceedings**, 2014.
146. Mitrofanov K. V., Egorov A. S., Piksaikin V. M., Goverdovskii A. A., Zolotarev K. I., Samylin B. F., Gremyachkin D. E., Sedyshev P. V., Zontikov A. O., Zeinalov Sh. S., Shvetsov V. N., Neutron-Physical Characteristics of a Neutron Source for the Production of Radioactive Isotopes Based on the Interaction of Electrons with Liquid Gallium. **Atomic Energy,** 2014, v. 116, p. 252-257.
147. Nekhoroshkov P.S., Kravtsova A.V., Frontasyeva M.V., Tokarev Yu. N., Neutron activation analysis and scanning electron microscopy of phytoplankton in the coastal zone of Crimea (The Black Sea). **American Journal of Analytical Chemistry**, 2014, v. 5, p. 323-334.
148. Nekhoroshkov P.S., Kravtsova A.V., Frontasyeva M.V., Tokarev Yu. N., Neutron activation analysis and scanning electron microscopy of phytoplankton in the coastal zone of Crimea (The Black Sea). **JINR Preprint,** E18-2014-11. Dubna, 2014, p.13.
149. Pavlov S.S., Dmitriev A.Yu., Chepurchenko I.A., Frontasyeva M.V., Automation system for measurement of gamma-ray spectra of induced activity for neutron activation analysis at the reactor IBR-2 of Frank Laboratory of Neutron Phsyics at the Joint Institute for Nuclear Research. **Physics of Elementary Particles and Niclei**, 2014, v. 11, № 6, p. 737–742.
150. Perny M, Huran J, Saly V, Vary M, Packa J, Kobzev AP. Electrical and structural characterization of carbon based

3. PUBLICATIONS

films prepared by RF-PECVD and ECR-PECVD techniques for photovoltaic applications. **Journal of Optoelectronics and Advanced Materials**, 2014, v.16, № 3-4, p. 306-310.

151. Qarri F., Lazo P., Bekteshi L., Stafilov T., Frontasyeva M., Harmens H., The effect of sampling scheme in the survey of atmospheric deposition of heavy metals in Albania by using moss biomonitoring. **Environmental Science and Pollution Research**, 2014, DOI: 10.1007/s11356-014-3417-3.
152. Qarri F., Lazo P., Stafilov T., Frontasyeva M., Harmens H., Bekteshi L., Baceva K., Goryainova Z., Multi-elements atmospheric deposition study in Albania. **Environmental Science and Pollution Research**, 2014, № 21, p. 2506–2518.
153. Sumets M, Ievlev V, Kostyuchenko A, Vakhtel V, Kannykin S, Kobzev A. Electrical properties of Si-$LiNbO_3$ heterostructures grown by radio-frequency magnetron sputtering in an Ar + O-2 environment. **Thin Solid Films**, 2014, v. 552, p. 32-38.
154. Vergel K.N., Goryainova Z.I., Vikhrova I.V., Frontasyeva M.V., Moss biomonitoring and employment of the GIS technology within the framework of the assessment of air aollution by industrial enterprises in the Tikhvin District of the Leningrad Region. **Ecology of Urban Areas**, 2014, № 2, p. 92-101.
155. Yastrubchak O., Sadowski J., Gluba L, Domagala J.Z., Rawski M., Zuk J., Kulik M., Andrearczyk T., Wosinski T. Ferromagnetism and the electronic band structure in (Ga,Mn)(Bi,As) epitaxial layers. **Applied Physics Letters** 2014, v. 105.
156. Zinicovscaia I., Mitina T., Lupascu T., Duca Gh., Frontasyeva M. V., Culicov O. A., Study of chromium adsorption onto activated carbon. **Water, Air, & Soil Pollution,** 2014, v. 225, №. 3,p. 1889- 1894.
157. Zinicovscaia I., Cepoi L., Valuta A., Rudi L., Culicov O. A., Frontasyeva M. V., Kirkesali E. I., Pavlov S. S., Mitina T., *Nostoc linckia* as biosorbent of chromium and nickel from electroplating industry wastewaters. **Journal of Material Science and Engineering B,** 2014, v.4, № 8, p. 242-247.
158. Антонова Л. Х., Демихов Т. Е., Троицкий А. В., Юрасов А. Д., Самойленков С. В., Дидык А. Ю., Кобзев А. П., Кулик М., Куликаускас В. С., Михайлова Г. Н., Влияние протонного облучения на критические параметры композитных высокотемпературных сверхпроводящих лент. **Перспективные материалы**, 2014, № 5, с. 34 – 38.

4. PRIZES AND AWARDS

MISCELLANEOUS

The PAC meeting for Condensed Matter Physics held a competition for the best poster presentation among young scientists. The poster “The magnetic structure of $HoCo_2$ and $ErCo_2$ compounds studies at high pressures” presented by **A. Rutkauskas** was selected as the best poster presentation. The PAC also noted two other high-quality posters: “Molecular dynamics simulation of human lactoferrin apoprotein” by **R. Erhan** and “High pressure diffractometer DN-6: current state” by **E. Lukin**.

JINR AND FLNP FELLOWSHIPS

In 2014, within the framework of the competition of the Association of Young Scientists and Specialists of JINR, the scholarships were awarded to:

1. grant for young PhD researchers
   - **I**.A. Bobrikov
   - V.M. Milkov
   - S.E. Kichanov

2. grant for young specialists
   - E.V. Lukin
   - Ye.A. Golubkov
   - V.S. Popov

3. grant for young researchers
   - Y.V. Alekseenok
   - S.M. Goryunov
   - Z.I. Goryaynova
   - K. Luczynska
   - A.V Rutkauskas
   - A.V. Tomchuk

4. grant for young workers
   - M.A. Bobrov
   - D.E. Pankratov
   - R. V. Chepurchenko

Since 2002, in FLNP a scholarship named after Academician of the USSR Academy of Sciences and first Director of the Laboratory of Neutron Physics **I.M. Frank** has been established in order to stimulate scientific and methodical research of young scientists.

In 2014 I.M. Frank scholarships were awarded to:

- In Neutron Nuclear Physics: I.I. Zinicovscaia
- In Condensed Matter Physics: D.V. Solovjov
- In Methodical Investigations: M.V. Bulavin
- In Development of basic facilities: A.V. Kutergin, K.V. Udovichenko

In 2014 **F.L. Shapiro scholarships** were awarded to:

- In «Neutron Spectroscopy» D.N. Groydanov, A.V. Nagornyi, G.S. Ahmedov

4. PRIZES AND AWARDS

JINR PRIZES

JINR Prizes are awarded annually for the best scientific, technical, methodical and applied research studies. In 2014, the following studies performed by the FLNP specialists or in collaboration with the employees from other JINR Laboratories or scientific institutions were awarded with the prizes of various degrees:

Experimental physics research:

Encouraging prizes

“Structure and properties of magnetic nanoparticles produced by bacteria Klebsiella oxytoca: comprehensive research and experimental validation of biomedical applications”

Authors: M. Balasoiu, D. Soloviov, A. Rogachev, L. Anghel, O. Orelovich, L. Ishchenko, S. Stolyar, R. Iskhakov, Yu. Raikher.

Scientific and Methodical Investigations:

Second prize

“The development of gas detectors for neutron investigations”

Authors: A Belushkin, A. Bogzdel, V. Zhuravlev, F. Levchanovski, E.Litvinenko, V. Milkov, Ts. Panteleev, V. Prikhodko, A. Churakov, V.Shvetsov.

Scientific and technical applied research:

Second prize

"Neutron diagnostics of perspective reactor materials".

Authors: A. Balagurov, G. Bokuchava, R. Vasin, I. Papushkin, V. Sumin.

FLNP SEMINARS

- **L.S. Dubrovinsky** (Bavarian Research Institute of Experimental Geochemistry and Geophysics University of Bayreuth, Germany) Internal structure of the Earth: results of studies of geological materials under extreme conditions. *(22.01.2014)*
- **N.D. Dikoussar** (LIT JINR) The basic element method (piecewise polynomial approximations of high orders). *(06.02.2014)*
- **A.B. Popov** (FLNP, JINR) From the history of neutron research in FLNP. Seminar dedicated to the 80th anniversary of A.B. Popov. (*19.02.2014*)
- **D.M. Itkis (**Lomonosov Moscow State University) Lithium intercalation into nanostructured vanadium oxides. *(21.04.2014)*
- **Dr. Sheldon Landsberger** (University of Texas at Austin, USA) Course: Gamma-Spectrometry and Advances in Nuclear Methodologies in Low Level Gamma Ray Counting: Applications in Environmental Analysis. *(14.04.2014-18.04.2014)*
- **V.I. Feldman** (Lomonosov Moscow State University) Investigation of radiation-induced chemical transformations in systems based on mesitylene and mesitylene-xylene mixtures. *(21.05.2014)*
- **I. Mukha** (GSI Helmholzzentrum für Schwerionenforschung, Germany) Neutron radioactivity. (*12.06.2014*)
- **P. Kopcansky** (Institute of Experimental Physics, Kosice, Slovakia) Cooperative phenomena in complex systems containing magnetic nanoparticles with perspective applications in biomedicine and industry. *(13.10.2014)*
- **F.I. Furman** Seminar dedicated to the 90th anniversary of L.B. Pekelner. (*10.11.2014*)
- **A.V. Belushkin** (FLPN JINR) Ireneusz Natkaniec and neutron scattering in Dubna. *(14.11.2014)*
- **J. Benkhoff** (European Space Agency, Germany) BepiColombo – a joint ESA/JAXA mission to explore Mercury. (*04.12.2014*)
- Seminar dedicated to the 80th anniversary of V.I. Luschikov. *(10.12.2014)*

L.B. Pikelner

A.B. Popov

V.I. Lushikov

5. EVENTS

CONFERENCES AND MEETINGS

On May 27-30, 2014 the XXII International Seminar on Interaction of Neutrons with Nuclei (ISINN-XXII) was held in Dubna. It is the traditional FLNP annual workshop in the field.

On June 24-27, 2014 FLNP organized a conference “Condensed Matter Research at IBR-2 reactor”. The aim of the conference was to bring together the users of the neutron facility for discussion of recent experimental results, prospects of future research and development of IBR-2 instruments.

ISINN-22

“Condensed Matter Research at IBR-2 reactor ”

On September 29 - October 03 the International Summer School and Workshop "Complex and Magnetic Soft Matter Systems: Physico-Mechanical Properties and Structure" was held in Dubna. The workshop was organized in collaboration with the Institute of Continuous Media Mechanics of Russian Academy of Sciences, Romanian Society of Physics, West University of Timisoara, and Horia Hulubei National Institute of Physics and Nuclear Engineering.

EDUCATIONAL PROGRAM

In 2014, the **V International Scientific School for Young Scientists and Students “Instruments and Methods of Experimental Nuclear Physics. Electronics and Automatics of Experimental Facilities”** (November 10-15, Dubna) was organized in the Frank Laboratory of Neutron Physics. The School brought together students, postgraduates and young scientists selected with regard to their specialization from 13 cities of Russia, Ukraine, Belarus, Kazakhstan, Armenia and Mongolia. The purpose of the School was to introduce the participants to the current state of the art in the instrumentation and methods of neutron experiments.

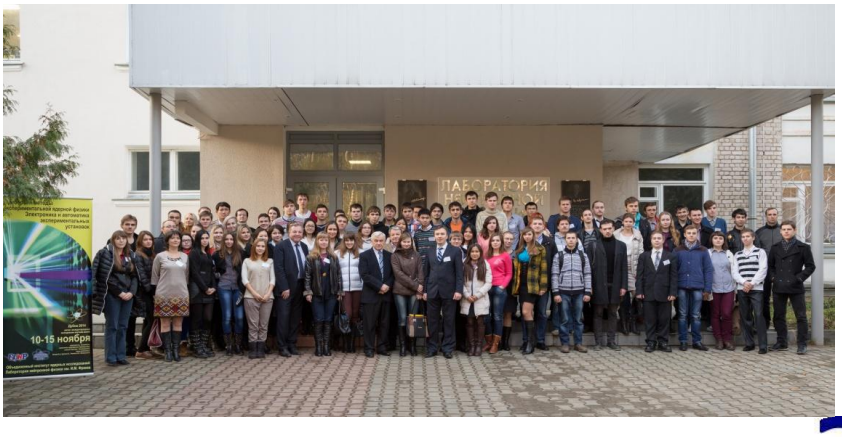

The FLNP successfully collaborates with the JINR University Centre in the organization of summer practical work for students from the JINR Member States (Belarus, Czech Republic, Poland, Romania, Slovakia,) and Associated countries (Egypt, South Africa).

Practice for Students from Arab Republic of Egypt

Student practice

Lectures and excursions to the FLNP facilities for teachers of physics from Russia and the JINR Member States were organized.

VISITS AT OUR FACILITIES

- Head of the Department of Nuclear Physics, Taras Shevchenko National Universiry, Prof. Dr. Igor Kadenko and Head of Materials Science Department of the Vinča Institute of Nuclear Sciences, Belgrade, Dr. Branko Matovic visited FLNP JINR in February 2014
- On February 25, Prof. Dr. Mohamed Salem Badawi from Alexandria University, Egypt visited FLNP JINR.
- On March 6, Dr. Douglas Glenzinski, spokesperson of theMu2e experiment at Fermilab, USA, visited the FLNP. During his visit, Dr. Glenzinski visited the IBR-2 reactor and IREN facility.
- On April 6, the staff members of the Embassy of the Republic of Poland in the Russian Federation in Moscow headed by the Deputy Ambassador Extraordinary and Plenipotentiary of the Republic of Poland to the Russian Federation Ksiazek Jaroslaw visited the Frank Laboratory of Neutron Physics. The guests visited the IBR-2 instruments (KOLKHIDA, REGATA) and IREN.

Members of the Embassy of the Republic of Poland in the Russian

Dr. Branko Matovic visit

- On June 17, the participants of the India-JINR Forum “Frontiers in Nuclear, Elementary Particle and Condensed Matter Physics” held in JINR from June 16 to June 20, 2014, visited the Laboratory. Members of the delegation met the Laboratory Directorate and visited the facilities on the IBR-2 reactor (REGATA and REMUR).
- On September 16, 2014 a delegation from India visited FLNP. Among the members of the delegation were the Science Attaché at the Indian Embassy, representatives of the Ministries, academic institutes and research centers. They met with the Laboratory Directorate and visited the IBR-2 reactor.

6. ORGANIZATION

STRUCTURE OF LABORATORY AND SCIENTIFIC DEPARTMENTS

Directorate:	
Director	*V.N. Shvetsov*
Deputy Director	*O.A. Culicov*
Deputy Director	*E.V. Lychagin*
Deputy Director	*N. Kucerka*
Deputy Director	*S.V. Kozenkov*
Chief engineer:	*A.V. Vinogradov*
Scientific Secretary	*D.M.Chudoba*
Laboratory Scientific Leader	*V.L. Aksenov*
Advisor to Directorate	*V.D. Ananiev*
Advisor to Directorate	*L.B.Pikelner*

Reactor and Technical Departments	Head
IBR-2 reactor	Chief engineer: *A.V. Dolgikh*
Mechanical maintenance division	*A.A. Belyakov*
Electrical engineering department	*V.A. Trepalin*
Design bureau	*A.A. Kustov*
Experimental workshops	*A.N. Kuznetsov*

Scientific Departments	Head
The Division of Condensed Matter Research and Developments	*A.V. Belushkin*
Nuclear physics department	*V.N. Shvetsov*

Administrative Services
Secretariat
Finances
Personnel

Scientific Secretary Group
Secretariat
Translation
Graphics

DIVISION OF CONDENSED MATTER RESEARCH AND DEVELOPMENTS

DEPARTMENT OF NEUTRON INVESTIGATION OF CONDENSED MATTER

Sub-Division	Title	Head
Head of the Department		*D.P.Kozlenko*
Sector 1: Neutron Diffraction. Head: *G D. Bokuchava*		
Group No.1	HRFD	*A.M. Balagurov*
Group No.2	DN-2	*A.I. Beskrovnyi*
Group No.3	DN-12	*B.N. Savenko*
Group No.4	Geomaterials	*D.M.Levin*
Group No.5	SKAT /Epsilon	*Ch. Scheffzük*
Sector 2: Neutron Optics. Head: *M.V. Avdeev*		
Group No.1	Physics of Surfaces	*Yu.V. Nikitenko*
Group No.2	Physics of Nanostructures	*V.I. Bodnarchuk*
Small angle scattering group		*A.I. Kuklin*
Inelastic scattering group		*D. Chudoba*

DEPARTMENT OF IBR-2 SPECTROMETERS COMPLEX

Sub-Division	Title	Head
Head of the Department		*S.A. Kulikov*
Group No.1	Detectors	*A.V. Churakov*
Group No.2	Electronics	*A.A. Bogdzel*
Group No.3	Information technologies	*A.S. Kirilov*
Group No.4	Sample environment and choppers	*A.P. Sirotin*
Group No.5	Cryogenic investigations	*A.N. Chernikov*
Group No.6	Cold moderators	*M.V. Bulavin*

NUCLEAR PHYSICS DIVISION

Sub-Division	Title	Head
Sector 1.	investigations of neutron-nuclear interactions	*Y.N. Kopatch*
Sector 2.	Investigation of neutron fundamental properties.	*Ye.V. Lychagin*
Sector 3.	Neutron Activation Analysis and Applied Research:	*M.V. Frontasyeva*
IREN facility		*V.G. Pytaev*

6.ORGANIZATION

PERSONNEL

DISTRIBUTION OF THE PERSONNEL PER DEPARTMENT

Theme	Departments	People
-1104-	Nuclear Physics Department	92
-1069-	Department of neutron investigation of condensed matter	93
-1075-	Department of IBR-2 spectrometers complex	43
-1105-	IBR-2 reactor	45
	Mechanical and Technical Department	49
	Electric and Technical Department	31
	Central Experimental Workshops	38
	Nuclear Safety Group	7
	Design Bureau	6
	FLNP infrastructure:	
	Directorate	10
	Services and Management Department	24
	Scientific Secretary Group	4
	Supplies Group	4
Total		**451**

PERSONNEL FROM THE JINR MEMBER STATES (BESIDES THE RF)

Country	People	of which young specialists (≤35 years)
Azerbaijan	5	4
Belarus	1	1
Bulgaria	9	5
Georgia	1	
Germany	1	
Kazakhstan	6	6
Moldova	2	2
Mongolia	9	9
Poland	10	3
Romania	7	2
Slovakia	1	
Ukraine	12	8
TOTAL	**64**	**42**

OUR PhD STUDENTS

In 2014 21 PhD students from 11 countries conducted their experimental research at the FLNP facilities.

Name	Country	PhD student of
Ahmedov G.S.	Azerbaijan	Institute of Radiation Problems ANAS
Alekseenok Yu.V.	Belarus	International Sakharov Environmental University
Hristozova G.	Bulgaria	Paisii Hilendarski University
Sanislo A.	Hungary	Obuda University
Bagdaulet M.	Kazakhstan	Al-Farabi Kazakh National University
Hramco C.	Moldova	University of the Academy of Science of Moldova
Nyamsuren B.	Mongolia	National University of Mongolia
Luczynska K.	Poland	Institute of Nuclear Chemistry and Technology
Ordon M.	Poland	Siedlce University of Natural Sciences and Humanities
Jaketov V.D.	Russia	JINR University centre
Eremin R.A.	Russia	JINR University centre
Rumyantsev I.	Russia	JINR University centre
Rutkauskas A.V.	Russia	JINR University centre
Vergel K.	Russia	Dubna International University for nature, Society and Man / FLNP JINR
Zontikov A.O.	Russia	Dubna International University for nature, Society and Man
Kravtsova A.V.	Russia	A.O. Kovalevsky Institute of biology of the Southern Seas
Nekhoroshkov P.	Russia	A.O. Kovalevsky Institute of biology of the Southern Seas
Ndlovu N.B.	South Africa	Stellenbosch University
Eze P.	South Africa	Western Cape University
Samoylenko S.A.	Ukraine	National University of Kyiv
Tomchuk A.V.	Ukraine	National University of Kyiv

In 2014, 9 BSc theses, and 4 MSc theses were defended using the experimental material obtained in FLNP. One of our employeer was conferred a Doctor of Science degree.

7. INTERNATIONAL COOPERATION AND USER INTERACTION

INTERNATIONAL COOPERATION

In 2014 the Frank Laboratory of Neutron Physics collaborated with 197 institutions from 22 JINRMember States or Associated Members of JINR and 41 institutions from 20 Non-Member States of JINR. The distribution of the institutions by country is presented below.

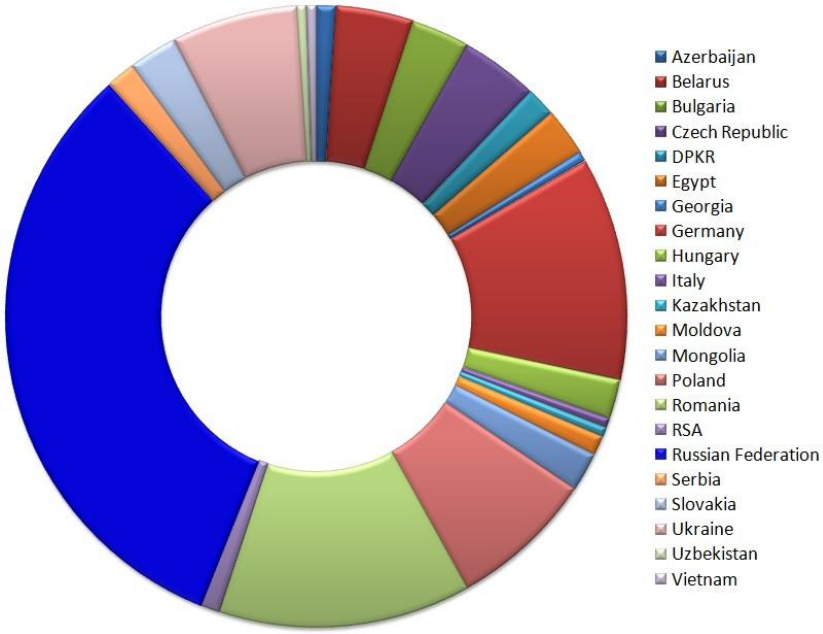

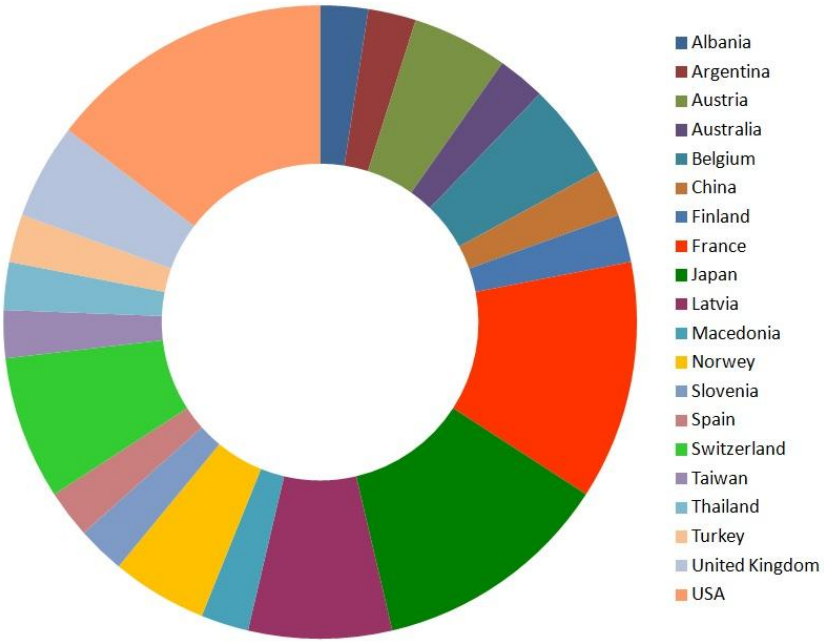

USER INTERACTION

In 2014 were two calls for proposals for experiments at the modernized IBR-2 reactor (01 September – 15 October 2013; Call-II: 01 March – 15 April 2014). A total of 163 proposals for conducting experiments were received from 17 different countries. The received proposals covered the broad spectrum of neutron research in physics, materials science, chemistry, geosciences, biology and applied sciences. 150 received proposals were admitted for realization.

Proposal distribution by applicant's affiliation

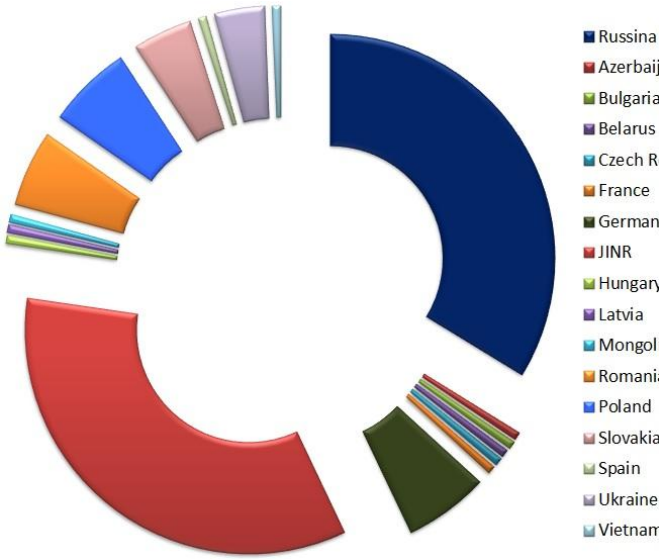

Proposal distribution by science

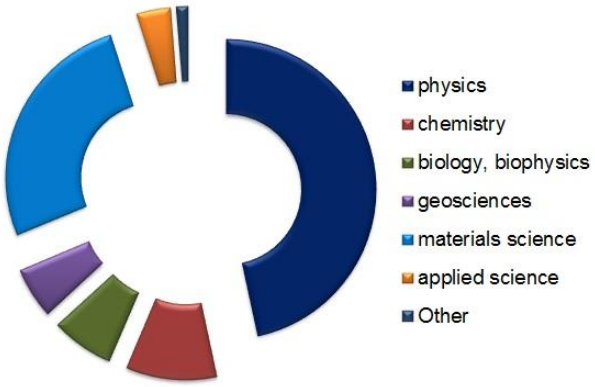

Proposal distribution by facilities

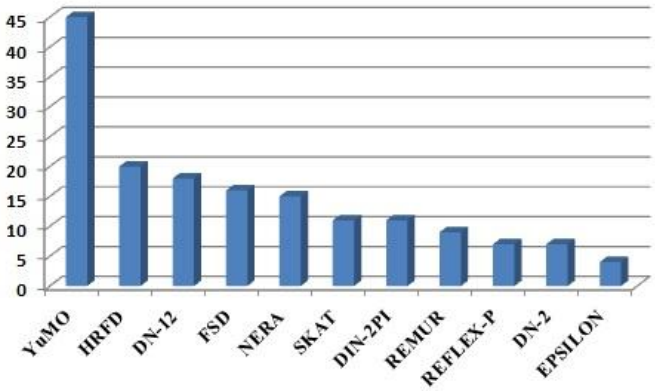

7. INTERNATIONAL COOPERATION AND USER INTERACTION

List of Visitors from the JINR Member States or Associated Members of JINR in 2014

Country	Nr of visitors
Azerbajan	1
Bulgaria	3
Czech Republic	2
Hungary	1
Germany	10
Georgia	2
Egypt	2
Kazakhstan	3
Moldova	1
Mongolia	3
Poland	18
Romania	9
Serbia	2
Slovakia	8
Ukraine	11
Czech Republic	2
RSA	1
Vietnam	1

List of Visitors from Non-Member States of JINR in 2014

Country	Nr of visitors
China	3
Australia	1
France	1
UK	1
Japan	1
Italy	1
Latvia	7
Norwey	1
Taiwan	2
Slovenia	2
Spain	2
Swizerland	2
USA	1

8. FLNP AND MASS-MEDIA

In the year 2014 Frank Laboratory of Neutron Physics was at center of interest of mass media.

NANO NEWS NET
22.01.2014
http://www.nanonewsnet.ru/news/2014/ibr-2-stanovitsya-fabrikoi-vysokikh-tekhnologii

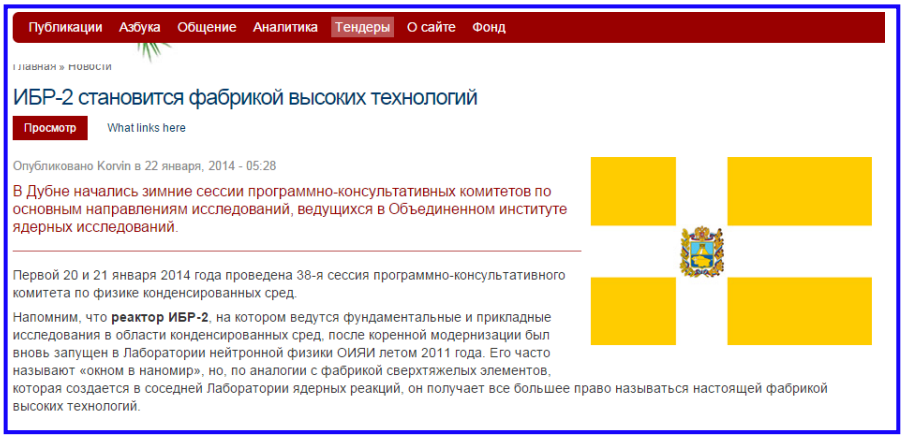

Russian Atomic Agency 24.02.2014
http://www.atomic-energy.ru/news/2014/02/24/46871

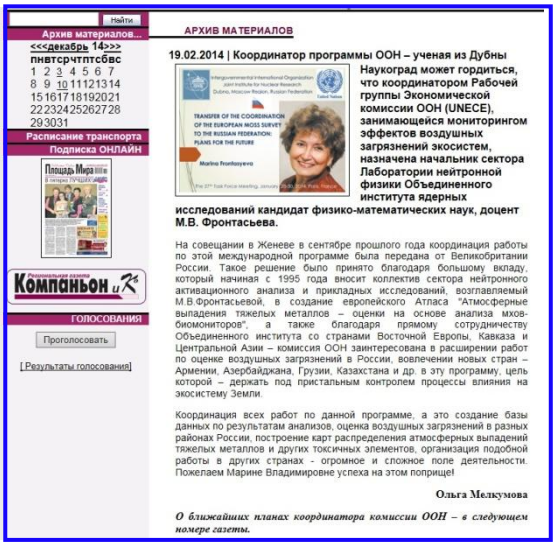

Газета "Площадь Мира" 19.02.2014
http://pressdubna.ru/archive_full.php?nid=12159

9. ANNIVERSARIES

V.G. SIMKIN

A lot of veterans work in JINR. And that's good! Continuity in science is the most important condition for its successful development. At a meeting held on February 3, 2009 in FLNP and dedicated to the 70th anniversary of birth of Valery G. Simkin, he was called a legend of the Condensed Matter Physics Department. During the past 5 years nothing has changed – V.G.Simkin continues years after his graduation from Kharkov State University, V.G.Simkin started to work in LNP, and since that time the Laboratory has become his home, where he knows everyone and everyone knows him. Over more than 20 years he worked in several experimental groups solving various challenging engineering problems. First he was involved in the development of magnetic quantum sensors, then of a very unusual method of correlation analysis of neutron scattering suggested by Hungarian physicists.

In the early 1990s V.G.Simkin was elected to the position of a researcher and started to work in the neutron diffraction group, where he has become one of the key figures in the construction of the world's first neutron high-resolution Fourier diffractometer (HRFD) at a pulsed neutron source. Owing to his efforts HRFD has long become an exemplary spectrometer and is a “must-see” place for excursions visiting IBR-2 during numerous conferences and schools. And no matter who the visitors are – eminent scientists or students – a great deal of sincere respect and admiration for this engineering marvel and people who created it, is guaranteed. At the above-mentioned jubilee party it was suggested to include a new paragraph in the duty instructions for all instrument-responsible scientists obliging them every three months to visit HRFD and adopt new developments and improvements made by V.G.Simkin.

V.G.Simkin is a repeated prize winner of JINR and FLNP scientific research competitions. He was awarded the honorary badge "Veteran of Nuclear Power Engineering and Iindustry." His never-failing friendliness, correctness in everything he does, his genuine desire to help, broad interests, and, above all, adherence to principles were the very qualities that allowed him to be elected as a chairman of comrades' court of the Laboratory (now-vanished but once important public authority body) for 15 years in a row. He spares no efforts to preserve the memory of the deceased colleagues.

He played a major role in the appearance of an alley in JINR named after Yu.M.Ostanevich, as well as in publishing collections of reminiscences about Yu.M.Ostanevich and D.A.Korneev.

10. CONTENT